

**Role of caveolin-1 in regulating membrane properties  
in cells in a 3D microenvironment**

**A THESIS**

**SUBMITTED IN PARTIAL FULFILLMENT OF THE REQUIREMENTS**

**OF THE DEGREE OF**

**DOCTOR OF PHILOSOPHY**

**BY**

**Trupti Nandkumar Thite**

**20113116**



**INDIAN INSTITUTE OF SCIENCE EDUCATION AND RESEARCH PUNE  
2016**

## DECLARATION

I declare that this written submission represents my ideas in my own words and where others' ideas have been included; I have adequately cited and referenced the original sources. I also declare that I have adhered to all the principles of academic honesty and integrity and have not misinterpreted or fabricated or falsified any idea/data/fact/source in my submission. I understand that the violation of the above will be a cause for a disciplinary action by the institute and can also evoke penal action from the sources which have thus not been properly cited or from whom proper permission has not been taken when needed.

*TN Thite*

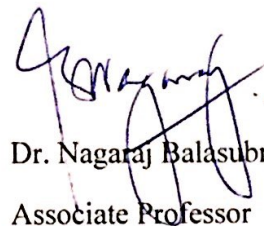
Trupti Nandkumar Thite

Reg. No. 20113116

Date: 16/6/2017

## CERTIFICATE

Certified that the work incorporated in the thesis entitled "**Role of Caveolin-1 in regulating membrane properties in cells in a 3D microenvironment**" submitted by **Trupti Thite** was carried out by the candidate under my supervision. The work presented here or any part of it has not been included in any other thesis submitted previously for the award of any degree or diploma from any other university or institution.



Dr. Nagaraj Balasubramanian  
Associate Professor

IISER, Pune.

Date: JUNE 16, 2017

## Acknowledgements

I would like to express my sincere gratitude to my Ph.D. supervisor Dr. Nagaraj Balasubramanian for his support and guidance for this project. I am thankful to him for giving me an opportunity to work in his lab and pursue my interest in this field. I am grateful to him for critically evaluating my experiments and scientific thinking.

I would like to acknowledge my Research Advisory Committee members, Dr. Aurnab Ghosh, Dr. Richa Rikhy and Dr. Pramod Pullarkat for their constant suggestions which helped me planning the project well. I am thankful to Dr. Thomas Pucadyil for his help with the analysis of FRAP experiments. I would also like to thank Dr. Girish Ratnaparakhi and Dr. L. S. Shashidhara for their support. AFM experiments were done with Dr. Abhijeet Majumdar and Pankaj Mogha (IIT Bombay). Dr. Chiam Keng Hwee (National University of Singapore) helped us with vesicle tracking experiments.

I thank IISER-Pune for funding during my Ph.D tenure and Wellcome-DBT India Alliance for funding the research in the lab. I am thankful to the facilities and authorities at IISER Pune for managing all the resources and equipments. I also acknowledge all the current and past members of Adhesion lab as well as other biology labs who helped me with help with reagents and technical assistance in experiments.

I was fortunate to make very special friends at IISER who stood by me all the time and encouraged me. Without them, it would have been difficult to survive for all these years. I sincerely thank Ayantika, Devika, Ketaki, Manasi, Maithilee, Roopali, Vibha for all the love and support. Music was a major stress-reliever during my PhD and so special thanks to Manasi, Abhijeet and Srikrishna with whom I share a great chemistry, not just related to music but even beyond that.

This thesis would have been difficult to achieve without the support of my family and friends. Special thanks to my extremely patient and supportive husband, Abhishek who kept me motivated during the difficult times of my PhD. All this would not have been possible without him.

## List of abbreviations

$\mu\text{M}$	macromolar
$\mu\text{l}$	microlitre
$\mu\text{g}$	microgram
Kd	Kilodalton
nm	Nanometer
BSA	Bovine serum albumin
CSD	Caveolin scaffolding domain
CBM	Caveolin binding motif
CEMM	Cholesterol enriched membrane microdomains
CLIC/GEEC	Clathrin-independent carriers (CLIC)/ Glycosylphosphatidylinositol- anchored protein (GPI-AP) enriched compartments (GEEC)
DMEM	Dulbecco's modified eagle's medium
ECM	Extracellular matrix
ER	Endoplasmic reticulum
EM	Electron microscope
FBS	Fetal bovine serum
FRAP	Fluorescent recovery after photobleaching
FRET	Förster resonance energy transfer
GFP	Green fluorescence proteins
GPI	Glycosylphosphatidylinositol

IL2	Interleukin-2
KO	Knockout
PBS	Phosphate buffered saline
PFA	Paraformaldehyde
PIP2	Phosphatidylinositol 4,5-bisphosphate
PACSIN2	Protein Kinase C And Casein Kinase Substrate In Neurons 2
SV40	Simian virus 40
RFP	Red fluorescence protein
TIRF	Total internal reflection fluorescence

## Abstract

Caveolae are 60-80 nm omega shaped structures on the plasma membrane which comprise of Caveolin-1 (Cav1), the major structural protein and are rich in cholesterol and sphingolipids. Caveolae play an important role in cellular signaling, endocytosis and mechanosensing. Apart from these functions, caveolae have been recently emerged as plasma membrane organizers and protectors. Their presence or absence changes the membrane composition, membrane order and membrane tension, further regulating signal transduction in cells. All these properties of plasma membrane are either known or expected to be different in cells which are cultured in a three-dimensional (3D) microenvironment as compared to conventional rigid two-dimensional (2D) tissue culture plate.

In this project, we have tried to elucidate the role of Cav1 in cells in a 3D microenvironment. We focused on two aspects - 1) how Cav1 modulate mobility of various membrane associated proteins and 2) whether and how Cav1 affect endocytosis in cells in a 3D microenvironment. pTyr14-cav1 is one of the important modification on Cav1 and we have studied its relevance in both these aspects. We compared mobility of various markers (K-Ras-CAAX-GFP, H-Ras-CAAX-GFP and GPI-GFP) in WT Cav1-KO MEFs (Mouse Embryonic Fibroblasts) and found it to be differentially regulated by Cav1 in 2D versus 3D. Mobility of K-Ras-CAAX-GFP on the plasma membrane by FRAP was found to be reduced in WT MEFs as compared to Cav1-KO MEFs. Interestingly, reconstitution of Cav1-KO MEFs with WT Cav1 or Y14F-Cav1 (phosphodeficient version) both reduced this mobility, suggesting pTyr14-Cav1 not being involved in regulating the mobility. H-Ras-CAAX-GFP and GPI-GFP did not have any difference in their mobility in WT MEFs versus Cav1-KO MEFs in 3D collagen. This altered mobility of K-Ras-CAAX-GFP could be because of altered plasma membrane properties (like fluidity or tension) of WT MEFs versus Cav1-KO MEFs.

Our studies looking at endocytosis in WT-MEFs in 3D collagen showed that, at concentrations 1.5 mg/ml and above, GM1-CTxB endocytosis was blocked. However, at lower collagen concentrations (0.5 mg/ml and 1 mg/ml) the endocytosis was supported. Cav1-KO MEFs did not show such differential uptake of GM1-CTxB at different collagen concentrations. Also, the mobility of K-Ras-CAAX-GFP was higher in WT MEFs embedded in 1 mg/ml than in 1.5 mg/ml collagen. Reconstitution of Cav1-KO MEFs with WT-Cav1 or Y14F-Cav1 both blocked the endocytosis at 1.5 mg/ml, again suggesting pTyr14-Cav1 not being involved in regulating GM1-CTxB endocytosis in 3D. Preliminary laser ablation and actin disruption experiments indicate to a possible mechanism for this differential regulation, which is, the membrane tension and / or cortical actin network could be different in WT MEFs embedded in different concentrations of collagen gels.



# Contents

<b>Sr. No.</b>	<b>Title</b>	<b>Pg. No.</b>
	Acknowledgements	
	Abstract	
	List of abbreviations	
	<b>Synopsis</b> .....	<b>i</b>
	<b>CHAPTER 1 : Review of literature and objectives</b>	
1.1	Caveolae.....	2
1.1.1	Structural proteins of caveolae - Caveolins and Cavins.....	3
1.1.2	The major structural protein - Cav1.....	5
1.1.3	Biogenesis of caveolae.....	6
1.2	Regulation of caveolar trafficking and function.....	8
1.2.1	Role of pTyr-14 Cav1.....	8
1.2.2	Role of integrins.....	9
1.2.3	Role of cytoskeleton.....	10
1.3	Functions of caveolae and caveolin-1.....	12
1.3.1	Caveolae, Cav1 and cellular signaling.....	12
1.3.2	Caveolar endocytosis and transcytosis.....	14
1.3.3	Caveolae mediated regulation of lipids.....	15
1.3.4	Caveolae and regulation of membrane properties.....	16
1.3.5	Caveolae and mechanotransduction.....	16
1.3.6	Cav1 and remodeling of extracellular matrix.....	18

1.4	Extracellular matrix : 2D v/s 3D.....	19
1.4.1	Different matrices used for 3D cell culture.....	20
1.4.2	Behavior of cells in 3D microenvironment.....	21
1.4.3	Integrins in 2D v/s 3D microenvironment.....	23
1.4.4	Plasma membrane in 2D v/s 3D microenvironment.....	24
1.4.5	Mechanotransduction in 2D v/s 3D microenvironment.....	25
1.4.6	Caveolae in 2D v/s 3D microenvironment.....	26
1.5	Objectives of the study.....	27

**CHAPTER 2 : Localization and mobility of Cav1 in cells in 2D v/s 3D microenvironment :  
Role of pTyr14-Cav1**

<b>2.1</b>	<b>Rationale.....</b>	<b>29</b>
<b>2.2</b>	<b>Materials and methods.....</b>	<b>31</b>
2.2.1	Plasmids and antibodies.....	31
2.2.2	Cell culture.....	31
2.2.3	Embedding MEFs in 3D collagen gels.....	31
2.2.4	Coating coverslips with collagen.....	32
2.2.5	Confocal imaging.....	32
2.2.6	Fluorescence Recovery After Photobleaching (FRAP).....	33
2.2.7	Extraction of cells using collagenase.....	34
2.2.8	Western blotting.....	34
2.2.9	Single particle tracking.....	34
2.2.10	Statistical analysis.....	35

<b>2.3</b>	<b>Results</b> .....	36
2.3.1	Standardizing embedding and imaging MEFs in 3D collagen gels.....	36
2.3.2	Localization of various Cav1 constructs in MEFs - 2D and 3D.....	38
2.3.3	Morphology of WT v/s Cav1-KO MEFs in 3D collagen.....	41
2.3.4	Cav1 and Cavin1 co-localization - 2D and 3d collagen.....	43
2.3.5	Standardizing FRAP in 3D - Using K-Ras-CAAX-GFP.....	45
2.3.6	Mobility of Cav1 in MEFs in 2D and 3D collagen - Role of pTyr14-Cav1.....	47
2.3.7	pTyr-Cav1 levels - 2D v/s 3D.....	51
<b>2.4</b>	<b>Discussion</b> .....	52
<b>2.5</b>	<b>Summary</b> .....	56

**CHAPTER 3 : Mobility of various membrane associated proteins in 2D v/s 3D  
microenvironment : Role of Cav1**

<b>3.1</b>	<b>Rationale</b> .....	58
<b>3.2</b>	<b>Materials and methods</b> .....	60
3.2.1	Plasmids.....	60
3.2.2	Cell culture.....	60
3.3.3	FRAP analysis and fitting - comparison of two equations.....	60
3.3.4	Embedding cells in 3D collagen.....	62
3.3.5	2D collagen coating.....	62
3.3.6	Statistical analysis.....	63

<b>3.3</b>	<b>Results</b> .....	64
3.3.1	Various membrane associated proteins used for FRAP experiments.....	64
3.3.2	Description of different bleach geometries used in FRAP experiments.....	66
3.3.3	Mobility of K-Ras-CAAX-GFP : 2D v/s 3D.....	68
3.3.4	Mobility of H-Ras-CAAX-GFP : 2D v/s 3D.....	70
3.3.5	Mobility of GPI-GFP : 2D v/s 3D.....	72
3.3.6	Mobility of EGFR-GFP : 3D.....	74
<b>3.4</b>	<b>Discussion</b> .....	75
<b>3.5</b>	<b>Summary</b> .....	78

**CHAPTER 4 : Regulation of endocytosis in a 3D microenvironment : Role of Cav1 and pTyr14 Cav1**

<b>4.1</b>	<b>Rationale</b> .....	80
<b>4.2</b>	<b>Materials and methods</b> .....	81
4.2.1	Reagents.....	81
4.2.2	Cell culture.....	81
4.2.3	Labeling cells in 3D collagen.....	81
4.2.4	Cytochalasin D and Latrunculin A treatment.....	82
4.2.5	FRAP.....	82
4.2.6	Atomic force microscopy (AFM).....	82

4.2.7	Second harmonic generation (SHG) imaging.....	83
4.2.8	Laser ablations.....	84
4.2.9	Statistical analysis.....	84
<b>4.3</b>	<b>Results.....</b>	<b>85</b>
4.3.1	Endocytosis of GM1-CTxB and transferrin upon loss of adhesion.....	85
4.3.2	Differential endocytosis of various markers in 3D collagen.....	86
4.3.3	GM1-CTxB endocytosis is blocked in WT MEFs in 1.5 mg/ml collagen.....	87
4.3.4	GM1-CTxB endocytosis in Cav1-KO MEFs.....	90
4.3.5	GM1-CTxB endocytosis in WT MEFs & Cav1-KO MEFs at higher collagen concentrations...91	
4.3.6	GM1-CTxB endocytosis in WT MEFs surrounded by Cav1-KO MEFs (3D collagen).....92	
4.3.7	GM1-CTxB endocytosis in Cav1-KO MEFs expressing WT Cav1 or Y14F Cav1.....94	
4.3.8	Mobility of K-Ras-CAAX-GFP at different collagen concentrations.....95	
4.3.9	Actin disruption triggers GM1-CTxB endocytosis in WT MEFs in 1.5 mg/ml collagen.....96	
4.3.10	Actin disruption increases mobility of K-Ras-CAAX-GFP in WT MEFs in 1.5 mg/ml collagen.....	98
<b>4.4</b>	<b>Discussion.....</b>	<b>100</b>
<b>4.5</b>	<b>Summary.....</b>	<b>108</b>
	<b>Future prospective.....</b>	<b>109</b>
	<b>Appendix.....</b>	<b>114</b>
	<b>Bibliography.....</b>	<b>120</b>

## Synopsis

## **Introduction**

**Caveolae** are 60-80 nm omega-shaped **invaginations present on the plasma membrane** of most mammalian cell types. These were first observed under electron microscope and are abundant in endothelial cells, fibroblast, adipocytes and muscle cells (Palade, 1953; Yamada, 1955). In the past few years there has been a lot of efforts understanding how these organelles are formed in cells (Hayer et al., 2010). **Caveolin and Cavin** are the two most important protein families which are the structural components of caveolae. There are total three caveolin proteins and 4 cavin proteins identified, amongst which caveolin-1 (Cav1) is the indispensable protein for caveolae formation (Fra et al., 1995).

**Cav1 is a 23KDa transmembrane protein** which is present as homo and hetero oligomers (with Cav2) at caveolae (Rothberg et al., 1992). It has a membrane scaffolding domain from amino acid residue 82 to 101 and both N and C termini face towards the cytoplasm. One of the important post-translational modification on Cav1 is - **tyrosine 14 phosphorylation (pTry14-Cav1)**, which is shown to be required for many cellular processes like focal adhesion dynamics (Joshi et al., 2008), Rho-A GTPase activation (Grande-Garcia et al., 2007), mechanotransduction (Joshi et al., 2012). Src, Abl and Fyn kinases have been shown to phosphorylate this site (Glenney and Soppet, 1992; Sanguinetti et al., 2003; Sanguinetti and Mastick, 2003). Unlike the protein Cav1, this phosphorylation is not dispensable for caveolae formation. The phospho deficient Cav1, when expressed in cells lacking Cav1, forms caveolae which are similar in number and size (del Pozo et al., 2005).

The main functions attributed to caveolae include **signaling, cholesterol homeostasis, endocytosis and mechanosensing** (Parton and Simons, 2007). The role of Cav1 in signaling has been explained in the field by the hypothesis that - Cav-1 has a **scaffolding domain (CSD)** which physically interacts with **Cav-1 binding domain (CBD)** present in many signaling molecules and controls signaling downstream (Couet et al., 1997; Okamoto et al., 1998). However, a detail **structure-based analysis** was done recently which showed that, the CBD is highly hydrophobic and hence is deeply buried inside the protein (of almost all signaling proteins) (Collins et al., 2012). Thus, a **direct physical interaction** between Cav-1 and signaling molecules containing CBD **is now being questioned**.

**Alternative hypothesis** suggests that **caveolae act as organizers of plasma membrane** and that eventually influence signaling downstream (Parton and del Pozo, 2013). A **comprehensive lipidomic analysis** showed that Cav1-KO MEFs have deregulated glycosphingolipid (GSL) and sphingolipid (SL) metabolism. It was also shown that Cav1-KO MEFs have alterations in glycerophospholipids, with a higher phosphatidylcholine (PC) / phosphatidylethanolamine (PE) ratio compared with WT-MEFs and altered phosphatidyl serine (PS) distribution. This was further reflected in differential clustering of Ras isoforms and hence signaling downstream (Ariotti et al., 2014). Caveolae are also known to affect other membrane properties, like **membrane order**. Using Laurdan probe, it shown that Cav1-KO MEFs have less abundant ordered membrane fraction as compared to WT-MEFs, making them more fluid. This was also shown to be dependent on Tyr14-Cav1 (Gaus et al., 2006). All these factors can eventually regulate signaling in cells.

In the current study, we have tried to explore the role of caveolin and phosphocaveolin in membrane of cells which are embedded in a **three-dimensional (3D) microenvironment**. Recently, studying cell behavior in a 3D microenvironment has proven to be more informative than conventional two-dimensional (2D) cultures. In vivo, cells experience a complex and dynamic 3D microenvironment and hence 3D cultures are considered to be **more close to physiological conditions than 2D**. Various phenomenon in cells including morphology of cells, integrin mediated adhesion structures, integrin signaling, arrangement of cytoskeleton, modes of migration etc., are shown to be different in 3D as compared to 2D (Baker and Chen, 2012; Cukierman et al., 2001).

Along with all these, **composition and properties of plasma membrane are also shown to be different in cells growing in 3D matrices**. Fibroblast cells were grown in 3D cell-derived matrices and, it was shown that cholesterol and sphingomyelin content in the membrane was more in 3D than 2D. Same study reported that the membrane cholesterol in cells growing in 3D was more susceptible to oxidation and was asymmetrically distributed among the two leaflets of plasma membrane (Staneva et al., 2011; Stefanova et al., 2009). Because of this asymmetric distribution, differences in the fluidity of the outer and the inner plasma membrane monolayers



were less pronounced in 3D than 2D cells. How caveolin and phosphocaveolin regulate membrane properties of cells in 3D is not known and we have tried to address that in this study.

To study this, we looked at two aspects - first, how Cav1 regulates diffusion of various membrane associated proteins and secondly, how Cav1 and pTyr-Cav1 regulate endocytosis of GM1-CTxB in cells in 3D collagen. We started the project by **standardizing embedding MEFs** (Mouse Embryonic Fibroblasts) in collagen gels, **image them live and standardizing FRAP** in these cells. The results obtained using these techniques are summarized below.

### **1. Role of pTyr14-Cav1 in regulating mobility of Cav1 in 2D v/s 3D microenvironments.**

We compared mobility by FRAP of WT-Cav1 in cells plated on 2D collagen versus those embedded in 3D collagen and the effect of pTyr-Cav1 on this mobility. We found that **mobile fractions of Y14F-Cav1 GFP (phosphodeficient version of Cav1) were lesser** as compared to WT-Cav1 GFP in cells embedded in **3D collagen and at the edge of the membrane in 2D cells**. Vesicle tracking experiments showed that the **Y14F-Cav1 vesicles move slower as compared to WT-Cav1 GFP vesicles** at the ventral surface in 2D cells. Levels of pCav1 (checked by western blotting) were comparable in 3D as compared to those in 2D. The differences between mobility of WT Cav1 and Y14F Cav1 could be because of differential association of these two proteins with the actin cytoskeleton, which needs to be tested further.

### **2. Role of Cav1 and pTyr14-Cav1 in regulating mobility of various membrane associated proteins - in 2D v/s 3d microenvironments.**

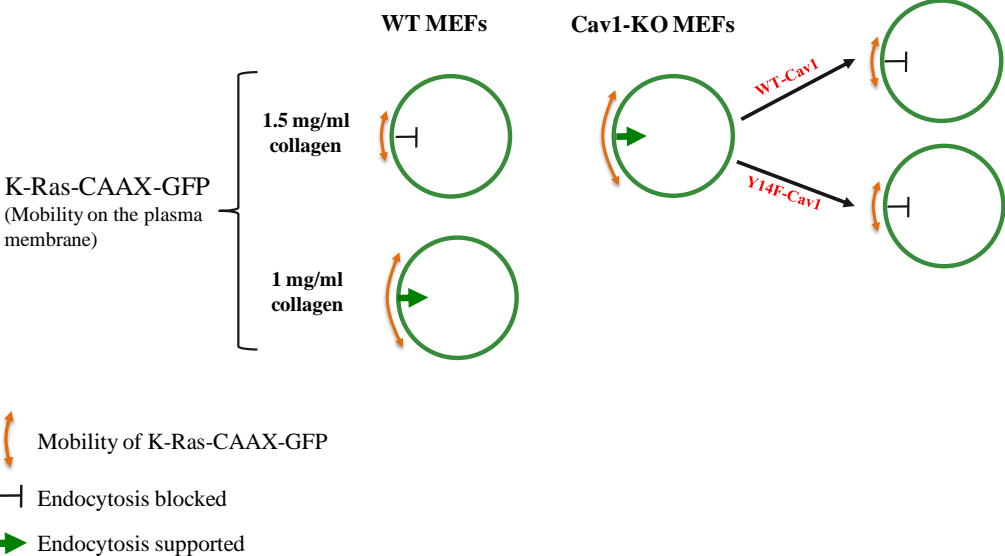
We compared mobility of various markers (**K-Ras-CAAX-GFP, H-Ras-CAAX-GFP and GPI-GFP**) in WT Cav1-KO MEFs in 2D and 3D by performing FRAP and deriving diffusion coefficient values from the FRAP data. Two of these markers K-Ras-CAAX-GFP, H-Ras-CAAX-GFP localize to the **inner leaflet** of plasma membrane and GPI-GFP localizes to the **outer leaflet**. In 2D, we performed FRAP experiments at two different planes of cells - **lower plane** which is in contact with the coverslip (collagen coated) and **upper plane**, which is not in

contact with the coverslip. There are inherent differences between these two planes like number of active integrins, adhesions formed with the substrate and tension on the membrane. Hence we decided to compare mobility at these two planes. We found that **mobility of all the three constructs was differentially regulated by Cav1 in 2D versus 3D**. Mobility of **K-Ras-CAAX-GFP** on the plasma membrane by FRAP was found to be **reduced in WT MEFs as compared to Cav1-KO MEFs**. Interestingly, reconstitution of Cav1-KO MEFs with WTCav1 or Y14F-Cav1 both reduced this mobility, **suggesting pTyr14-Cav1 not being involved** in regulating the mobility. H-Ras-CAAX-GFP and GPI-GFP did not have any difference in their mobility in WT MEFs versus Cav1-KO MEFs in 3D collagen. This altered mobility of K-Ras-CAAX-GFP could be because of altered plasma membrane properties (like fluidity or tension) of WT MEFs versus Cav1-KO MEFs. As a functional readout, we looked at mobility of a transmembrane marker, EGFR-GFP and found that to be also increased in Cav1-KO MEFs as compared to WT MEFs in 3D collagen.

### **3. Role of Cav1 and pTyr14-Cav1 in regulating endocytosis in cells embedded in 3D collagen gels.**

Endocytosis of **GM1-CTxB, transferrin and DQ-BSA** was studied in WT MEFs embedded in collagen gels of **different concentrations**. Transferrin and DQ-BSA were internalized by WT MEFs at all concentrations of collagen gels. However, we saw in **interesting concentration dependent phenomenon in GM1-CTxB endocytosis**. At concentrations 1.5 mg/ml and above, GM1-CTxB endocytosis was blocked. However, at lower collagen concentrations (0.5 mg/ml and 1 mg/ml) the endocytosis was supported. **Cav1-KO MEFs did not show such differential uptake** of GM1-CTxB at different collagen concentrations. Also, the mobility of K-Ras-CAAX-GFP was higher in WT MEFs embedded in 1 mg/ml than in 1.5 mg/ml collagen. Reconstitution of Cav1-KO MEFs with WT-Cav1 or Y14F-Cav1 both blocked the endocytosis at 1.5 mg/ml, again suggesting pTyr14-Cav1 not being involved in regulating GM1-CTxB endocytosis in 3D. Upon disruption of actin, GM1-CTxB endocytosis was triggered and also the mobility of K-Ras-CAAX-GFP was increased in WT MEFs at 1.5 mg/ml collagen.

We found that the two phenotypes - mobility of K-Ras-CAAX-GFP and endocytosis of GM1-CTxB correlate with each other. This is summarized in the following schematic :



## **References**

- Ariotti, N., Fernandez-Rojo, M.A., Zhou, Y., Hill, M.M., Rodkey, T.L., Inder, K.L., Tanner, L.B., Wenk, M.R., Hancock, J.F., and Parton, R.G. (2014). Caveolae regulate the nanoscale organization of the plasma membrane to remotely control Ras signaling. *J Cell Biol* 204, 777-792.
- Baker, B.M., and Chen, C.S. (2012). Deconstructing the third dimension: how 3D culture microenvironments alter cellular cues. *J Cell Sci* 125, 3015-3024.
- Collins, B.M., Davis, M.J., Hancock, J.F., and Parton, R.G. (2012). Structure-based reassessment of the caveolin signaling model: do caveolae regulate signaling through caveolin-protein interactions? *Dev Cell* 23, 11-20.
- Couet, J., Sargiacomo, M., and Lisanti, M.P. (1997). Interaction of a receptor tyrosine kinase, EGF-R, with caveolins. Caveolin binding negatively regulates tyrosine and serine/threonine kinase activities. *J Biol Chem* 272, 30429-30438.
- Cukierman, E., Pankov, R., Stevens, D.R., and Yamada, K.M. (2001). Taking cell-matrix adhesions to the third dimension. *Science* 294, 1708-1712.
- del Pozo, M.A., Balasubramanian, N., Alderson, N.B., Kiosses, W.B., Grande-Garcia, A., Anderson, R.G., and Schwartz, M.A. (2005). Phospho-caveolin-1 mediates integrin-regulated membrane domain internalization. *Nat Cell Biol* 7, 901-908.
- Fra, A.M., Williamson, E., Simons, K., and Parton, R.G. (1995). De novo formation of caveolae in lymphocytes by expression of VIP21-caveolin. *Proc Natl Acad Sci U S A* 92, 8655-8659.
- Gaus, K., Le Lay, S., Balasubramanian, N., and Schwartz, M.A. (2006). Integrin-mediated adhesion regulates membrane order. *J Cell Biol* 174, 725-734.
- Glenney, J.R., Jr., and Soppet, D. (1992). Sequence and expression of caveolin, a protein component of caveolae plasma membrane domains phosphorylated on tyrosine in Rous sarcoma virus-transformed fibroblasts. *Proc Natl Acad Sci U S A* 89, 10517-10521.
- Grande-Garcia, A., Echarri, A., de Rooij, J., Alderson, N.B., Waterman-Storer, C.M., Valdivielso, J.M., and del Pozo, M.A. (2007). Caveolin-1 regulates cell polarization and directional migration through Src kinase and Rho GTPases. *J Cell Biol* 177, 683-694.
- Hayer, A., Stoeber, M., Bissig, C., and Helenius, A. (2010). Biogenesis of caveolae: stepwise assembly of large caveolin and cavin complexes. *Traffic* 11, 361-382.
- Joshi, B., Bastiani, M., Strugnelli, S.S., Boscher, C., Parton, R.G., and Nabi, I.R. (2012). Phosphocaveolin-1 is a mechanotransducer that induces caveola biogenesis via Egr1 transcriptional regulation. *J Cell Biol* 199, 425-435.

- Joshi, B., Strugnell, S.S., Goetz, J.G., Kojic, L.D., Cox, M.E., Griffith, O.L., Chan, S.K., Jones, S.J., Leung, S.P., Masoudi, H., *et al.* (2008). Phosphorylated caveolin-1 regulates Rho/ROCK-dependent focal adhesion dynamics and tumor cell migration and invasion. *Cancer Res* 68, 8210-8220.
- Okamoto, T., Schlegel, A., Scherer, P.E., and Lisanti, M.P. (1998). Caveolins, a family of scaffolding proteins for organizing "preassembled signaling complexes" at the plasma membrane. *J Biol Chem* 273, 5419-5422.
- Palade, G.E. (1953). Fine structure of blood capillaries. *J Appl Phys* 24, 1424-1436.
- Parton, R.G., and del Pozo, M.A. (2013). Caveolae as plasma membrane sensors, protectors and organizers. *Nat Rev Mol Cell Biol* 14, 98-112.
- Parton, R.G., and Simons, K. (2007). The multiple faces of caveolae. *Nat Rev Mol Cell Biol* 8, 185-194.
- Rothberg, K.G., Heuser, J.E., Donzell, W.C., Ying, Y.S., Glenney, J.R., and Anderson, R.G. (1992). Caveolin, a protein component of caveolae membrane coats. *Cell* 68, 673-682.
- Sanguinetti, A.R., Cao, H., and Corley Mastick, C. (2003). Fyn is required for oxidative- and hyperosmotic-stress-induced tyrosine phosphorylation of caveolin-1. *Biochem J* 376, 159-168.
- Sanguinetti, A.R., and Mastick, C.C. (2003). c-Abl is required for oxidative stress-induced phosphorylation of caveolin-1 on tyrosine 14. *Cell Signal* 15, 289-298.
- Staneva, G., Lupanova, T., Chachaty, C., Petkova, D., Koumanov, K., Pankov, R., and Momchilova, A. (2011). Structural organization of plasma membrane lipids isolated from cells cultured as a monolayer and in tissue-like conditions. *J Colloid Interface Sci* 359, 202-209.
- Stefanova, N., Staneva, G., Petkova, D., Lupanova, T., Pankov, R., and Momchilova, A. (2009). Cell culturing in a three-dimensional matrix affects the localization and properties of plasma membrane cholesterol. *Cell Biol Int* 33, 1079-1086.
- Yamada, E. (1955). The fine structures of the gall bladder epithelium of the mouse. *J Biophys Biochem Cytol* 1, 445-458.

## CHAPTER 1

### Review of literature and objectives

## **1.1 Caveolae**

Eukaryotic cell membranes are organized into domains of distinct function and this is a characteristic feature of them. Caveolae are one such type of specialized microdomains found in most mammalian cell types. Caveolae are different from rest of the plasma membrane biochemically, as they are rich in cholesterol and sphingolipids. They have a characteristic omega shape and their size ranges from 60-80 nm.

Caveolae were first observed by electron microscope back in 1953 by G. E. Palade who called them "plasmalemmal vesicles". Later in 1955 they were named as "caveola intracellularis" by E. Yamada, because of their typical "cave-like shape". Caveolae are abundant in endothelial cells, fibroblast, adipocytes and muscle cells (Palade, 1953; Yamada, 1955). These are present as single invaginations or can also form complex rosette like structures which contain multiple caveolae. Caveolae are present on all over the plasma membrane but are known to polarize in migrating cells, where these are highly concentrated at the rear of the cell (Hill et al., 2008; Hill et al., 2012; Howes et al., 2010; Parat et al., 2003).

After the discovery of caveolae, initially these were often confused with "lipid rafts". According to the consensus definition of lipid rafts which is accepted by the field, these are highly dynamic microdomains present on the plasma membrane which are also rich in cholesterol and sphingolipids (like caveolae). Even though both these structures are similar in their composition, caveolae are still distinct because they have a fixed structure and shape. Other difference is that caveolae are generally quite static structures whereas lipid rafts are fairly dynamic. Size of lipid rafts ranges from approximately 10 nm to 200 nm. Small raft domains can fuse with each other to form bigger domains and stabilize to form signaling platforms in cells (Simons and Sampaio, 2011).

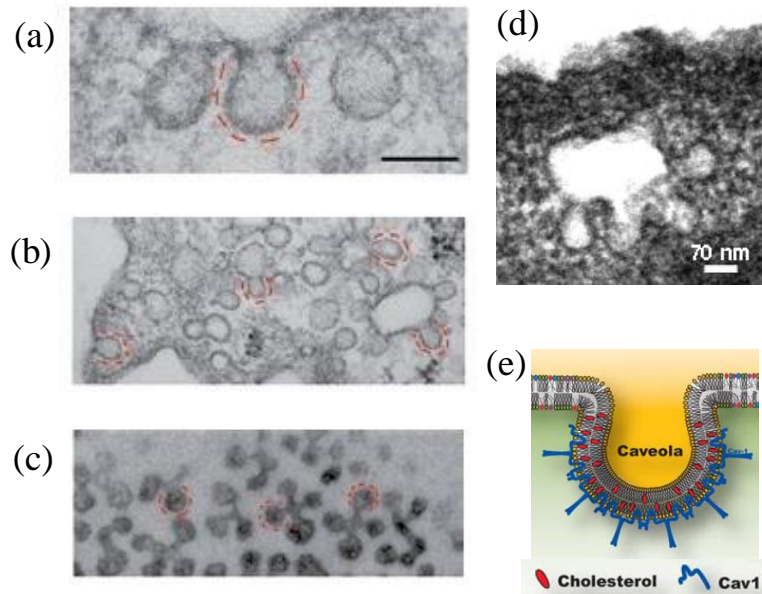


**Fig 1.1 : Structure of caveolae.** Electron micrographs showing the ultrastructure of caveolae in (a) fibroblasts (b) adipocytes and (c) skeletal muscle. Rosette-like structures are shown in (d) in Hela cells. (e) Shows organization of single caveola on the plasma membrane. Figure adapted from (Goetz et al., 2008; Parton and del Pozo, 2013; Rothberg et al., 1992).

### **1.1.1 Structural proteins of caveolae - Caveolins and Cavins**

Caveolin and Cavin are the two most important protein families which are the structural components of caveolae. There are three Caveolin (Cav) proteins - Cav1, Cav2 and Cav3 identified till date. Out of these three, Cav1 and Cav2 are expressed in all cell types, and Cav3 is specific to skeletal muscle cells (Wary et al., 1998). Caveolins were the first structural proteins identified (Glenney and Soppet, 1992; Rothberg et al., 1992). These are transmembrane proteins which have a transmembrane domain in the middle and both N and C termini face the cytoplasm. Genetic ablation of Cav1 results in loss of caveolae and re-expression of Cav1 in cells lacking endogenous Cav1 is enough to form caveolae in those cells (Fra et al., 1995).

Cavin family of proteins contain four proteins, Cavin1 or PTRF (polymerase I and transcript release factor), Cavin2 or SDPR (serum deprivation protein response), Cavin3 or SBRC (SDR-



related gene product that binds to c-kinase) and Cavin4 or MURC (muscle-restricted coiled-coil protein) (Briand et al., 2011) Amongst the four cavin proteins, cavin1, 2 and 3 are expressed in all cell types but cavin4 is muscle specific. Like Cav1, the knockdown of cavin1 also results in loss of caveolae and lysosomal degradation of Cav1 (Hill et al., 2008).

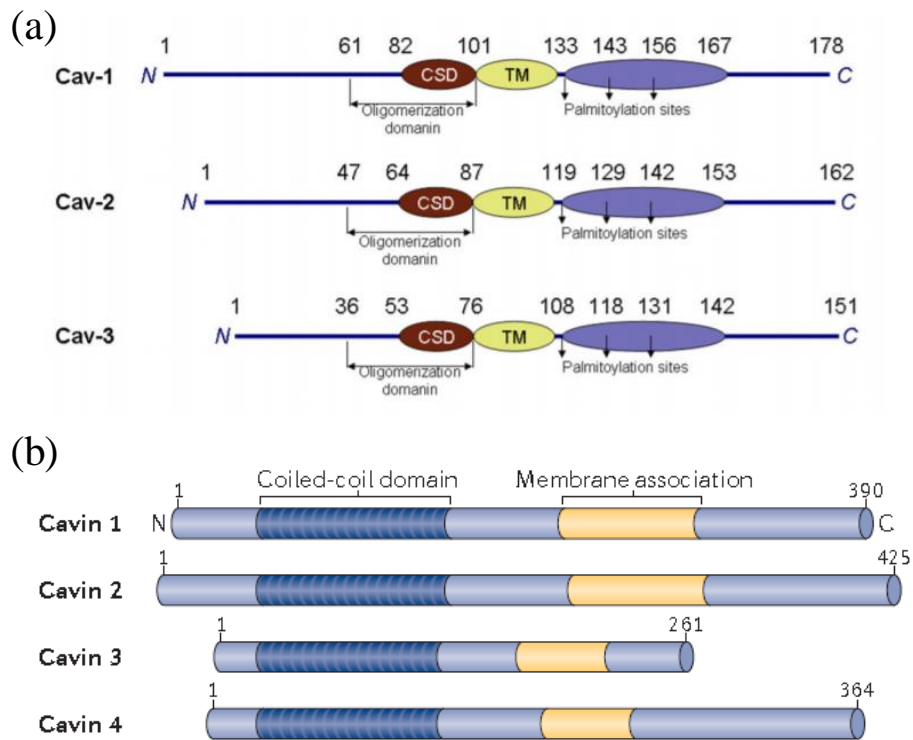


**Fig 1.2 : Schematic representation of caveolin and cavin protein families.** Caveolin proteins (a) have two common domains, CSD (Caveolin Scaffolding Domain) and TM (Transmembrane domain) whereas cavin proteins (b) have coiled-coil domain and membrane association domains in common. Fig adapted from (Norica Branza-Nichita et al., 2012; Parton and del Pozo, 2013).

### 1.1.2 The major structural protein - Cav1

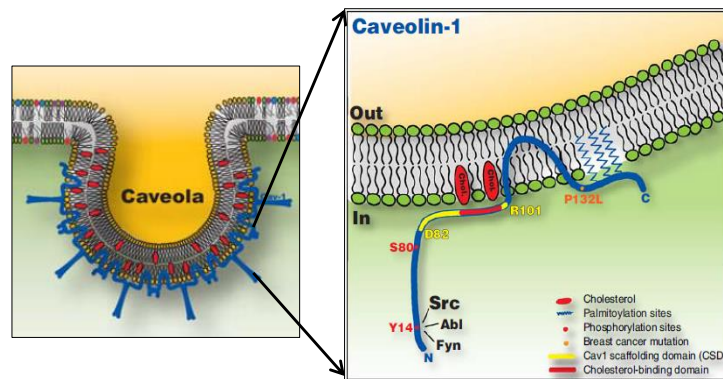


**Fig 1.3 : Detail schematic of Cav1 protein.** Cav1 is a transmembrane protein with both N and C termini exposed inside the cytoplasm. Different post-translational modifications are indicated in the right panel. Fig adapted from (Goetz et al., 2008).

After the first observation of caveolae in cells, the structural protein Cav1 was identified after almost 40 years. Cav1, also called as VIP21 (Vesicular integral membrane protein) was identified as a substrate for Src kinase (Glenney, 1989). Although it is primarily a membrane protein, there are studies describing cytosolic and secreted pools too (Liu et al., 1999). Cav1 is a 21KD protein which contains 1) oligomerization domain (aa 61 to 101), responsible for forming oligomers with either Cav1 or Cav2 (Scherer et al., 1997), 2) the hydrophobic transmembrane domain (aa 102 to 134) which exhibits a helix-break-helix structure (Lee and Glover, 2012) and 3) Caveolin scaffolding domain or CSD (aa 81 to 101) which has been implicated in interaction of Cav1 with various signaling molecules. In cells, two isoforms of Cav1 are expressed, viz. Cav1- $\alpha$  (expresses all 178 amino acids) and Cav1- $\beta$  (lacks first 31 amino acids). Both isoforms are translated from same mRNA transcript but Cav1- $\beta$  is expressed from a internal start codon (Scherer et al., 1995). The functional relevance of these two isoforms has not been studied yet in detail.

Cav1 has various known post-translational modifications including palmitoylation (amino acid 133, 143 and 156) and phosphorylation (tyrosine 14 and serine 80). The palmitoylations are required to stabilize caveolin oligomers but not required for the membrane localization of

caveolin (Dietzen et al., 1995). Serine 80 phosphorylation is suggested to have a role in Cav1 and cholesterol binding (Fielding et al., 2004). Tyrosine 14 phosphorylation is discussed in detail further in this chapter (section 1.2.1).

Cav1 is expressed in other metazoan as well, including zebrafish, *C. elegans*, and *Apismellifera*. It is however absent in *Drosophila melanogaster*. The mammalian ortholog of Cav1 in zebrafish causes embryonic lethality (Fang et al., 2006). *C. elegans* Cav1 does not form caveolae in both the animal itself or when expressed in mammalian cells. On the other hand, Cav1 *Apismellifera* when expressed in mammalian cells induces formation of caveolae (Kirkham et al., 2008). These studies indicate the fact that Cav1 may have other roles than just formation of caveolar structures, but more studies are required to completely understand role and regulation of non-mammalian caveolins.

### **1.1.3 Biogenesis of caveolae**

Assembly of caveolae starts with SRP dependent, co-translational insertion of Cav1 into the membrane of ER (Monier et al., 1995). Following this, there is homo-oligomerization of Cav1 where 150-200 KDa primary oligomers (also known as 8S complexes) are formed consisting of 7-10 monomers (Scheiffele et al., 1998). These primary oligomers get concentrated at ER exit site by virtue of "DXE" sequence in the N-terminal region and are further transported to the Golgi in a COPII dependent manner Cav1 complexes increase in size during transport through Golgi, lose their diffusional mobility, get associated with cholesterol and eventually become 70S complexes. These newly synthesized Cav1 scaffolds further undergo transport to the plasma membrane in the form of vesicular carriers. Independently, cavin is recruited to the plasma membrane as 60S complexes. Cavin complexes then get associated with Cav1 scaffolds and form caveolae on the plasma membrane (Hayer et al., 2010a).

Cavin-1 oligomerization in the cytoplasm starts with trimerisation through HR1 domain. These oligomers can bind negatively charged membranes and are stabilized only in presence of caveolins (Kovtun et al., 2015). Caveolin scaffolds are known to co-localize with PIP2 (Simone

et al., 2013) and phosphatidyl serine (Fairn et al., 2011) and this subsequent recruitment of cavin oligomers can further increase local concentration of negatively charged lipids which leads to membrane curvature. PACSIN-2 or syndapin-2, a F-BAR domain containing protein is also implicated in caveolae biogenesis. PACSIN-2 co-localizes with Cav1 on the plasma membrane and loss of PACSIN-2 results in loss of caveolar morphology (Hansen et al., 2011). Other member of the cavin family, cavin-2 has also been linked to generation of caveolar membrane curvature (Hansen et al., 2009).

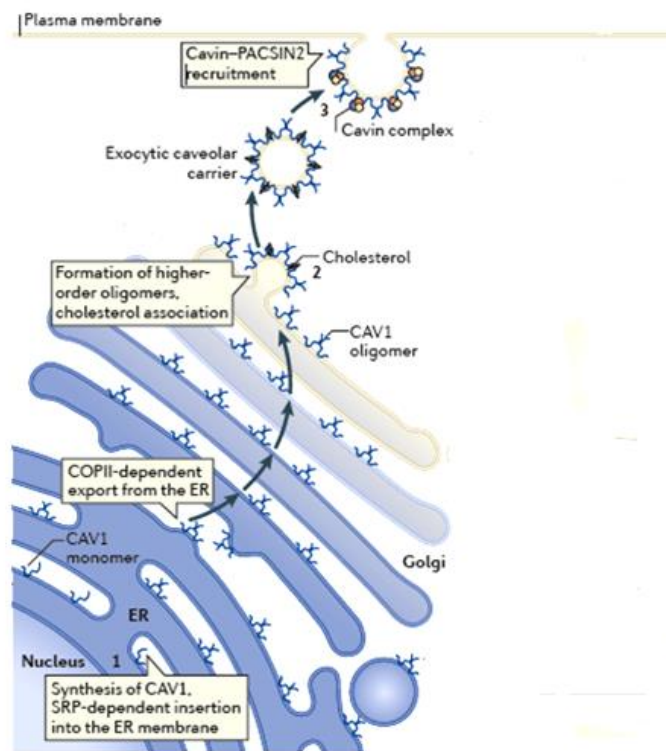


**Fig 1.4 Biogenesis of caveolae.** Schematic showing synthesis and exit of Cav1 from ER to Golgi and further to plasma membrane. COPII dependent oligomerization, cholesterol association and recruitment of accessory proteins like cavin and PACSIN2 are some of the major steps in this process. Figure adapted from (Parton and del Pozo, 2013).

We still do not completely understand all aspects of caveolae formation process and the role of accessory proteins in this. One such important study which re-emphasized this was conducted in

bacteria. It was shown that expression of mammalian Cav1 in *E. Coli* results in formation of caveolae-like structures in the bacteria. These structures were similar in size, curvature to what is seen in mammalian cells (Walser et al., 2012). As only Cav1 was enough to make caveolae in such a simple membrane system, it indicates to the fact that role of membrane composition and accessory proteins in caveolae formation needs to be studied in detail. As explained earlier, in many cell types (eg. adipocytes), formation of caveolae further continues and generates rosette-like structures or higher order structures of caveolae. The mechanism behind the formation of such structures is not completely understood. Role of cavin proteins or other curvature sensing proteins in this context is still not explored as well.

## **1.2 Regulation of caveolar trafficking and function**

The density of caveolae on plasma membrane at a given point has impact on downstream functions of caveolae in cells. Identifying and understanding the regulators of caveolar trafficking and functions will provide information about role of caveolae in diseases like muscular dystrophy and cancer. Some of the key regulators are discussed below.

### **1.2.1 Role of pTyr-14 Cav1**

Phosphorylation at 14<sup>th</sup> tyrosine residue is one of the important post translational modification of Cav1. Cav1 was in fact first identified as a substrate for Src kinase (Glenney, 1989) and later shown to be phosphorylated by other kinases such as c-Abl and Fyn (Sanguinetti et al., 2003; Sanguinetti and Mastick, 2003). This phosphorylation is stimulated in response to biochemical as well as mechanical cues like growth factor treatment, osmotic stress, shear stress, etc (Kim et al., 2000; Volonte et al., 2001). It has also been shown to be involved in focal adhesion dynamics and tumor cell migration and invasion (Joshi et al., 2008). Cav1 regulates cell migration by controlling activities of small GTPases like RhoA, Rac and Cdc42 (Grande-Garcia et al., 2007). Cav1 negatively regulates RhoA activity by controlling plasma membrane localization of a GAP for Rho, p190RhoGAP. In Cav1-KO cells, RhoA activation is higher and with re-expression of

WT-Cav1, it reverses to the levels present in WT cells. However a phosphodeficient variant of Cav1, Y14F-Cav1 was not able to rescue this phenotype.

Similarly, this phosphorylation is required during endocytosis of CEMM (Cholesterol Enriched Membrane Microdomains) markers (particularly CTxB) upon loss of integrin mediated adhesion. Rescue of Cav1-KO MEFs with Y14F-Cav1 was not able to endocytose CTxB while WT-Cav1 did endocytose (del Pozo et al., 2005). Other function regulated by caveolae which is discussed earlier is membrane fluidity. Authors have shown that Cav1-KO MEFs (mouse embryonic fibroblasts) have higher fluid fraction than WT-MEFs. Further, they show that rescue with WT-Cav1 restores the membrane order in Cav1-KO MEFs but Y14F-Cav1 cannot (Gaus et al., 2006). Interestingly, this phosphorylation has also been shown to have mechanosensory function in cells. During prolonged cycles of membrane stretch leads to pTyr14-Cav1 and this further regulates transcription of Cav1 and Cavin1 via a transcription factor early growth response protein1 (EGR1) (Joshi et al., 2012). This positive feedback loop could help the cells cope with membrane stress by increase in caveola biogenesis.

Another known phosphorylation on Cav1 is at the residue Serine80 which is required for its retention in the endoplasmic reticulum and further entry into the regulated secretory pathway (Schlegel et al., 2001). Like pTyr14-Cav1, Cav2 is phosphorylated on 19<sup>th</sup> tyrosine residue by Src kinase. This phosphorylation primarily acts as a signal for dissociation from Cav1 oligomers (Lee et al., 2002).

### **1.2.2 Role of integrins**

Formation and function of caveolae both are closely linked to integrins, which are the primary sensors of the ECM.  $\beta$ 1 integrin, along with gangliosides was shown to regulate caveola formation (Singh et al., 2010). Integrins also regulate internalization of CEMM domains which happens majorly through caveolar route. Integrin mediated caveolar trafficking further regulates cell migration by controlling targeting of a small GTPase Rac1 to the plasma membrane (del Pozo et al., 2004). Absence of Cav1 leads to deregulation of this process and helps the cells to acquire anchorage independence.

In turn, caveolae also regulate integrin dependent signaling and trafficking. Some integrins are known to be the cargo molecules internalized via caveolar route (discussed in section 1.3.2). In another study, it was shown that caveolae dependent internalization of  $\beta 1$  integrin in mesenchymal stem cells is required for their differentiation to neuronal cells when cells are plated on soft matrices (Du et al., 2011).

Integrins and caveolar trafficking are correlated in another important process, mitosis. Caveolae get redistributed during mitosis (Boucrot et al., 2011) which regulates cyclin-D activation downstream of Rac1. Activation of cyclin-D is an important checkpoint for entering into G1 phase of cell cycle (Cerezo et al., 2009).

### **1.2.3 Role of cytoskeleton**

All the cytoskeletal components, actin filaments (Kanzaki and Pessin, 2002; Rothberg et al., 1992), microtubules (Wickstrom et al., 2010) and intermediate filaments (Nixon et al., 2007) have been shown to be associated with caveolae. These studies were done using electron microscopy - both two and three dimensional. There are a few functional studies done in this context, however, there aren't as comprehensive as those with clathrin-mediated endocytosis and trafficking. These studies indicate to the fact that actin is one of the key regulator of caveolar endocytosis (Mundy et al., 2002; Parton, 1994).

Filamin-A is the protein which is an important link between actin and caveolae. Filamin-A directly binds Cav1 (Ravid et al., 2008; Stahlhut and van Deurs, 2000) and this protein has also been implicated in trafficking of various cargos, for example opioid receptor (Onoprishvili et al., 2003), calcitonin receptor (Seck et al., 2003) and albumin transcytosis across endothelium (Sverdlov et al., 2009). Serine phosphorylation on Filamin-A is reported to be crucial for its role in regulating caveolar trafficking upon loss of adhesion. Filamin-A depletion makes caveolae unstable and increases their dynamics (Muriel et al., 2011; Stahlhut and van Deurs, 2000).

The abundance of stress fibers dictates plasticity of caveolar domains at the plasma membrane and are essential for their internalization upon loss of integrin mediated adhesion. mDIA-1 (a protein from formin family) and a tyrosine kinase Abl together polymerize actin into stress fibers

and organize a pool of caveolae linked to them. In the absence of any one of these protein, actin undergoes depolymerization and this affects localization of caveolar domains on plasma membrane (they form clusters on the membrane) and subsequent internalization in the cell. On the other hand, over expression of active mDIA-1 causes excess actin polymerization leading to flattening of caveolae (Echarri et al., 2012). The other major pathway of actin polymerization, which depends on Arp2/3 complex, however is not crucial for caveolae-actin linkage.

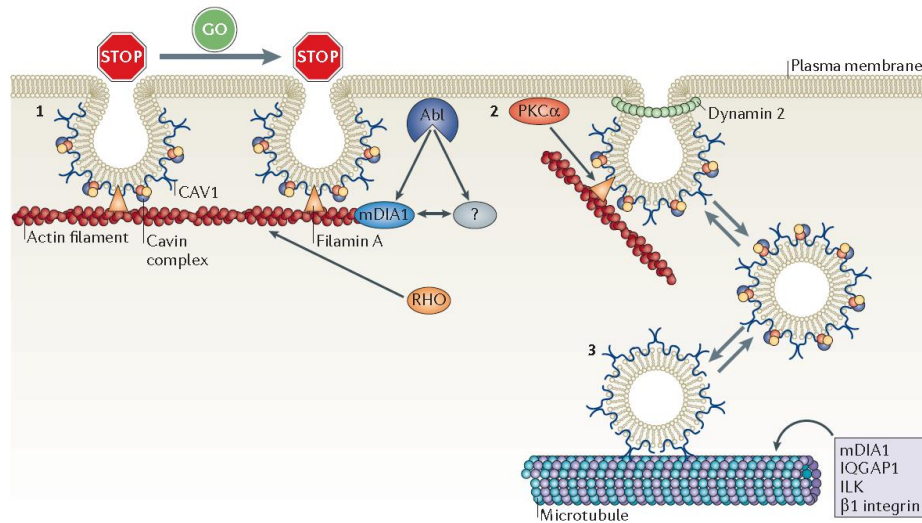


**Fig 1.5 Caveolae and cytoskeleton.** Schematic showing dynamics of caveolae regulated by actin and microtubules. Filamin A, mDIA1 and Rho mediate interaction of caveolae with actin and ILK, mDIA1, IQGAP regulate interaction with microtubules. Figure adapted from (Parton and del Pozo, 2013).

In keratinocytes, knockdown of  $\beta 1$  integrins or ILK (integrin linked kinase) leads to loss of caveolae (Wickstrom et al., 2010). These two are essential for stabilization of microtubules via recruitment of IQGAP (IQ motif containing GTPase-activating protein-1) to the cell cortex. At the cortex, it interacts with mDIA-1 and leads to stabilization of microtubules. Trafficking of caveolae from the plasma membrane to inside and also back to plasma membrane both depend on intact microtubular network. This strong linkage of caveolae with the cytoskeleton could be the mediator in mechanotransduction via caveolae.



## **1.3 Functions of caveolae and caveolin-1**

Because of the structural resemblance between clathrin-coated pits and caveolae, initially caveolae were thought to be an important player in the process of endocytosis. However, later many other functions have been attributed to them including cellular signaling, transcytosis, regulation of lipids, mechanotransduction, and regulation of membrane properties.

### **1.3.1 Caveolae, Cav1 and cellular signaling**

Caveolae and Cav1 have been implicated in cell signaling since many years. The earlier hypothesis was, Cav1 recruits and regulates many signaling molecules and controls signaling downstream either positively or negatively. This interaction happens via Caveolin Scaffolding Domain (CSD) in Cav1 (amino acids 81-101) which interacts with a hydrophobic patch  $\Psi X \Psi X X X X \Psi$  in signaling molecules - known as Caveolin Bonding Motif (CBM) (Couet et al., 1997a; Okamoto et al., 1998). One such extensively studied signaling molecule is eNOS, which is negatively regulated by CSD-CBM interaction (Garcia-Cardena et al., 1997). Many other signaling molecules and receptor tyrosine kinases are known to be regulated by this interaction and these are summarized in following table (table 1.1).

Majority of these earlier studies which validated the CSD-CBM interaction hypothesis were done using a isolated CSD peptide. However, recently, a detail structure-based analysis showed that, CBD, being highly hydrophobic in nature, is deeply buried inside the protein (all signaling proteins) and hence direct physical interaction between Cav1 and signaling molecules containing CBD is being questioned (Collins et al., 2012). There is an alternative hypothesis in the field now which claims that caveolae control cellular signaling by altering membrane organization and composition which is described in detail in section 1.3.4.

Signaling proteins	Regulation by Cav1 (Positive / Negative)	References
Akt	Positive	(Zhuang et al., 2002)
Erk1/2	Negative	(Engelman et al., 1998a) (Galbiati et al., 1998)
NO synthase	Negative	(Venema et al., 1997) (Ju et al., 1997)
	Positive	(Isshiki et al., 2002) (Parat et al., 2003)
Csk	Positive	(Cao et al., 2001)
Grb2	Positive	(Biedi et al., 2003)
Phospholipase C	Positive	(Jang et al., 2001)
Phospholipase D	Positive	(Czarny et al., 2000)
	Negative	(Kim et al., 1999)
Protein kinase A	Negative	(Razani and Lisanti, 2001)
Protein kinase C	Positive	(Waschke et al., 2006)
	Negative	(Prevostel et al., 2000)
Receptor tyrosine kinases	Role of Cav1	References
Transforming growth factor (TGF) beta receptor	Negative	(Razani et al., 2001)
Insulin receptor	Positive	(Yamamoto et al., 1998)
Epidermal growth factor (EGF) receptor	Negative	(Lajoie et al., 2007) (Couet et al., 1997b)
	Positive	(Agelaki et al., 2009) (Zhang et al., 2007)
Neural growth factor (NGF) receptor	Negative	(Bilderback et al., 1999) (Bilderback et al., 1997)

**Table 1.1 : Signaling proteins regulated by Cav1 and caveolae**

Cav1 can independently contribute to certain signaling pathways in cells outside caveolae as well. One such example is regulation of small GTPases like Rho, Rac and Cdc42 which are involved in directional cell migration. Cav1-KO MEFs have altered profile of activation of these

three GTPases and hence spread and migrate differently as compared to WT MEFs (Grande-Garcia et al., 2007).

### **1.3.2 Caveolar endocytosis and transcytosis**

Internalization of few cargos has been reported to happen through the caveolar route, for example CTxB (Cholera Toxin B subunit), shiga toxin, GPI linked proteins, BSA, SV40 virus and some bacteria, IL2 receptors, etc (Johannes and Lamaze, 2002; Nichols and Lippincott-Schwartz, 2001; Pelkmans and Helenius, 2002). Caveolar endocytosis was identified as a dynamin dependent process (Henley et al., 1998) and the internalized cargo molecules were shown to reside in a novel endosomal compartment called "caveosomes" (Nichols, 2003). This compartment had neutral pH and did not accumulate lysosomal dye or fluid phase markers or ligands of clathrin pathway and hence was distinguished as unique and distinct from existing endocytic compartment. However, few years later, the same group who had identified and named this compartment raised the concern about how extent of over expression of exogenous Cav1 can affect interpretations of caveolar endocytosis and trafficking (Hayer et al., 2010b). Importantly, they found no evidence for existence of "caveosomes" and proposed that the term should be discontinued. They identified this as late endosomal compartment or multivesicular bodies (MVBs). Clearly, more work is required to completely understand the exact path taken by cargos which are internalized via caveolae. One more issue in studying caveolar endocytosis has been the lack of specific markers. For example, SV40 virus, which was earlier considered to be endocytosed only via caveolar route was later shown to be endocytosed through caveolin independent pathways too (Damm et al., 2005).

Unlike endocytosis, the model for transcytosis in endothelial cells is well established for many years. Transcytosis of albumin in pulmonary endothelial cells has been shown to majorly occur through caveolae (with a little fraction via caveolin independent pathways) (Oh et al., 2007). In endothelial cells, caveolae have been proposed to bud from the surface which faces bloodstream (luminal surface) and fuse with albuminal surface hence mediating efficient transport from the blood to underlying tissues.

Contribution of caveolar endocytosis in regulating signaling also has been reported in literature. Caveolar trafficking results into endocytosis or exocytosis of certain proteins or receptors which modulate their surface levels in a cell. This further results in regulating downstream signaling via that particular protein. One such important example has been endocytosis of components of ordered domains of the plasma membrane which down regulates Akt and Erk signaling pathways during detachment of cells from ECM (del Pozo et al., 2005). Other components which are reported include certain growth factor receptors, components of adherens junctions and integrins ( $\beta 1$ ). Regulation of  $\beta 1$  integrin endocytosis can be both positively (Shi and Sottile, 2008; Upla et al., 2004) or negatively (Arjonen et al., 2012) regulated by caveolin. There are other factors involved too, including cell type specificity and specific cellular function which result in these differences. Caveolae can regulate exocytic trafficking of certain proteins (e.g. calcium channel TRPC1) and hence modulate signaling (Pani et al., 2009).

One interesting aspect which is recently reported is how caveolin and cavin proteins regulate clathrin independent endocytosis pathways in cells (CLIC/GEEC pathways) (Chaudhary et al., 2014). Several studies had earlier suggested this cross talk to be possible but now the molecular mechanism of how caveolar proteins negatively regulate CLIC/GEEC pathways is known. Cav1 and Cav3 were shown to inhibit CLIC/GEEC pathways upon over expression. Cavin-1 and Cavin-3 were also identified as inhibitors of CLIC/GEEC in a process independent of caveola formation.

### **1.3.3 Caveolae mediated regulation of lipids**

Cav1 directly binds free cholesterol (FC) and helps in maintaining cholesterol homeostasis in cells (Murata M et al., 1995). FC has selective affinity for sphingolipids and it condenses phospholipid acyl chains. By virtue of these properties, it modifies the properties of plasma membrane locally (K. Bloch, 1991). This Cav1 and FC interaction was hence attributed to regulation of signaling downstream in response to cues from the ECM (Fielding and Fielding, 2000). In the absence of Cav1, FC accumulates in the mitochondria and results in ROS induced cell death (Bosch et al., 2011).

Apart from cholesterol, Cav1 is also known to bind fatty acids (Brasaemle et al., 2004) and facilitate their endocytosis (Meshulam et al., 2006). In cultured cells as well as *in vivo* Cav1 localizes to lipid droplets (Pol et al., 2004). These droplets are reservoirs of triglycerides in cells which are utilized during fasting condition. Cav1 is also implicated in normal lipid homeostasis which is supported by the studies in Cav1-KO mice. These mice are insulin resistant, have smaller adipocytes, reduced fat mass and are resistant to diet induced obesity as well (Razani et al., 2002) . They have low levels of adiponectin hormone which regulated lipid and hydrocarbon metabolism (Asterholm et al., 2012). Like Cav1, Cavin-1 may also have similar effects. Cavin-1 null mice too, have reduced fat mass and are insulin resistant (Liu et al., 2008).

#### **1.3.4 Caveolae and regulation of membrane properties**

Caveolae being one of the important membrane microdomains, are shown to regulate organization of the plasma membrane and certain membrane properties. Using Laurdan dye technique it was shown that fibroblast cells which express Cav1 have higher ordered fraction (28.6%) as compared to Cav1 KO MEFs (8.1%) (Gaus et al., 2006). Changes in cholesterol levels and distribution could be one reason for this difference. In another comprehensive lipidomic analysis it was found that Cav1-KO MEFs have deregulated glycosphingolipid (GSL) and sphingolipid (SL) metabolism. It was also shown that Cav1-KO MEFs have alterations in glycerophospholipids, with a higher phosphatidylcholine (PC) / phosphatidylethanolamine (PE) ratio compared with WT-MEFs and altered phosphatidyl serine (PS) distribution. This was further reflected in differential clustering of Ras isoforms and hence signaling downstream (Ariotti et al., 2014). These studies have opened up a whole new concept in the field that caveolae act as organizers of the plasma membrane which in turn affects signaling downstream. This is emerging as an exciting hypothesis in finding role of caveolae in cellular signaling.

#### **1.3.5 Caveolae and mechanotransduction**

Caveolae are abundant in muscle cells, endothelial cells, fibroblasts - all experience variety of mechanical cues *in vivo*. This encouraged to study whether and how of caveolae are involved in mechanosensing or mechanotransduction. An important property of caveolar domains which

plays protective role in response to mechanical stress is flattening of caveolae. In response to shear stress, mechanical stretch and osmotic stress, caveolae were shown to disassemble and flatten out in various cell types such as endothelial, skeletal muscle, cardiomyocytes, fibroblasts (Dulhunty and Franzini-Armstrong, 1975; Lee and Schmid-Schonbein, 1995; Sinha et al., 2011).

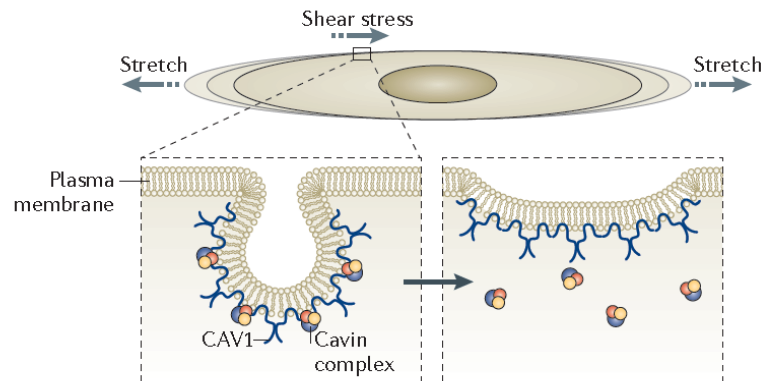


**Fig. 1.6 Caveolae disassemble in response to mechanical stress.** Shear stress or stretch causes caveolae to flatten and disassemble which results in release of cavin complex in the cytoplasm. Figure adapted from (Parton and del Pozo).

Earlier studies had reported this phenomenon using EM images however Sinha *et. al.* have explained this process in depth using improved imaging techniques like TIRF. This flattening provides buffer membrane to the cell and protects from rupturing. Caveolae were earlier shown to be acting as membrane reserves and limiting increase in membrane tension (Kozera et al., 2009). Sinha *et. al.* further confirmed that caveolae disassemble in cells as well as plasma membrane spheres and also found that this process is passive as it continues in ATP depleted cells as well. The recovery of caveolae however after the stress is released, is not passive and requires ATP (Sinha et al., 2011). Upon flattening of caveolae, Cavin complex gets dissociated from caveolar membrane and released inside the cytoplasm. Cavin-1 was first identified and characterized as a transcription factor, PTRF, and it is speculated that upon disassembly from caveolar membrane in response to stretch, PTRF enters the nucleus and alters gene expression.

In addition to this flattening phenomenon, caveolae are also involved in active signaling in response to mechanical forces. For example, in endothelial cells they can sense flow and activate Akt signaling and in muscle cells they can sense stretch and respond to it through MAPK signaling (Albinsson et al., 2008). However, whether this is dependent on caveolae disassembly is not known yet. Other components of the caveolar system, Cav-3 and Cavin1 have also been implicated in membrane release after injury (Cai et al., 2009; Zhu et al., 2011). To understand the exact molecular mechanism in caveolae mechanosensing more studies are needed, but it is interesting to note that caveolae might have a universal protective role in response to membrane stress and they minimize the damage.

### **1.3.6 Cav1 and remodeling of extracellular matrix**

The role of Cav1 in cancer progression is still unclear (Goetz et al., 2008). In majority of primary tumors Cav1 is down regulated which leads to anchorage independence, proliferation and angiogenesis however, metastatic stage is correlated with re-expression of Cav1 leading to survival, invasion and multidrug resistance (Goetz et al., 2008). Most of the studies focus on function of Cav1 in tumor cells and how that contributes to progression of the disease. However, it is equally important to look at the role of Cav1 in the stromal microenvironment. Extracellular matrix (ECM) remodeling plays an important role in tumor cell migration, invasion and tumor growth. Stromal fibroblasts or cancer associated fibroblasts (CAFs) are majorly involved in ECM secretion and remodeling. These cells express high levels of Cav1, which regulates mechanical properties of the tumor microenvironment (Goetz et al., 2011). Through regulation of Rho, Cav1 promotes actomyosin contractility in cells which leads to ECM fibrillogenesis and this stiffens the microenvironment. Higher actomyosin contractility also leads to parallel arrangement of ECM fibers which facilitates tumor cell migration. ECM remodeling is required for maintenance of proper architecture of normal organs rich in ECM, like mammary glands. Loss of Cav1 has been shown to cause disorganized ECM in mammary glands and altered ductal architecture in mice (Thompson et al., 2017). This might explain the reduced invasiveness of tumor cells injected in Cav1-KO mice.

These studies emphasize the fact that both tumor cells and tumor stroma need to be evaluated in the context of disease progression. This also partly explain the debated role of Cav1 in tumorigenesis as the pro-tumorigenic effects of Cav1 might not depend on its expression in tumor cells but in stromal cells. However whether this remodeling of ECM depends only on just caveolins or caveolae is still an open question. But this raises an interesting possibility in the context of mechanosensory role of caveolae. It can be hypothesized that flattening of caveolae in response to mechanical forces could also change cell-ECM interaction and could influence downstream pathways that alter expression and secretion of various ECM components.

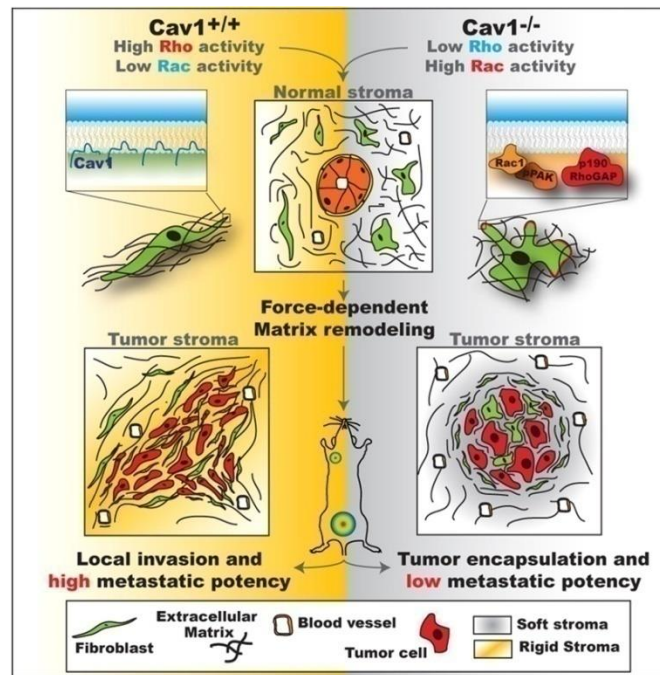


**Fig 1.7 ECM remodeling by Cav1 in tumor stroma.** Stromal fibroblasts (also called cancer associated fibroblasts) which express high levels of Cav1 have higher actomyosin contractility and hence leads to parallel alignment of ECM fibers. This facilitates migration and invasion of cancer cells (Goetz et al., 2011).

### 1.4 Extracellular matrix : 2D v.s. 3D

Extracellular matrix (ECM) proteins form the intercellular meshwork in tissues and provide structural support to cells. ECM proteins contain multiple independently folded domains which



are highly conserved across organisms. ECM however has many important consequences on cell behavior rather than just providing a structural support. The composition and mechanical properties such as stiffness of the ECM influence differentiation, polarization, migration etc. ECM composition is shown to be constantly altering during development and hence considered as a guidance clue for differentiation (Bode et al., 2003). ECM stiffness is known to affect cell behavior in many ways. Cells grown on soft substrates are often round with nascent focal adhesions as compared to cells growing on stiff matrices which spread completely and possess mature focal adhesion complexes (Choquet et al., 1997).

In past few years the importance of three-dimensional cell culture has been much appreciated among cell biologists as it is more physiological. Conventional cell culture practices involve growing cells on rigid plastic culture vessels. But *in vivo* cells grow in much different microenvironment. Growing cells on rigid substrates like plastic could greatly affect their behavior and this might not be the reflection of how cells behave *in vivo*. The concept of growing cells in a 3D matrix is not very recent. Elsdale and co-authors in 1972 had come up with the idea of growing fibroblasts in collagen-I gels, which is more physiologically relevant to these cells (Elsdale and Bard, 1972). Mina Bissell was one of the pioneers in establishing 3D cell culture for cancer cells. Her group showed that metastatic potential of breast cancer cells could be reversed by using anti-integrin antibody to block integrins (Weaver et al., 1997). This was a completely novel finding and was not possible in 2D cultures. Since then, many efforts have been taken in the field to understand how cells respond to their 3D microenvironments and how biochemical as well as biomechanical cues guide cells for various processes.

#### **1.4.1 Different matrices used for 3D cell culture**

Cell derived matrices (CDMs) are commonly used to grow normal as well as cancer cells. In this approach, fibroblasts are grown for about 8 days with ascorbic acid supplement which is required for collagen synthesis. These cells then form a thin (~20-30  $\mu\text{m}$ ) layer which is rich in fibronectin and collagen. Cells are then extracted by detergent treatment, CDMs are washed extensively and new cells are seeded on them (Beacham et al., 2002). Matrigel<sup>TM</sup> is basement membrane based gel which is also quite commonly used. Matrigel<sup>TM</sup> is composed of laminin,

collagen type IV and proteoglycans and is produced from Engelbreth-Holm-Swarm mouse sarcoma cells and forms a non-fibrous dense mesh-work gel (Kalluri, 2003). The limitation with such natural, cell derived matrices is that the composition, stiffness and uncharacterized population of growth factors might vary within batches (Hughes et al., 2010).

Another approach to grow cells in 3D is using gels made of one or more ECM component. Collagen-1 gels have been extensively used for this purpose as it is the most abundant ECM component (Grinnell, 2003). Another ECM component which is used is fibrin that is formed after cleavage of fibrinogen by active thrombin. After cleavage it forms a fibrous mesh which acts as a scaffold and promotes wound healing (Lord, 2007). Fibrin gels have mainly been used to study cell invasion and vasculogenesis (Clark et al., 2004; Zhou et al., 2008) and these gels are composed of thinner, shorter and straighter fibers as compared to collagen gels (Alavi and Stupack, 2007).

In last ten years rapid advancement has taken place in development of synthetic gels which provide greater control over physical properties as compared to natural gels (Liu et al., 2017; Lutolf and Hubbell, 2005). These synthetic gels contain cell-binding ligands and a structural backbone which are cross-linked to each other. Polyethylene glycol is the most common example of such gels and has been extensively used (Mann et al., 2001; Miller et al., 2010). Self-assembling peptides are also quite commonly used as 3D matrices for growing cells (Kisiday et al., 2002; Mata et al., 2009). Recent research in the field is focused on designing more types of synthetic materials which will be highly tunable in terms of their mechanical as well as biochemical properties.

#### **1.4.2 Behavior of cells in 3D microenvironment**

The difference in the microenvironment of cell in terms of dimensionality has been shown to affect the cell behavior drastically. Fibroblasts spread when cultured on a 2D surface and acquire forced polarity (apical-basal), but show spindle-shaped morphology which is more *in vivo* like when they are grown in collagen gels (Grinnell, 2003). Although the apical-basal polarity is relevant for some cell types, like epithelial cells, it is not natural for most mesenchymal cells.

Also, apart from morphology, certain signaling pathways in fibroblasts grown in collagen gels were found to be different (Rhee and Grinnell, 2007).

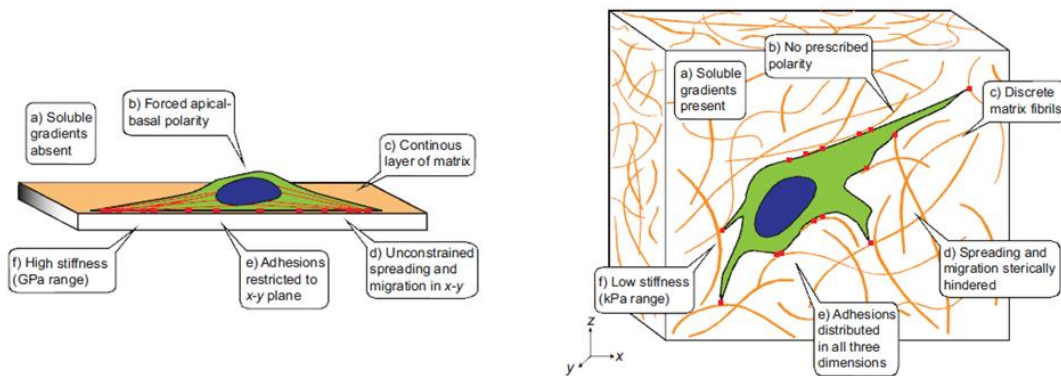


**Fig 1.8 Comparison of 2D v.s. 3D microenvironment.** Cell plated on a 2D dish (left) v.s. embedded in a 3D gel (right) and differences listed between the two different microenvironments. Figure adapted from (Baker and Chen, 2012).

Migration on 2D surfaces involves the following highly coordinated steps: extension of leading edge, formation of adhesive contact with the surface, generation of traction force and subsequent retraction of the trailing edge (Lauffenburger and Horwitz, 1996; Ridley et al., 2003). Migration in 3D matrices is much more complex and depends upon topography of the matrix, ECM degradation and steric hindrance (Doyle et al., 2009; Zaman et al., 2006). Two main modes of migration have been described in 3D: mesenchymal (which depends upon proteolytic degradation of ECM) and amoeboid (where cells move without proteolytically degrading the matrix, instead they squeeze through matrix pores and this movement is entirely dependent on actin-myosin contractility (Wolf et al., 2003). Recent studies have explained how cortical actin and focal adhesions help cells switch to amoeboid kind of mobility (Liu et al., 2015; Ruprecht et al., 2015). Another interesting study showed that one of the major mechanisms in tumor cells migrating in 3D confined microenvironments is directed water permeation (Stroka et al., 2014).

The arrangement of cytoskeleton is drastically different in 2D versus 3D. In 2D actin is seen as long bundles along the cell axis (stress fibers) but in 3D, actin bundles are majorly present on

lateral sides of the extensions produced by cells (Beningo et al., 2004). Myosin distribution and microtubule arrangement is also different in 3D (Murshid et al., 2007).

### **1.4.3 Integrins in 2D v.s. 3Dmicroenvironment**

Integrins are the heterodimeric receptors on plasma membrane which connect cells to the ECM and since in 3D the ECM (its architecture, physical properties) is different, it can be speculated that integrins will function differently in 3D matrices. Integrin activation and clustering majorly depends on their interaction with cytoskeleton, diffusion on plasma membrane and interaction with membrane lipids. All these factors are again thought to be different in a 3D microenvironment than 2D. In a theoretical model, authors compared single integrin cluster attached to either a 2D collagen film or a 3D collagen fiber and compared their lifetimes. They found the clusters to be more dynamic in 3D microenvironment which agrees with experimental results as well (Lepzelter et al., 2012).

After anchoring to the ECM, engagement of integrins leads to formation of membrane-associated protein complexes at sites called cell-matrix adhesions. These adhesion structures mature over time from focal complexes to focal adhesion to fibrillar adhesions and this maturation process requires actin-myosin contractility generated within the cell (Zamir and Geiger, 2001). Focal complexes are the nascent adhesions formed when cells just start to spread after attaching to the substrate. These are very small and very dynamic, which become stable over time and are then called focal adhesions. Finally, the most stable adhesive structures are called fibrillar adhesions which lead to the stretching of cell surface fibronectin and formation of long fibronectin fibrils.

In 3D, the number and arrangement of such adhesion structures are expected to be different as the cell is in contact with the ECM from all sides as against 2D, where only dorsal side is attached to the ECM and ventral side is not. A lot of efforts have been made to visualize adhesion structures in 3D matrices but there have been a few technical limitations to this like over expression of fluorescently tagged proteins, background fluorescence and difficulties in imaging dynamic structures in 3D and 4D. Although there exists contradicting reports regarding existence of focal adhesion like structures in 3D matrices (Fraley et al., 2010; Kubow and Horwitz, 2011), a general consensus in the field has been such adhesions do exist in 3D but are

smaller in size and are more dynamic (Doyle et al., 2015). These contradicting studies were done in cells embedded in hydrogels, however, in cells plated on cell derived matrices (CDMs), 3D adhesions are quite extensively studied (Cukierman et al., 2001b)

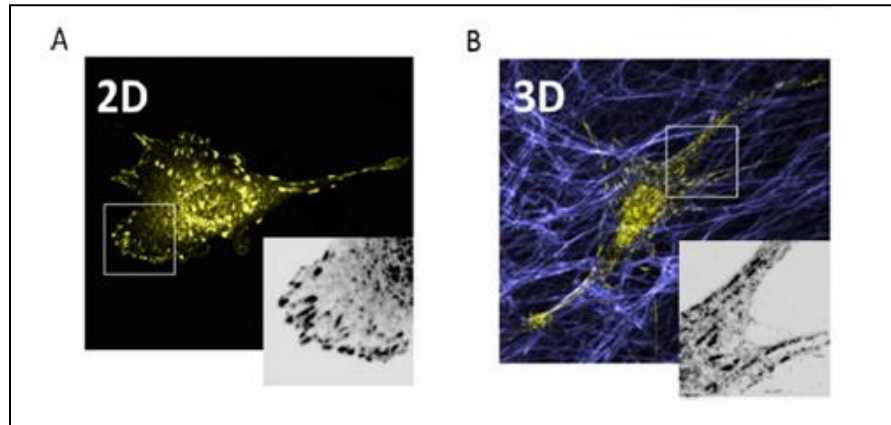


**Fig 1.9 Adhesion structures in 2D and 3D.** NIH-3T3 (mouse embryonic fibroblasts) cells expressing paxillin-GFP, plated on 2D fibronectin coated surface (A) or seeded on cell-derived matrix (B). Figure Adapted from (Jayo and Parsons, 2012).

Integrin mediated signaling is also shown to be different in 3D than 2D. FAK (focal adhesion kinase) – the important component of many integrin initiated signaling pathways shows altered phosphorylation status, in that it is almost four-fold less phosphorylated in cells growing in 3D microenvironments (Cukierman et al., 2001b). Interestingly, phosphorylation of paxillin is not affected. This suggests that FAK dependent signaling pathways could be majorly affected. Among other signaling pathways affected, MAPK/Erk activation is enhanced by about 25% (Wozniak et al., 2003).

#### **1.4.4 Plasma membrane in 2D v.s. 3D microenvironment**

The surface area of cells in 3D collagen gels is almost half as compared to that of the cells growing on 2D surfaces (Goetz et al., 2011). It can also be speculated that tension on the membrane will be different when cells are grown on 2D versus 3D because of differences in cytoskeleton; however, this has not yet been calculated experimentally.

In another study, plasma membrane composition was found to be different in fibroblasts growing in CDMs as compared to 2D culture. Particularly, cholesterol and sphingomyelin content in the membrane was more in 3D than 2D. Same study reported that the membrane cholesterol in cells growing in 3D was more susceptible to oxidation and was asymmetrically distributed among the two leaflets of plasma membrane. Because of this asymmetric distribution, differences in the fluidity of the outer and the inner plasma membrane monolayers were less pronounced in 3D than 2D cells. (Stefanova et al., 2009). It should be noted here that the cells were plated on CDMs, which are slightly different than 3D hydrogels. They are much more complex, as they contain more than one ECM protein. Also, these are quite thinner (few micrometers as against few millimeters in the case of hydrogels). CDMs have higher stiffness (Young's modulus in the range of few KPa). Hydrogels are softer as compared to CDMs, with Young's modulus in the range of few Pa. All of these factors could affect how certain processes are regulated in CDMs versus 3D hydrogels.

#### **1.4.5 Mechanotransduction in 2D v.s. 3D microenvironment**

Mechanotransduction is defined as the process of converting mechanical stimuli into biochemical signals. Eukaryotic cells exhibit a diverse array of molecules which sense and transmit mechanical cues inside cells (mechanosensors and mechanotransducers). These include integrins, cadherins, cytoskeletal components, ion-channels, etc. (Ingber, 2006). All of these components eventually transmit information regarding mechanical cues from the ECM to the nucleus via the LINC complex (linker of nucleoskeleton and cytoskeleton) (Crisp et al., 2006). This further leads to changes in gene expression by regulating nuclear architecture or certain activity of certain transcription factors.

To study mechanotransduction, the primary model which is used in the field is 2D substrates with different but uniform stiffness (uniform across the gel). Various cellular factors and processes like contact guidance, cell adhesion and migration, cellular morphology etc have been studied using such systems (Lo et al., 2000; Weiss and Garber, 1952). However, 3D ECM models provide unique properties like dimensionality which are closer to physiology. In 2D models the only factor cells respond to and differentiate is ECM stiffness, but in 3D, along with

matrix stiffness there other factors like ECM ligand density, pore size, alignment and cross-linking of ECM fibers, etc. This is certainly a complex model and recently few studies done using these have revealed important dimension and architecture dependent differences in 3D gels(Doyle and Yamada, 2016).

Another interesting factor which is specific to only 3D ECM models is gel stiffness v.s. fiber stiffness. It is observed that although individual fibers of ECM components like collagen or fibrin have stiffness in the range of MPa, the stiffness of the hydrogel can be significantly softer (even up to several orders of magnitude) (An et al., 2004; Guthold et al., 2007). The reason behind this discrepancy is that the bulk stiffness of a hydrogel majorly depends on fiber architecture than stiffness of individual fiber or strength (Lee et al., 2014; Pedersen and Swartz, 2005). Because of this, a cell can locally sense part of a matrix as soft (if generated by a fiber aligned perpendicular to the cell) or stiff (if generated by a fiber aligned perpendicular to the cell). ECM fiber alignment also correlates with size of adhesion sites in cells (Kubow et al., 2013)

Our understanding of mechanotransduction in 3D microenvironment is still very preliminary. More comprehensive studies are needed to completely understand contribution of all the parameters like ECM composition, nature of ECM fibers (linear / non-linear elasticity), phenotype of cells etc. Other than integrin mediated adhesions, other mechanotransducory pathways like ion channels, cytoskeleton are also speculated to be differentially regulated in 3D.

Like mechanosensory pathways, many complex cellular phenomenon remain to be understood in 3D. These include organization of plasma membrane, properties of plasma membrane, membrane trafficking in 3D, etc. Caveolae are one important organelles in cells which have emerged as plasma membrane organizers and protectors and how their function and regulation happens in 3D is not known.

#### **1.4.6 Caveolae in 2D v.s. 3D microenvironment**

Majority of the literature reviewed here in context of caveolar trafficking and function till now has been done using 2D microenvironment as a model system. Except a few studies which have

looked at ECM remodeling by Cav1, nothing is known about role and regulation of caveolae in a 3D microenvironment. Integrins and cytoskeleton, the primary regulators of caveolar trafficking and function, both are different in 3D (as discussed earlier) and hence it will be interesting to speculate that regulation of caveolae will also be differentially regulated in 3D. Caveolae are also emerging as mechanosensory or mechanotransducory organelles in cells and how many mechanosensory pathways are regulated (including caveolae) is not known. Considering all these factors, in this project we have explored the role of Cav1, caveolae and pTyr-14-Cav1 in a 3D microenvironment in the context of organization of plasma membrane and endocytosis.

### **1.5 Aims and objectives of current study**

In this project, we have elucidated the role of Cav1 and hence caveolae in cells in a 3D microenvironment. We focused on two aspects – AIM 1) Mobility in 2D versus 3D microenvironments. Role of caveolin-1 and its Y14 phosphorylation and AIM 2) Endocytosis in 3D matrix microenvironment. Role of Cav1 and its Y14 phosphorylation.

The detail specific aims of the study are as follows :

1. To standardize embedding MEFs in collagen gels, image them live and do quantitative live imaging (FRAP) in 3D gels.
2. To investigate the role for caveolin-1 phosphorylation (pY14Cav-1) on mobility Cav1 on the plasma membrane in 2D v.s. 3D microenvironments.
3. To investigate the role of caveolin-1 and its phosphorylation (pY14Cav-1) on the mobility of membrane markers in 2D v.s. 3D microenvironments.
4. To investigate the role of caveolin-1 and its phosphorylation (pY14Cav-1) in endocytosis of membrane markers in 3D collagen gels of increasing concentration.



## CHAPTER 2

Localization and mobility of Cav1 in cells in 2D v.s. 3D  
microenvironment : Role of pTyr14-Cav1

## **2.1 Rationale**

Caveolin-1 is an important structural protein required for formation of caveolae, distinct invaginations on the plasma membrane that play a vital role in trafficking, signaling and mechanosensing. Formation of caveolae starts with synthesis of Cav1 in ER, subsequent oligomerization and trafficking through Golgi, association with cholesterol (Hayer et al., 2010a). Eventually these oligomers travel to the plasma membrane where with accessory proteins like Cavins and syndapin, invaginations on the plasma membrane are formed (Hansen et al., 2011; Hill et al., 2008). Caveolae, once formed, are reported to be quite stable structures unlike clathrin-coated pits. The reason behind this is caveolae are quite closely associated with the cytoskeleton - both actin and microtubules (Mundy et al., 2002). Upon disruption of actin with known drugs like latrunculin A, caveolae become dynamic which is measured earlier by comparing mobility of fluorescently tagged Cav1 in control and treated cells by FRAP (fluorescence recovery after photobleaching) (Tagawa et al., 2005).

There are two pools of Cav1 on the plasma membrane : caveolar and non-caveolar. Majority of the Cav1 present on the plasma membrane is inside caveolae (the caveolar pool). Some of the Cav1, however, is present outside caveolae (the non-caveolar pool). The non-caveolar Cav1 has been implicated in various cellular functions mainly in prostate cancer cells (Aung et al., 2011; Gould et al., 2010) which are independent of its ability to form caveolae. The disruption of cytoskeleton hence could flatten caveolar structures and increase non-caveolar Cav1 pool in a cell. This could result in the increased mobile fraction of Cav1 on the plasma membrane. Thus, mobility of Cav1 on the plasma membrane is quite closely related to caveolar functions. Apart from cytoskeleton, proteins like EHD2, Cavins as well as cholesterol all have been shown to regulate mobility of Cav1 on the plasma membrane. The scaffolding domain of Cav1 protein is also implicated in its mobility. Here we have explored the importance of a modification on Cav1-pTyr14-Cav1 in regulating mobility of Cav1.

pTyr14-Cav1 is known to affect many important caveolar functions like focal adhesion dynamics (Joshi et al., 2008), activation of Rho GTPase (Grande-Garcia et al., 2007), mechanotransduction (Joshi et al., 2012). This phosphorylation is shown to be critical in CTxB endocytosis via caveolar route upon loss of integrin mediated adhesion (del Pozo et al., 2005). However, whether this phosphorylation affects the mobility on the plasma membrane and hence caveolar functions

is not known. Even though a phosphodeficient version of Cav1 (Y14F-Cav1) results in formation of caveolae in cells which are similar in number and size as the WT-Cav1, they are not characterized in detail. Using advanced microscopy techniques like quantitative 4D imaging, TIRF and FRET, it was recently shown that pTyr14-Cav1 leads to separation or spreading of neighboring negatively charged N-terminal phospho tyrosine residues causing swelling and subsequent release of caveolae from the plasma membrane (Zimnicka et al., 2016). The fact that caveolae comprising Y14F-Cav1 mutant fail to endocytose upon loss of adhesion might be because of differential engagement of these caveolae with the cytoskeleton as compared to those with WT-pY14Cav1 which could also reflect on mobility of Cav1 on the plasma membrane.

We have compared mobility of Cav1 and Y14F Cav1 in cells in a 2D versus 3D microenvironment as we hypothesize that the caveolar function and trafficking could be differentially regulated in a 3d microenvironment. This is because all the parameters which regulate caveolae trafficking and function (cytoskeleton, integrins, membrane tension and composition) are all either shown or speculated to be different in 3D.

## **2.2 Materials and methods**

### **2.2.1 Plasmids and antibodies**

Primary antibodies used were Cav1 (Santa Cruz Biotech SC-894), pCav1 (BD 611338) and tubulin (DSHB Clone E7). HRP conjugated secondary antibodies (anti-rabbit and anti-mouse) were from Jackson Immuno Research Laboratories. Plasmids Cav1-mRFP and Y14F Cav1 mRFP plasmids were kind gift from Dr. Ivan Nabi's lab. Cav mCherry and Y14F-Cav1 mCherry plasmids were a kind gift from Dr. Miguel Del Pozo's lab. K-Ras-CAAX-GFP was a kind gift from Dr. Konstadinos Moissoglu. Cavin1-mEGFP was procured from Addgene (plasmid #27709). Cav1 GFP and Y14F Cav1 GFP were a kind gift from Dr. Martin Schwartz's lab.

### **2.2.2 Cell culture**

Mouse embryonic fibroblasts (MEFs) - WT MEFs and Cav1-KO MEFs (from the lab of Dr. Richard Anderson, University of Texas Health Sciences Center, Dallas TX) were cultured in high glucose DMEM medium with 5% fetal bovine serum, penicillin and streptomycin (Invitrogen). For transfections  $1 \times 10^5$  cells were seeded in a 35 mm petri plate. After they had attached and started spreading (after about 2-3 hours), they were transfected with  $2 \mu\text{g}$  of DNA.  $4 \mu\text{l}$  of Plus reagent and  $5 \mu\text{l}$  of Lipofectamine-LTX (Invitrogen Cat. No. 15228100) was added to the transfection mix. Transfection mix was prepared in  $500 \mu\text{l}$  OptiMEM (Invitrogen, Cat. No. 5198509) and incubated for 30 minutes before adding to cells. Cells were incubated with  $1.5 \text{ ml}$  complete DMEM +  $0.5 \text{ ml}$  transfection mix for 12 hours. Medium was changed after 12 hours and cells were used for further experiment.

### **2.2.3 Embedding MEFs in 3D collagen gels**

48 hours Post transfection, cells were detached with trypsin and embedded in  $1.5 \text{ mg/ml}$  Collagen Type-1, Rat tail (Corning - Cat no. 354236). A mixture of  $10\text{X}$  PBS, sterile mili-Q water and collagen (to make final concentration to  $1.5 \text{ mg/ml}$ ), in a total volume of  $400 \mu\text{l}$ . This

amount varies according to the stock bottle concentration). This mixture was kept on ice for 5 mins.  $4 \times 10^4$  cells were mixed with this collagen solution and 1N NaOH was added (final concentration in the gel is 0.006N). After proper mixing, this collagen I (volume 400  $\mu$ l) with cells was transferred to one well of a LabTek chamber (Thermo Scientific). The chamber was kept in 37C incubator with 5% CO<sub>2</sub> supply for about 30 minutes. The gel polymerized in 30 minutes, after which 400  $\mu$ l DMEM (5% FBS) was added on top and the chamber was further kept at 37<sup>0</sup>C for 12 more hours.

#### **2.2.4 Coating coverslips with collagen**

Coverslips (from VWR) were first washed with KOH + methanol solution (25g KOH in 500ml methanol) and thoroughly washed with MiliQ water. Washed coverslips are stored in 100% ethanol and are flame-dried and subjected to UV sterilization for 30 minutes before using. Collagen coating is done in two steps. First step involved a 4  $\mu$ g/ml collagen solution made in 70% ethanol (molecular biology grade). This solution was added on the coverslip to cover it fully (about 200  $\mu$ l, varies depending on the size of the coverslip). The coverslips were then allowed to air dry under UV (until all the solution evaporated). After this 100  $\mu$ g/ml collagen solution (made in DPBS) was added (2 ml) and coverslips were incubated at 4<sup>0</sup>C overnight. Next day, collagen solution was aspirated and coverslips were washed twice with 1X PBS and then used to seed cells.

#### **2.2.5 Confocal imaging**

Images were acquired using a 63X oil immersion objective on Zeiss LSM 780 confocal microscope, NA 1.4. For Z stacks, the step size was kept at 0.8  $\mu$ m. Z stacks were reconstructed using Huygens software and object analyzer module was used to calculate volume and surface area. For co-localization analysis, JACOP (Just Another Co-localization Plug-in) in ImageJ software was used.

### **2.2.6 Fluorescence recovery after photobleaching (FRAP)**

Cells were transfected 24 hours prior to photobleaching experiment. During FRAP experiments, cells were maintained in CO<sub>2</sub> independent Leibovitz L-15 medium (Invitrogen, 21083-027). Images were acquired using a 63X oil immersion objective on Zeiss LSM 780 confocal microscope, NA 1.4, at 2.2X digital zoom. A region of interest 20X10, 20X20, 20X30 or 20X50 were used for photobleaching on the plasma membrane (1 pixel = 0.12 μm) For photobleaching, we used the 488 nm laser line. 100% laser power was used for photobleaching (200 iterations for bleaching) after 10 scans of pre bleach, and image acquisition was performed every 0.5 sec. Images were analyzed using Zen 2011 FRAP Analysis module to calculate mobile fraction and T<sub>half</sub>. For Cav1 constructs, mobile fractions were calculated from normalized intensity v.s. time graphs using following formula :

$$\text{Mobile fraction} = \frac{F_{\text{end}} - F_{\text{post}}}{F_{\text{pre}} - F_{\text{post}}}$$

Where,

F<sub>end</sub> = Fluorescence intensity in the bleach box after recovery

F<sub>post</sub> = Fluorescence intensity in the bleach box immediately after bleaching

and

F<sub>pre</sub> = Fluorescence intensity in the bleach box before bleaching.

Double normalization of the FRAP data was done as follows :

Intensity of background region was subtracted from intensity of bleached area. This was divided by intensity in the reference region (unbleached box of similar size, drawn on the plasma membrane). This value is called "A". Mean of pre-bleach intensities was taken and referred to as "B". Then A divided by B gives normalized intensity values. A graph of normalized intensity v.s. time was plotted.

### **2.2.7 Extraction of cells using collagenase**

Cells were embedded in collagen as explained above in section 2.2.3. Instead of LabTek chambers, 24 well plates were used for this protocol. In each well of a 24 well plate, the final 400  $\mu$ l gel mixture was added and incubated for 12 hours before starting extraction. After 12 hours, first DMEM was removed and gels were twice washed with 1X PBS (400  $\mu$ l PBS was added and kept for 2 minutes, 2 such washes were given). Collagenase P was procured from Roche (Cat. No. 11 213 857 001, stock - 10 mg/ml). Working concentration was 2 mg/ml, dilution made in HBSS (Hank's Buffered Salt Solution from Invitrogen) and kept protected from light. 400  $\mu$ l of 2 mg/ml collagenase solution was added onto the gel and the 24 well plate was kept at very slow shaking in an 37<sup>0</sup>C incubator for 30 minutes. After the gel was completely dissolved (after 30 minutes), 800  $\mu$ l DMEM (containing FBS) was added and the cells were spun down in a centrifuge at 1000 rpm, for 5 minutes. Pellets were lysed in 30  $\mu$ l 1X Laemmli and processed further for Western blotting.

### **2.2.8 Western blotting**

Cells were lysed in Laemmli buffer and cell equivalent volumes of lysates were resolved by SDS PAGE (12.5 %, 1.5 mm gels), transferred to PVDF membrane and blocked with 5% non-fat dry milk in TBS+0.5% Tween-20 (TBS-T). Blots were probed with primary antibodies overnight at 4<sup>o</sup>C. Concentrations of primary antibodies were : Cav1 - 1:10,000, pCav1 - 1:500, Tubulin - 1:5000, made in 2.5 % non-fat dry milk in TBS+0.5% Tween-20 (TBS-T). Following the respective secondary antibody incubations (done at room temperature for 60 minutes), blots were developed using chemiluminiscent substrates from Thermo-Fischer using the LAS 4000 developing system (Fujifilm-GE). Densitometric analyses of blots were done using Image J software (NIH) to calculate the pCav1/total Cav1 ratio.

### **2.2.9 Vesicle tracking experiments**

Cells expressing WT Cav1-GFP or Y14F-Cav1-GFP were plated on 35 mm glass bottom petri

plates and time lapse movies were acquired on a confocal microscope (LSM 780). Images were acquired with a 63X oil objective, with zoom factor 1 at 512X512 pixels. The frame rate (3.94 sec) and zoom factor (1) was kept constant for all the time lapse movies. The vesicle tracking analysis was done by Dr. Chiam Keng Hwee (NUS, Singapore).

#### **2.2.10 Statistical analysis**

Statistical analysis of data was done using Mann-Whitney test as the data sets had non-normal distribution (confirmed by Shapiro–Wilk test). All analysis was done using Prism Graphpad analysis software. Statistical significance was considered at  $p < 0.05$ . For figure 2.10, one sample T test was used as one of the dataset is normalized to other dataset.



## **2.3 Results**

### **2.3.1 Standardizing embedding and imaging MEFs in 3D collagen gels**

We have used mouse embryonic fibroblasts (MEFs) which either express Cav1 (WT-MEFs) or MEFs coming from a Cav1-KO mouse (Cav1-KO MEFs) in this study. Fibroblasts do have abundant caveolae and are hence a good choice to study caveolar functions. *In vivo*, fibroblasts are the primary cells present in the stroma and they remodel the stroma which is rich in collagen. To study fibroblasts in 3D microenvironment, collagen has been a very widely used as the ECM component. It forms visco-elastic hydrogel which is quite close to the stroma and is also optically clear making imaging of cells in the collagen gels easier. The physical properties like pore size and stiffness of this gel can also be easily modulated by changing polymerization conditions for the gel.

We have used the commercially available rat tail collagen type 1 from Corning to make hydrogels. The solution is in acetic acid and when it is brought to pH 7 by adding 1N NaOH, collagen starts polymerizing and forms hydrogel. The temperature at which polymerization occurs affects the thickness of collagen fiber and hence pore size of the gel. The amount of NaOH added and concentration of collagen both again affect physical properties of the gels (Achilli and Mantovani, 2010). We chose a range of concentrations - 0.5 mg/ml, 1 mg/ml, 1.5 mg/ml and 2 mg/ml with a constant NaOH amount and embedded cells in these different gels. We mixed the cells with unpolymerized collagen solution and then added NaOH. This ensures that the cells are completely trapped inside the gel and even the early adhesion events occur in a 3D microenvironment.

We embedded WT-MEFs in different concentrations of collagen gels and followed the cells (imaged live) at different time points. This was done using LabTek chambers, as they have a glass bottom which makes it possible to image cells live when they are still embedded in 3D collagen (fig 1.1 a). At 1.5 mg/ml collagen after 12 hrs post embedding, fibroblasts had the typical 3D morphology as reported earlier by others. At earlier time points, cells were mostly round with very little or no protrusions. At lower concentrations and longer time points, all the cells were settled to the bottom of the chamber and were no longer embedded inside the gel. The

different morphologies observed at different gel concentrations and different time points are listed in fig 1.1 b. We used this concentration and this time point for further experiments.

(a)

Cells incubated for	Collagen conc. (mg/ml)	Observations
6 hrs	0.5	Very few cells seen in the gel, most of them were settled
	1	Most were still round. Some had started producing protrusions
	1.5	
	2	
12 hrs	0.5	Almost all the cells had spread
	1	Majority of them were spread (These were likely at the bottom)
	1.5	Lesser number of cells were spread (as compared to 1mg/ml)
	2	Many were still round (May be 2mg/ml is too stiff for the cells)
23 hrs	0.5	Almost all the cells had spread
	1	
	1.5	
	2	

(b)

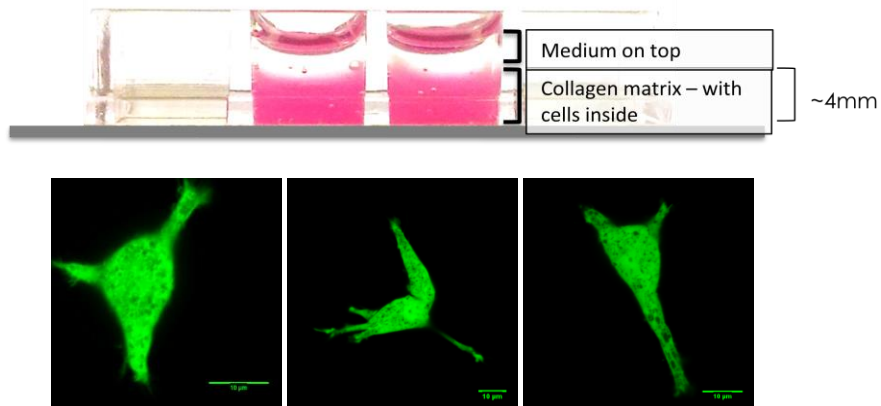


**Fig 2.1 Standardizing embedding and imaging MEFs in collagen gels.** (a) Table summarizing morphology of WT MEFs observed at various collagen concentrations and time points (b) Experimental set up for live cell imaging – LabTek chamber containing collagen gel with cells embedded inside. Below the chamber are confocal images of cells expressing empty GFP.

### 2.3.2 Localization of various Cav1 constructs in MEFs - 2D and 3D

The fluorescent tag attached to Cav1 has been shown to affect its processing through the secretory pathway or oligomerization properties. We hence checked localization of GFP tagged and mCherry tagged WT-Cav1 (known to be phosphorylated on pY14) and a phospho-deficient version of Cav1, i.e. Y14F-Cav1.

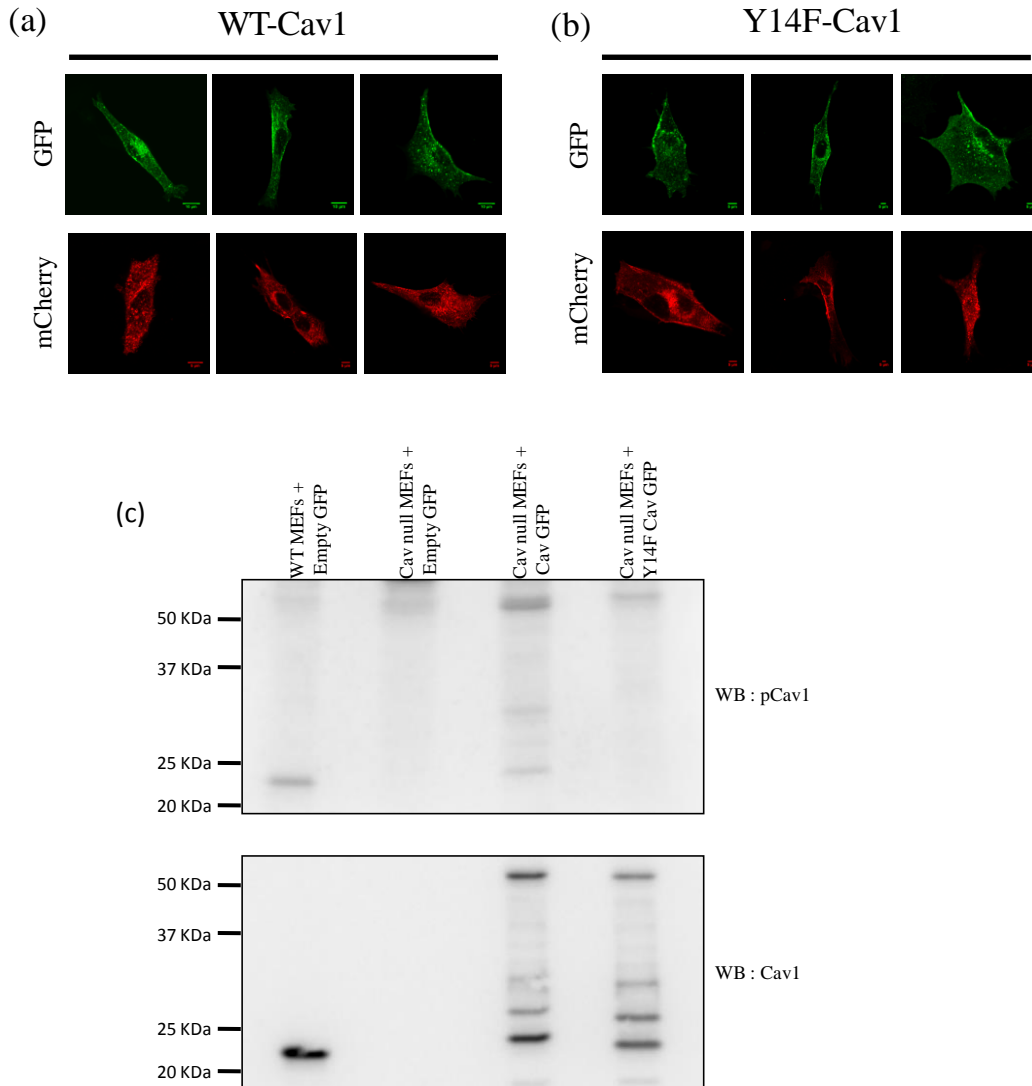


**Fig 2.2 Localization of various Cav1 and Y14F-Cav1 constructs in WT-MEFs (2Dcollagen)**  
(a) WT-Cav1 and (b) Y14F-Cav1, GFP or mCherry tagged. Cells were plated on collagen coated coverslips, fixed after 12 hours and then imaged under confocal microscope Images represented here are cross sections from 3 independent experiments. (c) Western blot to verify that Y14F-Cav1-GFP construct can not get phosphorylated.

The phospho-deficient construct was used as a way to comment on whether and how this Tyr-14 phosphorylation affects localization of Cav1. The only commercially available antibody for pTyr14-Cav1 is not suitable for immunofluorescence as it cross-reacts with phospho-paxillin and phospho vinculin (Hill et al., 2007). Hence we had to rely on this indirect approach of using Y14F-Cav1 construct to comment on localization. Note that these cells have their endogenous Cav1 which can still get phosphorylated. Hence, the further localization studies (in 3D) were done in Cav1-KO MEFs too.

As shown in fig 2.2, in WT MEFs plated on 2D collagen, there wasn't any obvious difference in localization of WT versus the phosphodeficient construct (both GFP and mCherry tagged). All the four constructs showed a punctate localization as expected. WT MEFs showed a spindle-shaped morphology on 2D collagen coated coverslips (after 12 hours of plating). No morphological differences were observed between cells expressing WT-Cav1 or Y14F-Cav1.

We next checked the localization of these constructs in cells embedded in 3D collagen - both WT MEFs and Cav1-KO MEFs. Cells were imaged live after embedding in 1.5 mg/ml collagen gels for 12 hours. Fig 2.3 shows cross-sections of cells imaged using a confocal microscope. In both the cell types, GFP-tagged constructs showed proper membrane localization (with a little cytoplasmic pool, as expected). However mRFP and mCherry tagged constructs formed aggregates in the cytoplasm with very little membrane localization. This was more prominent in WT MEFs than in Cav1-KO MEFs. We tested only mCherry tagged constructs in Cav1-KO MEFs and both WT -Cav1-mCherry and Y14F-Cav1-mCherry showed mainly membrane localization with lesser aggregates in the cytoplasm.

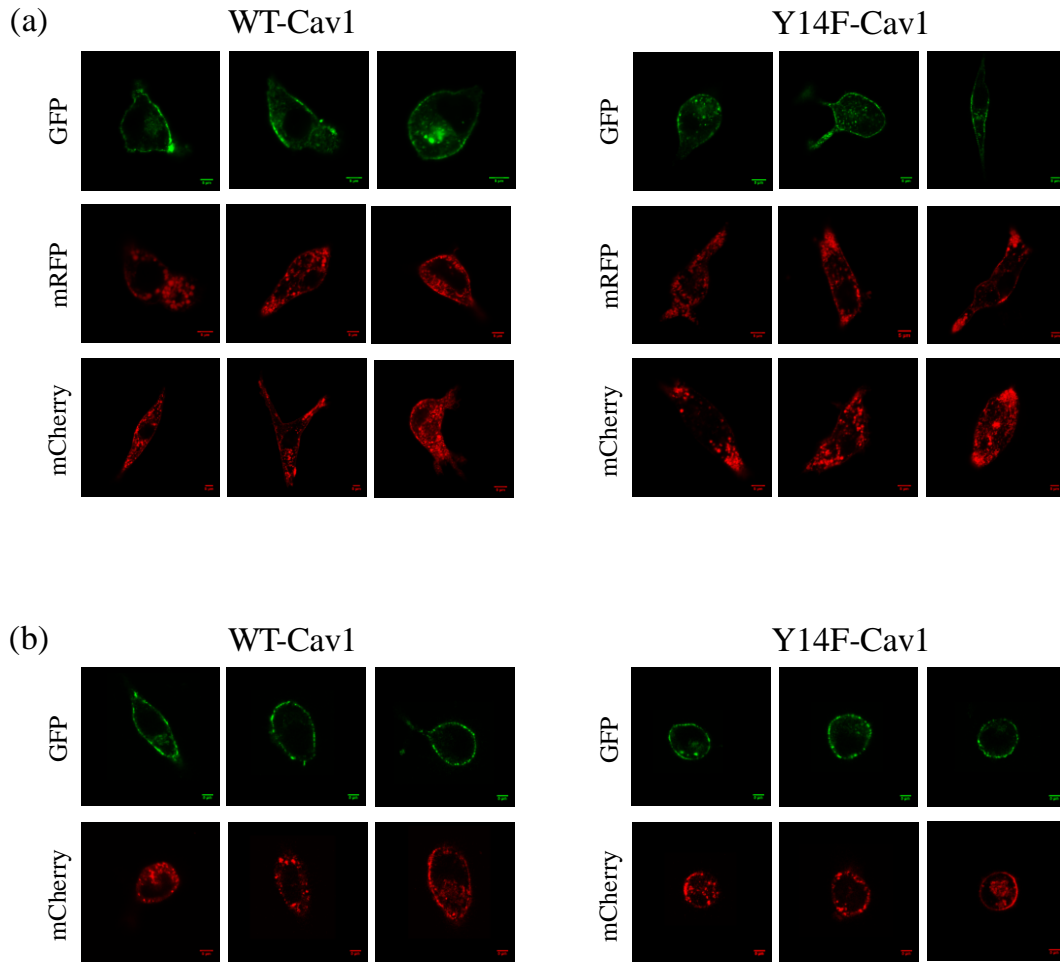


**Fig 2.3 Localization of various Cav1 and Y14F-Cav1 constructs in WT-MEFs and Cav1-KO MEFs (3D collagen)**(a) WT MEFs and (b) Cav1-KO MEFs expressing GFP or RFP or cherry tagged Cav1 constructs. Cells imaged live under confocal microscope after 12 hours of embedding at 1.5 mg/ml collagen gels.

Both GFP and mCherry tagged caveolin-1 constructs indicated some morphological differences, mainly in Cav1-KO MEFs. Cells expressing WTCav-1 (GFP and mCherry tagged) appeared more elongated as compared to those expressing Y14F Cav-1 (GFP and mCherry tagged). These differences were assessed and discussed in detail in the next section.

### **2.3.3 Morphology of WT v.s. Cav1-KO MEFs in 3D collagen gels**

As mentioned above, in the cross sections of cells embedded in 3D collagen gels, we saw some morphological difference between cells expressing WT-Cav1 and the cells expressing Y14F-Cav1. We did detail analysis with reconstituted Z stacks of these two cell types and analyzed following parameters : cell surface area, cell volume and aspect ratio (ratio of longest axis to the shortest axis of a cell). Fig 2.4 shows representative images and quantitation of the analysis done using object analyzer module of Huygens software. WT MEFs and Cav1-KO MEFs expressing empty GFP were taken as controls.

We compared Z stacks of cells embedded in 1.5 mg/ml collagen gels for 12 hours. We did not find any significant difference between all four cell types : WT MEFs, Cav1-KO MEFs, Cav1-KO MEFs + WT Cav1 GFP and Cav1-KO MEFs + Y14F-Cav1 GFP in their surface area or volume. However, interestingly, there was a difference between the aspect ratio of WT MEFs and Cav1-KO MEFs. As WT MEFs were more elongated with more number of protrusions and Cav1-KO MEFs were mainly round with no or very small protrusions, the aspect ratio of WT MEFs was significantly higher as compared to Cav1-KO MEFs. When Cav1-KO MEFs reconstituted with WT-Cav1 when analyzed was seen to recover its aspect ratio, becoming comparable to control WT MEFs. The phosphodeficient construct, Y14F-Cav1, could not rescue this phenotype in Cav1-KO MEFs.

Similar observation has been reported in literature earlier, and in that study also Y14F-Cav1 did not reverse the phenotype but WT-Cav1 did (Goetz et al., 2011). The authors in this study have attributed this difference to differential Rho GTPase activation in WT MEFs versus Cav1-KO MEFs. WT MEFs have higher Rho activation and hence higher acto-myosin contractility. This leads to more elongated morphology in collagen gels of concentration 1 mg/ml. Cav1-KO MEFs by virtue of having low Rho GTPase activity, lacks protrusions and remains largely round in these gels.

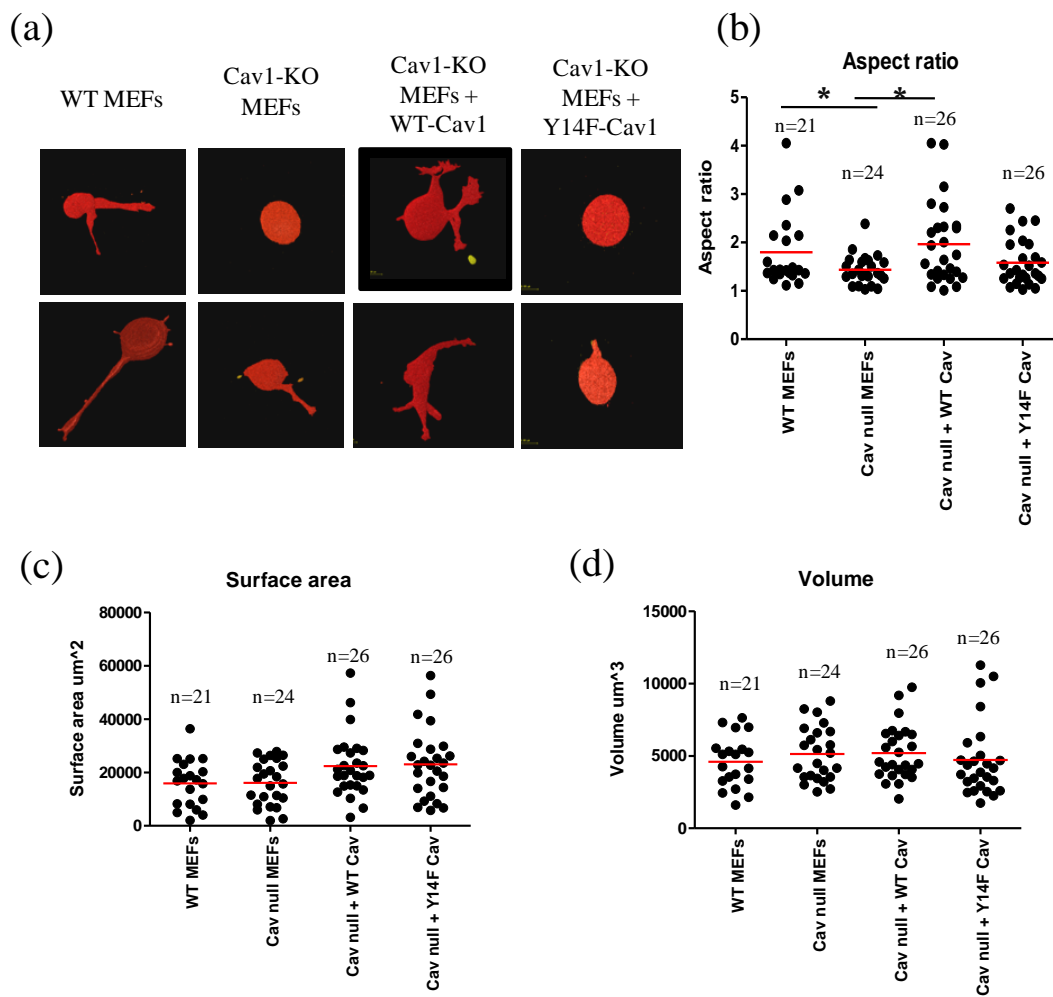


**Fig 2.4 Morphology of MEFs in 3D collagen – role of Cav1 and pTyr14Cav1.** (a) representative Z stacks : images constructed using Huygens (b) aspect ratio (c) surface area and (d) volume of cells calculated using Huygens software.  $p < 0.005$ , significance calculated by unpaired two tailed T-test, wherever indicated. Images analyzed from 4 independent experiments. For detail statistics refer appendix.

#### **2.3.4 Cav1 and Cavin1 co-localization - 2d and 3D collagen**

Cavin1 (also known as PTRF) is an important accessory protein present at caveolae. Like Cav1, Cavin1 also forms oligomers and they are taken to the plasma membrane independently from Cav1 oligomers. Cavin1 is believed to stabilize caveolar structure on the plasma membrane. Cavin1 is known to co-localize with Cav1 at the plasma membrane at ultra structural level and it is supposed to be an important parameter of caveolar function (Hill et al., 2008). It is not known yet whether pTyr14-Cav1 interacts or localizes differentially with Cavin1 as against WT Cav1. We checked the co-localization of Cavin1 with either WT or Y14F Cav1 in 2D as well as 3D collagen.

In 2D, both these proteins are shown to co-localize at the trailing edge and have a role in regulating cell migration (Hill et al., 2012). We saw similar co-localization at the trailing edge - for both WT Cav1 as well as Y14F-Cav1 with Cavin1 (Fig 2.5 - b). In the cytoplasm, the extent of co-localization is less and that is reflected in the Pearson's coefficient calculations (Fig 2.5 - a). In 3D cells, at cross sections mainly membrane localization of both Cav1 and Cavin1 is seen and hence the Pearson's coefficients are higher as compared to 2D cells. (Fig 2.5 - a). There doesn't seem to be a difference between co-localization of Cavin1 with WT Cav1 and Y14F Cav1 (as Pearson's coefficients are comparable).



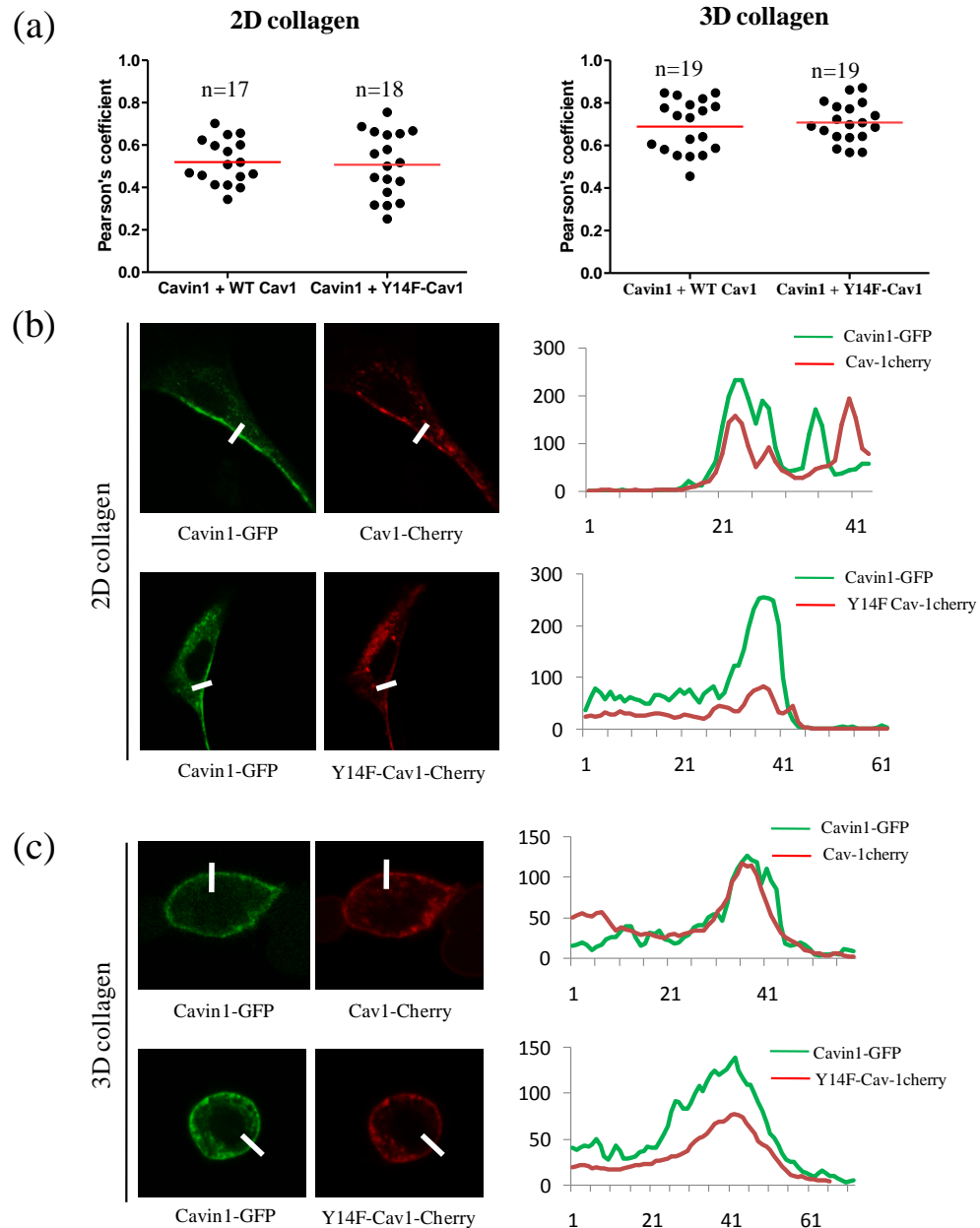


**Fig 2.5 Co-localization of Cav1 and Cavin1 in WT-MEFs in 2D and 3D collagen : Role of pTyr14-Cav1.** (a) Shows Pearson's coefficient for Cavin1-GFP and WT-Cav1 Cherry or Y14F-Cav1-Cherry. (b) Images of cells plated on 2D collagen and (c) embedded in 3D collagen. Line scans on the right show overlap between Cavin-1 and WT Cav1 and Y14F Cav1. Images represented here are from three independent experiments.

### **2.3.5 Standardizing FRAP in 3D - Using K-Ras-CAAX-GFP**

As Cav1 is a membrane protein, its mobility on the plasma membrane is linked with its function. Once formed, caveolae are quite static structures relative to clathrin-coated pits and hence mobility of Cav1 reported in literature is quite low (Tagawa et al., 2005; Thomsen et al., 2002). Even though these move slower than clathrin-coated pits, the mobility of Cav1 protein reflects on caveolar versus non-caveolar pools and hence function. The role of pTyr14-Cav1 in mobility of Cav1 was also something we wanted to explore here. Also, all earlier studies have been carried out in cells plated on 2D surfaces and we also eventually wanted to compare their mobility to those in cells embedded in 3D collagen gels. For this purpose we standardized a technique called Fluorescence Recovery After Photobleaching (FRAP), first using a highly mobile membrane diffusion marker : K-Ras-CAAX-GFP.

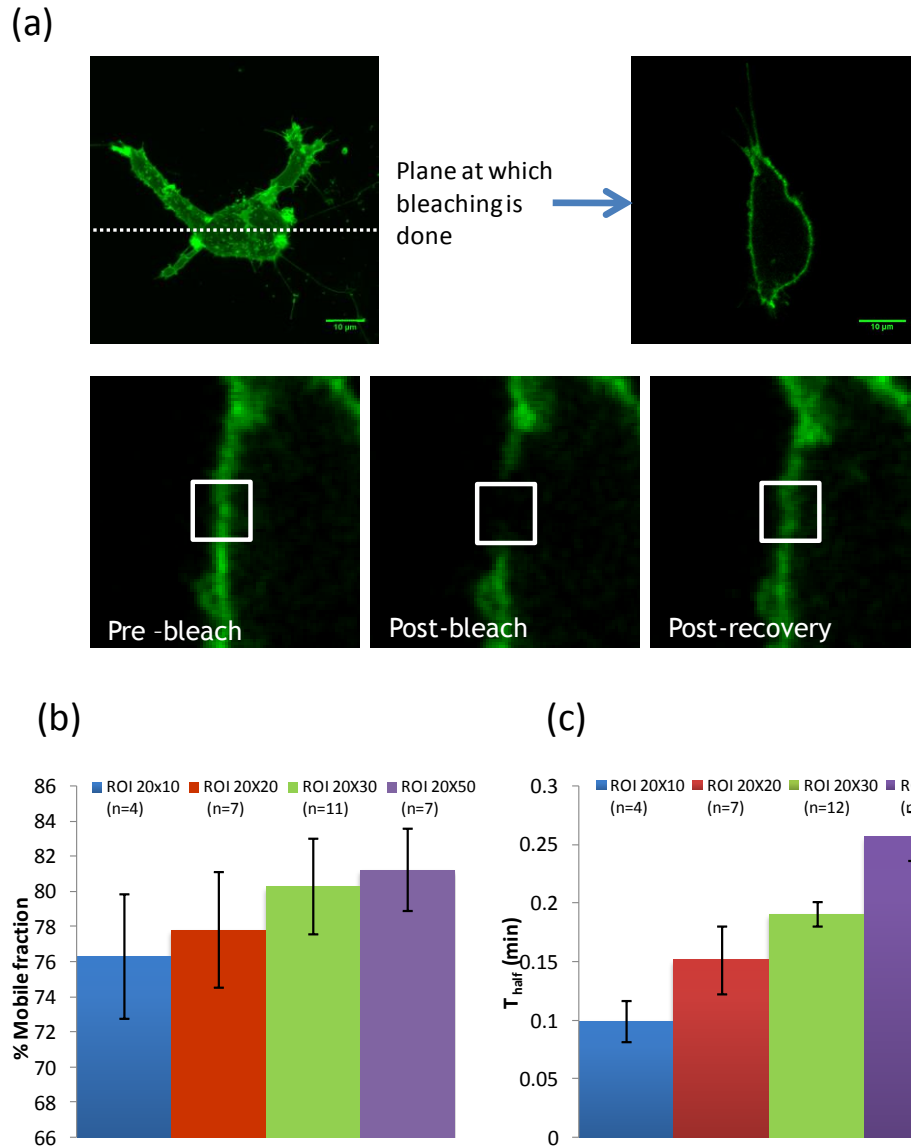


**Fig 2.6 Standardization of FRAP in WT MEFs in 3D – using K-Ras-CAAX-GFP** (a) Schematic showing how FRAP is done in cells embedded in collagen gels. (b) Mobile fractions and (c)  $T_{\text{half}}$  for K-Ras-CAAX-GFP expressed in WT MEFs. Bleaching done at three ROIs – 20X20, 20X30 and 20X50. Analysis done using Zenlight software. Data represented from 6 independent experiments. For detail statistics refer appendix.

The construct used for this standardization is the C terminal CAAX motif and the hypervariable region of K-Ras tagged to GFP. This protein associates with the inner leaflet of the plasma membrane mainly via electrostatic interactions between the hypervariable (lysine rich) region on

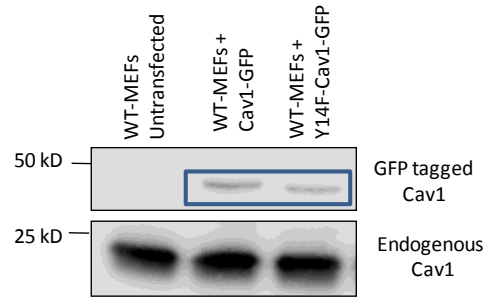
the protein and the plasma membrane. It is supposed to diffuse freely along the inner leaflet as it does not have any affinity towards cholesterol-enriched domains on the plasma membrane. WT MEFs were transfected with this construct and were embedded in 1.5 mg/ml collagen gels for 12 hours. FRAP was carried out at the middle cross section of the cell (see Fig 2.6 - a) using region of interest (ROIs) of increasing size - 20X10, 20X20 pixels, 20X30 pixels and 20X50 pixels. Mobile fractions were calculated by taking the ratio of fluorescence intensities before bleach and after bleach. Double normalization was performed on the data before calculating ratios to take into account bleaching in a reference (unbleached region) as well as background fluorescence. (for more details please refer materials and methods section 2.2.6).

For a molecule whose recovery is mainly diffusion based, increasing the size of ROI should increase both its mobile fraction and T-half. Upon increasing the size of the ROI, we did see an increase in the mobile fraction as well as  $T_{\text{half}}$  (Fig 2.6 - b and c). We made use of this to validate and confirm that our FRAP protocol and analysis is correct and can be used for other molecules (mainly Cav1). We hence went ahead with the same protocol and compared mobility of Cav1 and Y14F-Cav1.

### **2.3.6 Mobility of Cav1 in MEFs in 2D and 3D collagen - Role of pTyr14-Cav1**

We first checked mobility of WT Cav1 GFP and Y14F-Cav1 GFP in WT MEFs embedded in 3D collagen (1.5 mg/ml). WT MEFs were transiently transfected with either of these constructs and FRAP was performed after 12 hours of embedding in collagen. While performing transient transfections, we confirmed by Western blot that the levels of over expressed protein are actually less than the endogenous Cav1 levels (Fig 2.7).

(a) WT MEFs



(b) Cav1-KO MEFs

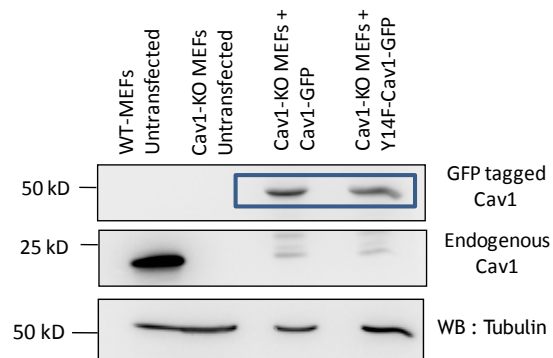


**Fig 2.7 Levels of over expressed Cav1 constructs in WT MEFs and Cav1-KO MEFs.** Cells were transiently transfected with either WT Cav1 or Y14F Cav1 and cell equivalents were loaded on a Western blot. Blots were probed with anti-Cav1 antibody. Cav1 (for WT MEFs) and tubulin (for Cav1-KO MEFs) were used as an internal loading control.

We transiently expressed WT Cav1-GFP and Y14F Cav1-GFP in WT MEFs and compared mobile fractions by FRAP. We found that the percent mobile fraction for Y14F Cav1-GFP was less as compared to WT Cav1-GFP (Fig 2.8). The difference however was not significant. One possible reason for this could be since these are WT MEFs, they will still have their endogenous Cav1 which can get phosphorylated. Hence we further compared mobility of these two constructs in Cav1-KO MEFs.

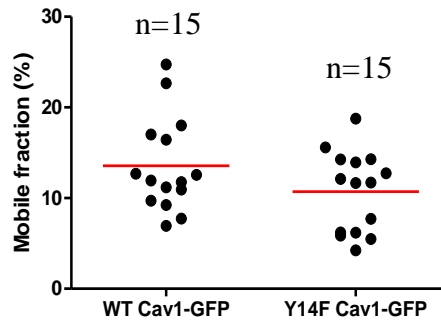


**Fig 2.8 Mobility of Cav1-GFP in 3D by FRAP in WT MEFs : Role of pTyr14-Cav1.** Mobile fractions for WT-Cav1-GFP and Y14F Cav1-GFP expressed in WT MEFs. Bleaching was done in ROI of 20X20 pixels. Data represented from four (for WT-Cav1 GFP) and five (Y14F-Cav1 GFP) independent experiments. For detail statistics refer appendix.

We next decided to compare mobility of these two constructs in Cav1-KO MEFs as those results will not be affected by the presence of endogenous Cav1. Cav1-KO MEFs were transiently transfected with either WT-Cav1-GFP or Y14F-Cav1-GFP and their mobility was measured by FRAP For Cav1-KO MEFs experiments, we used a smaller ROI, 20X10 pixels.

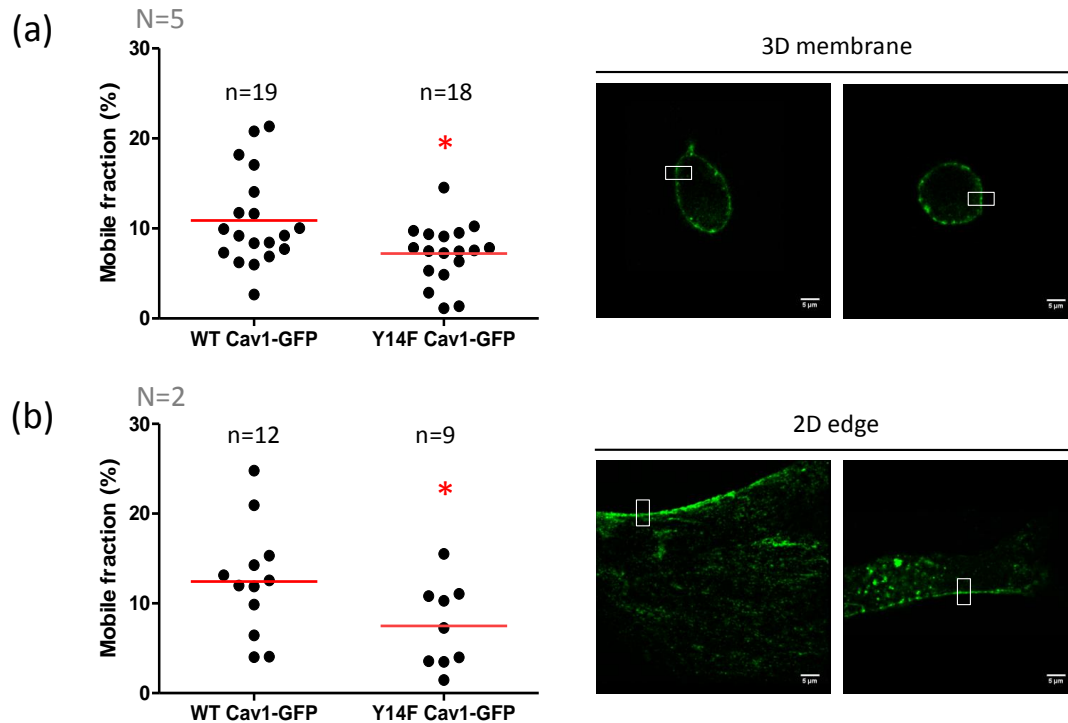


**Fig 2.9 Mobility of Cav1-GFP in 3D by FRAP in Cav1-KO MEFs : Role of pTyr14-Cav1.** Mobile fractions calculated at (a) membrane in 3D cells and (b) trailing edge in 2D cells. Representative images at each are shown on right. White box indicates region of bleaching, 20X10 pixels.  $P < 0.005$ , calculated by Mann-Whitney test. For detail statistics refer appendix.

When we compared the mobile fractions of the two proteins in cells embedded in 3D collagen gels, the results were similar to what is seen in WT MEFs, that is, mobile fraction of Y14F-Cav1 was less as compared to WT Cav1. Also, in Cav1-KO MEFs, this difference was statistically significant. WT-Cav1-GFP has mobile fraction of  $10.88 \pm 1.18$  % and Y14F-Cav1-GFP has  $7.2 \pm 0.77$  % (Fig 2.8 c).

Caveolae are shown to be enriched at the trailing edge in migrating cells in 2D where it is shown that Cav1 co-localizes with Cavin-1 (Hill et al., 2012), a protein which stabilizes caveolar structure. We earlier saw that Cav1 and Cavin1 co-localize in 3D and at the trailing edge in 2D cells (Fig 2.5 b and c). Hence we compared mobility of Cav1 and Y14F-Cav1 at the trailing

edge. At the trailing edge, again, Y14F-Cav1-GFP was found to be less mobile (mobile fraction  $7.48\% \pm 1.56$ ) as compared to WT-Cav1GFP (mobile fraction  $12.44\% \pm 1.78$ ) (Fig 2.8 b).

### **2.3.7 pTyr14-Cav1 levels - 2D v.s. 3D**

Phosphorylation status of a number of proteins is known to be different in a 3D microenvironment, like pFAK (Cukierman et al., 2001a), pMAPK (Wozniak et al., 2003), pMLC (Zhong et al., 2012), etc. One of the important regulator of pY14Cav-1 is integrins and integrin clustering and signaling has been earlier shown to be different in 3D as compared to 2D.

We hence checked whether pCav1 levels also change in 3D as compared to 2D. pCav1 levels are known to increase as a response to certain mechanical stimuli (Kim et al., 2000; Volonte et al., 2001). To check this, cells were extracted from 3D collagen and were compared to cells plated on 2D collagen. As 3D matrices have very low stiffness as compared to 2D dishes, there is a possibility that pCav1 levels will be altered in 3D. However, we did not find any difference between levels of pCav1 in 3D as compared to 2D (Fig 2.10). This also indicated that the effects seen because of pTyr14-Cav1 (differences in morphology or on mobility of Cav1) are not because of altered levels of pCav1 in 3D relative to 2D. This indicates that regulation of Cav1 phosphorylation in 2D and 3D is similar, unlike phosphorylation of FAK. However, in response to a particular stimulus whether the pTyr14-Cav1 levels change in 2D versus 3D remains to be addressed.



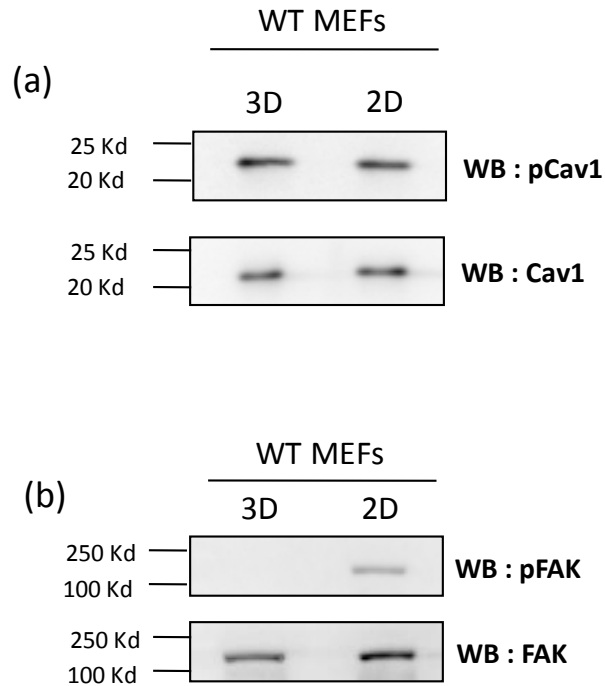


**Fig 2.10 Levels of pTyr-Cav1 : 2D v.s. 3D in WT MEFs.** (a) Representative Western blot comparing pCav1 levels in cells extracted from 3D collagen v.s. cells plated on 2D collagen. (b) pFAK was used as a positive control. Blots representative of three independent experiments.

## 2.4 Discussion

In order to study caveolar function in 3D, we first standardized how to embed MEFs in collagen gels and image them live. Cav1 is the major structural protein of caveolae and is used to study caveolar localization, trafficking and function as well. It is a **transmembrane protein** with its both N and C termini facing towards cytoplasm. Various tagged constructs of Cav1 are widely used, including fluorescently tagged constructs. Cav1 is an **oligomerizing protein** (both homo and hetero - with Cav2) and this is essential for formation of caveolae. Adding a tag at N-terminal interferes with oligomerization of the protein and hence **C-terminally tagged Cav1 constructs are used**. Recently, there are a few studies published which comment on how different tags affect localization and processing of Cav1 and also the extent of over expression of tagged constructs. There is a known mutation in Cav1, P132L, which has been suggested to have a role in breast cancer. This protein is known to get trapped in Golgi and hence this has been

thought to be the mechanism in regulating disease related phenotypes. However, the authors showed that only P132L-GFP was getting trapped in the Golgi, but P132L-Cherry was properly targeted to the plasma membrane (Han et al., 2015). Other study shows that even a WT Cav1 behaves like a dominant negative mutant if over expressed many folds above the endogenous Cav1 and is excluded from the oligomers formed by endogenous proteins (Hanson et al., 2013).

We confirmed using Western blot that the extent of over expression in our cells is lesser than endogenous Cav1 (Fig 2.7), which is what is generally advisable in the field. We also compared localization of GFP as well as mCherry constructs and found that GFP constructs showed proper membrane localization. **mCherry constructs** in 2D showed proper localization however, **in 3D**, they formed **big aggregates inside the cytoplasm** with very little membrane pool (Fig 2.3). The aggregation phenotype was more profound in WT MEFs as compared to Cav1-KO MEFs (in 3D). We do not know the exact reason for this formation of aggregates but we speculate that the specific fluorescent tag leads to this phenomenon. We hence used GFP tagged constructs in all further experiments.

**Cav1 regulates activity of small GTPases like Rac, Rho and Cdc42.** Rho is more active in WT MEFs as compared to Cav1-KO MEFs, however Rac and Cdc42 are less active in WT MEFs as compared to Cav1-KO MEFs(Grande-Garcia et al., 2007). These GTPases are critical in regulating the cytoskeleton and hence cell polarization, spreading and morphology of cells. We hence compared at the morphology of WT MEFs and Cav1-KO MEFs in 3D collagen. There was no difference between surface area and volume of the two cell types. However, **the aspect ratios were significantly different for WT MEFs versus Cav1-KO MEFs.** Aspect ratio is the ratio of length of longest axis to the shortest axis in a cell and hence is a parameter of elongation of cells. This analysis revealed that WT MEFs are more elongated in 3D collagen (1.5 mg/ml concentration) as compared to Cav1-KO MEFs, reflecting their having more or longer protrusions (Fig 2.4). Cav1-KO MEFs mainly remained round with no or very small protrusions. Reconstitution of Cav1-KO MEFs with WT Cav1 restored their aspect ratio confirming the role caveolin-1 has in mediating the shape of these cells. Interestingly the phosphodeficient Y14F-Cav1 mutant failed to do so, suggesting a role of caveolin-1 phosphorylation in mediating the same. A similar difference in morphology of WT MEFs and Cav1-KO MEFs and a role of caveolin-1 phosphorylation in controlling this morphology has been reported earlier (Goetz et al.,

2011). In this study, in subsequent experiments this effect was attributed to differential Rac and Rho activation in these cells. Further it was shown that reconstitution with the phosphodeficient mutant of Cav1 could not reverse the phenotype but WT Cav1 did. We see a similar result in our set up as well.

pTyr14-Cav1, has been implicated as an important regulator of caveolar endocytosis. Upon loss of adhesion, WT Cav1 can internalize CEMMs however Y14F-Cav1 can't (del Pozo et al., 2005). In the context of 3D microenvironment however, nothing is known about how pTyr14Cav-1 affects caveolar trafficking. Whether it has any effect on Cav1 mobility on the membrane is not known. To check this, we decided to look at mobility of Cav1 on the plasma membrane. We made use of the technique called FRAP, which essentially indicates mobile and immobile fractions of a particular protein. There are two pools of Cav1 present on the plasma membrane - caveolar (present inside caveolae) and non caveolar (present outside caveolae) and while bleaching, we did not particularly look at a particular pool versus the other. However, once Cav1 enters caveolae, it gets associated with actin cytoskeleton and other structural proteins like cavins and it relatively becomes less mobile. Hence, differences in mobile - immobile fractions of Cav1 could also reflect on the amounts of caveolar versus non-caveolar pools in a cell.

We compared mobility of WT Cav1 and a phosphodeficient version of Cav1 in cells in 2D and 3D. In **2D, the ventral membrane is different than the edge** in certain aspects. One major difference is **co-localization of Cavin1 and Cav1**. These two proteins co-localize only at the edge, suggesting caveolae are enriched at this part of the cell. This means that we were predominantly looking at caveolin-1 that is localized in caveolae.. We found that, the **mobile fractions of Y14F-Cav1 GFP were lesser** as compared to WT-Cav1 GFP **at the edge of the membrane**. This suggests an interesting possibility of pTyr-Cav1 affecting mobility of Cav1 only when it is in association with Cavin1, that is, when it is present in caveolae. In cells in 3D collagen, we found co-localization of Cav1 and Cavin1, exactly like the edge in 2D.

Interestingly, even in 3D, **mobile fractions of Y14F-Cav1 GFP were lesser** as compared to WT-Cav1 GFP. Whether the 2D edge is exactly similar to membrane in 3D in other contexts (presence of other proteins, actin polymerization, membrane density) are all open questions

which remain to be addressed. The differences in mobility of Y14F-Cav1 and WT-Cav1 could be because of differential engagement with the actin cytoskeleton, however the exact mechanism remains to be elucidated.

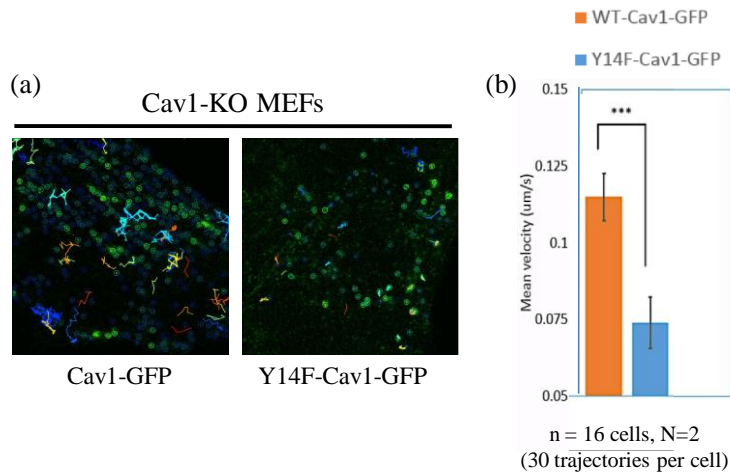


**Fig2.11 Mobility of Cav1-GFP in 2D by vesicle tracking : Role of pTyr14-Cav1.** (a) Cross sectional view of a cell plated on 2D collagen with tracks of vesicles used for analysis (b) Velocities of WT Cav1-GFP and Y14F-Cav1-GFP vesicles measured and compared by two-tailed T-test.  $p < 0.001$ .

We further compared the vesicular trafficking of Cav1 in cells in 2D and checked the effect of pTyr14-Cav1 on this. Our results showed that Y14F-Cav1-GFP vesicles move significantly slower (mean velocity =  $0.0738 \pm 0.007 \mu\text{m}/\text{sec}$ ) than WT-Cav1-GFP (mean velocity =  $0.115 \pm 0.008 \mu\text{m}/\text{sec}$ ) (Fig. 2.10). This was however done at the ventral surface of the cell (the part of the membrane which is in contact with the coverslip). All these results indicate that pTyr14-Cav1 does regulate mobility of Cav1 in MEFs in 2D as well as 3D. The effect of pTyr14-Cav1 seems to be similar in 2D and 3D. Levels of this phosphorylation do not change in 3D unlike FAK. Both of these phosphorylations are partly dependent on integrins but their regulation seems very different in 3D. In response to a particular stimulus like growth factor or mechanical stimulus,

whether levels of pTyr14-Cav1 and also its effect on mobility of Cav1 change in 3D remains to be tested.

## **2.5 Summary**

We standardized embedding, imaging and FRAP in cells in 3D collagen gels. Standardization of FRAP was done using the K-Ras-CAAX-GFP construct, evaluating the effect increasing ROIsize on its recovery. This indicates that the recovery of K-Ras-CAAX-GFP is indeed majorly via diffusion. We further compared the mobility of WT-Cav1 in cells plated on 2D collagen versus those embedded in 3D collagen and evaluated the role its phosphorylation on the tyrosine-14 residue has on the same. We find that when expressed in caveolin-1 null cells embedded in 3D the mobile fractions of Y14F-Cav1 GFP was significantly lesser than WT-Cav1 GFP. This when compared in 2D cells at the cell trailing edge was seen to be similar, that is, Y14F-Cav1 was found to be less mobile at these two places. We checked co-localization of Cavin1 and Cav1 at these three places. Ventral membrane had the least extent of co-localization and edge and 3D membrane had highest co-localization. Levels of pCav1 were comparable in 3D as compared to those in 2D. Both of these results suggest that levels of pTyr14-Cav1 and its effect on Cav1 mobility on the plasma membrane are comparable in 2D and 3D.

## CHAPTER 3

Mobility of various membrane associated proteins in cells in  
2D v.s. 3D microenvironment : Role of Cav1

### **3.1 Rationale**

The main functions attributed to caveolae include signaling, cholesterol homeostasis, endocytosis and mechanosensing. Caveolae and Cav1 have been implicated in cell signaling for many years. The hypothesis was, Cav-1 has a scaffolding domain (CSD) which physically interacts with Cav-1 binding domain (CBD) present in many signaling molecules and controls signaling downstream (Couet et al., 1997b; Okamoto et al., 1998). However, recently, a detail structure-based analysis showed that, this CBD is deeply buried inside the protein (all signaling proteins) and hence direct physical interaction between Cav-1 and signaling molecules containing CBD is being questioned (Collins et al., 2012). Recently, alternative hypothesis has come up in the field that caveolae act as organizers of plasma membrane which eventually influence signaling downstream. A comprehensive lipidomic analysis showed that Cav1-KO MEFs have deregulated glycosphingolipid (GSL) and sphingolipid (SL) metabolism. It was also shown that Cav1-KO MEFs have alterations in glycerophospholipids, with a higher phosphatidylcholine (PC) / phosphatidylethanolamine (PE) ratio compared with WT-MEFs and altered phosphatidyl serine (PS) distribution. This was further reflected in differential clustering of Ras isoforms and hence signaling downstream (Ariotti et al., 2014). Apart from altering membrane composition, caveolae have also shown to affect membrane order (Gaus et al., 2006). Using Laurdan probe, the authors have shown that Cav1-KO MEFs have less abundant ordered membrane fraction as compared to WT-MEFs. This was also shown to be dependent on Tyr14-Cav1. Altered membrane order could also be a factor which will eventually affect cellular signaling.

Here, we have explored the role of caveolin and phosphocaveolin in membrane of cells which are embedded in a three-dimensional (3D) microenvironment. Recently, studying cell behavior in a 3D microenvironment has proven to be more comprehensive than conventional two-dimensional (2D) cultures. *In vivo*, cells experience a complex and dynamic 3D microenvironment and hence 3D cultures are considered to be more close to physiological conditions than 2D. Various phenomenon in cells including morphology of cells, integrin mediated adhesion structures, integrin signaling, arrangement of cytoskeleton, modes of migration etc., are shown to be different in 3D as compared to 2D. Along with all these, composition and properties of plasma membrane are also shown to be different in cells growing in 3D matrices. Fibroblast cells were grown in cell-derived matrices and, it was shown that

cholesterol and sphingomyelin content in the membrane was more in 3D than 2D. Same study reported that the membrane cholesterol in cells growing in 3D was more susceptible to oxidation and was asymmetrically distributed among the two leaflets of plasma membrane (Stefanova et al., 2009). Because of this asymmetric distribution, differences in the fluidity of the outer and the inner plasma membrane monolayers were less pronounced in 3D than 2D cells. All these properties of the plasma membrane regulate crucial cellular processes like receptor clustering, endocytosis and exocytosis, etc. Thus, studying how membrane properties are different in 3D than 2D will provide information on these cellular functions as well.

How caveolin and phosphocaveolin regulate membrane properties of cells in 3D is not known and we have addressed that in this chapter by comparing mobility of various membrane associated proteins in WT versus Cav1-KO MEFs. Our results indicate to the fact that membrane in 2D and 3D is indeed different as the mobility of all these constructs is differentially regulated in 2D versus 3D.



## **3.2 Materials and methods**

### **3.2.1 Plasmids**

H-Ras-CAAX-GFP and K-Ras-CAAX-GFP were a kind gift from Dr. Konstadinos Moissoglu. Cav1-flag and Y14F-flag was a kind gift from Dr. Martin Schwartz's lab. GPI-GFP was a kind gift from Dr. Steve Lacy's lab. EGFR-GFP was procured from Addgene (plasmid # 32751).

### **3.2.2 Cell culture**

Mouse embryonic fibroblasts (MEFs) - WT MEFs and Cav1-KO MEFs (from the lab of Dr. Richard Anderson, University of Texas Health Sciences Center, Dallas TX) were cultured in high glucose DMEM medium with 5% fetal bovine serum, penicillin and streptomycin (Invitrogen). For transfections  $1 \times 10^5$  cells were seeded in a 35 mm petri plate. After they had attached and started spreading (after about 2-3 hours), they were transfected with  $2 \mu\text{g}$  of DNA.  $4 \mu\text{l}$  of Plus reagent and  $5 \mu\text{l}$  of Lipofectamine-LTX (Invitrogen Cat. No. 15228100) was added to the transfection mix. Transfection mix was prepared in  $500 \mu\text{l}$  OptiMEM (Invitrogen, Cat. No. 5198509) and incubated for 30 minutes before adding to cells. Cells were incubated with  $1.5 \text{ ml}$  complete DMEM +  $0.5 \text{ ml}$  transfection mix for 12 hours. Medium was changed after 12 hours and cells were used for further experiment.

### **3.3.3 FRAP analysis and fitting - comparison of two equations**

The diffusion coefficients (D) of K-Ras-CAAX-GFP, H-Ras-CAAX-GFP and GPI-GFP were calculated by FRAP with two different equations :

1) Ellenberg's equation :

$$I_{(t)} = I_{(\text{final})} (1 - (w^2 (w^2 + 4\pi Dt)^{-1})^{1/2})$$

Where,

$I_{(t)}$  = intensity as a function of time,

$I_{(\text{final})}$  = final intensity reached after complete recovery,

w = width of bleach box,

D = effective one-dimensional diffusion coefficient.

2) Yguerabide's equation :

$$F(t) = \frac{F(0) + F(\infty)(t/t_{1/2})}{1 + (t/t_{1/2})}$$

Where,

$F_{(t)}$  = fluorescence intensity as a function of time,

$F_{(0)}$  = fluorescence intensity at time 0,

$F_{(\infty)}$  = final fluorescence intensity reached after complete recovery,

$t_{1/2} = T_{\text{half}}$

D was further calculated using this equation :

$$T_{\text{half}} = w^2/4D$$

Where,

w = width of bleach box,

D = effective one-dimensional diffusion coefficient.

Ellenberg's equation (Ellenberg et al., 1997) assumes one-dimensional diffusion whereas Yguerabide's equation (Yguerabide et al., 1982) assumes two-dimensional diffusion of proteins on the membrane.

### **3.3.4 Embedding cells in 3D collagen**

48 hours Post transfection, cells were detached with trypsin and embedded in 1.5 mg/ml Collagen Type-1, Rat tail (Corning - Cat no. 354236). A mixture of 10X PBS, sterile mili-Q water and collagen (to make final concentration to 1.5 mg/ml), in a total volume of 400µl. This amount varies according to the stock bottle concentration). This mixture was kept on ice for 5 mins.  $4 \times 10^4$  cells were mixed with this collagen solution and 1N NaOH was added (final concentration in the gel is 0.006N). After proper mixing, this collagen I (volume 400 µl) with cells was transferred to one well of a LabTek chamber (Thermo Scientific). The chamber was kept in 37C incubator with 5% CO<sub>2</sub> supply for about 30 minutes. The gel polymerized in 30 minutes, after which 400 µl DMEM (5% FBS) was added on top and the chamber was further kept at 37<sup>0</sup>C for 12 more hours

### **3.3.5 2D collagen coating**

Coverslips (from VWR) were first washed with KOH + methanol solution (25g KOH in 500ml methanol) and thoroughly washed with MiliQ water. Washed coverslips are stored in 100% ethanol and are flame-dried and subjected to UV sterilization for 30 minutes before using. Collagen coating is done in two steps. First step involved a 4 µg/ml collagen solution made in 70% ethanol (molecular biology grade). This solution was added on the coverslip to cover it fully (about 200 µl, varies depending on the size of the coverslip). The coverslips were then allowed to air dry under UV (until all the solution evaporated). After this 100 µg/ml collagen solution (made in DPBS) was added (2 ml) and coverslips were incubated at 4<sup>0</sup>C overnight. Next day, collagen solution was aspirated and coverslips were washed twice with 1X PBS and then used to seed cells.

### **3.3.6 Statistical analysis**

Statistical analysis of data was done using Mann-Whitney test as the data sets had non-normal distribution (confirmed by Shapiro–Wilk test). All analysis was done using Prism Graphpad analysis software. Statistical significance was considered at  $p < 0.05$ .

### **3.3 Results**

#### **3.3.1 Various membrane associated proteins used for FRAP experiments**

<b>Construct</b>	<b>Description</b>	<b>Localization</b>
K-Ras-CAAX-GFP	CAAX motif and polybasic region of K-Ras 4B tagged to GFP	Inner leaflet of plasma membrane
H-Ras-CAAX-GFP	CAAX motif and hypervariable region of H-Ras tagged to GFP	Inner leaflet of plasma membrane
GPI-GFP	Glycosylphosphatidylinositol anchor tagged to GFP	Outer leaflet of plasma membrane
EGFR-GFP	Full length EGFR (human) tagged to GFP	Transmembrane

**Table : 3.1: List of constructs used for FRAP experiments.**

To study how plasma membrane in cells embedded in 3D is different in those plated on 2D, we decided to look at mobility of different constructs. To elucidate the contribution of Cav1 in regulating this, we compared the mobility in WT MEFs versus Cav1-KO MEFs. The list of all constructs is given in the table above. The localization of these in WT MEFs versus Cav1-KO MEFs looked exactly the same (Fig 3.1). They localize to different parts of the plasma membrane - inner leaflet / outer leaflet / transmembrane. This however could not be resolved in confocal microscopic images.

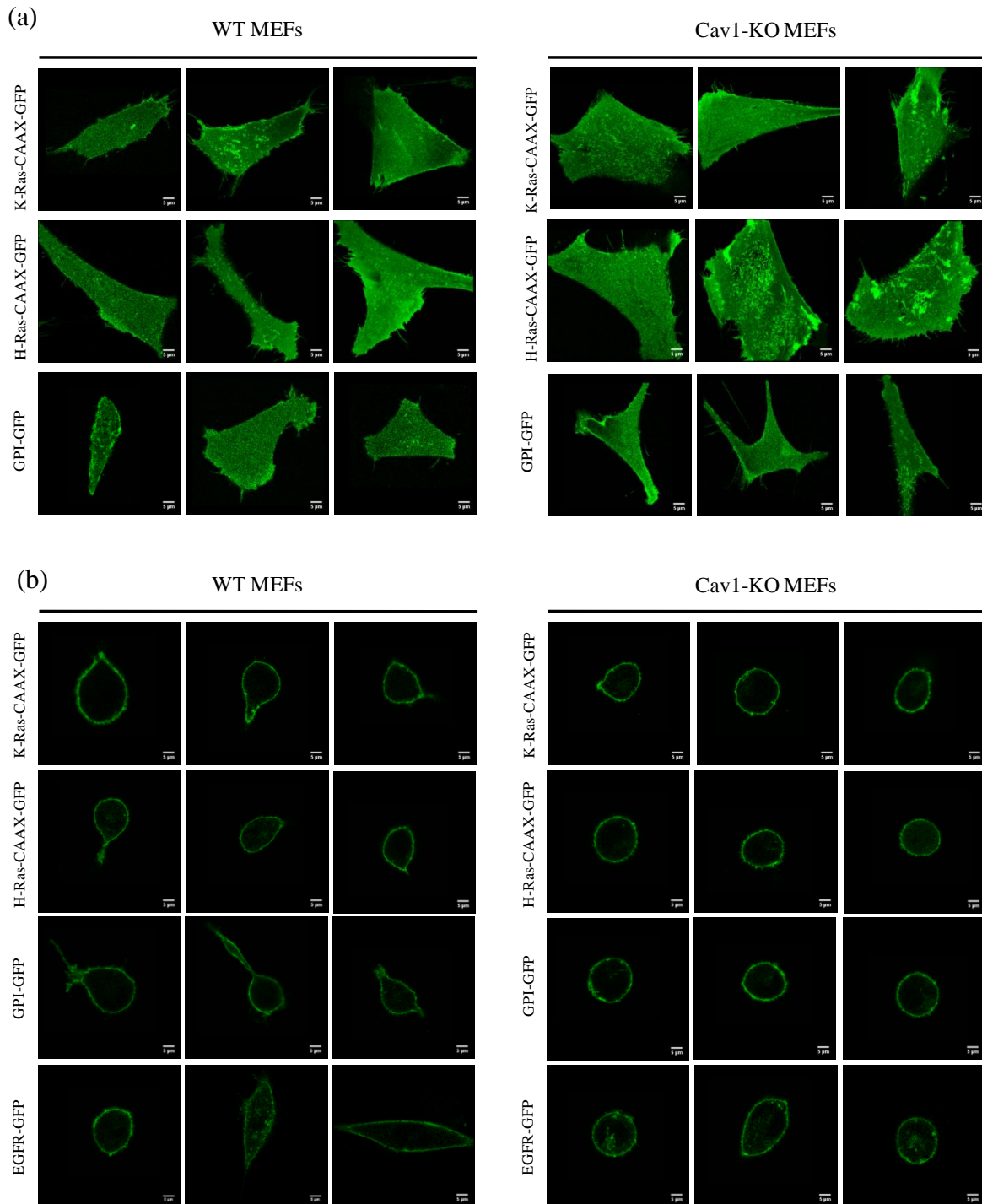


**Fig 3.1 Localization of all constructs (2D and 3D).** (a) Cells plated on 2D collagen and (b) cells embedded in 3D collagen gels, expressing the specified construct. Images are recorded on confocal microscope, cross sections are represented. Images are representative from at least four different experiments.

### 3.3.2 Description of different bleach geometries used in FRAP experiments

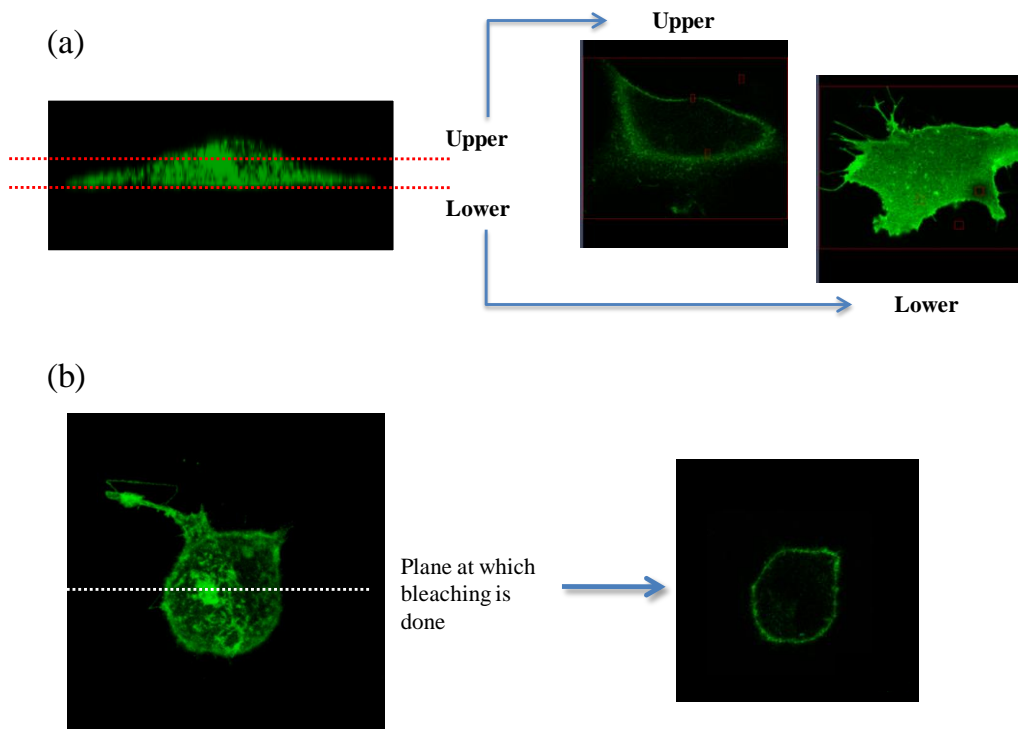


**Fig 3.2 Schematic explaining different bleach geometries.** (a) Cells plated on 2D collagen – bleaching done at lower plane and upper plane, (b) Cells embedded in 3D collagen. Upper plane in 2D and 3D membrane data fitted using one dimensional diffusion equation and lower plane in 2D fitted with two dimensional diffusion equation .

Photobleaching experiments were performed at two different planes in cells plated on 2D collagen -

- 1) lower plane of the cells, which is attached to the coverslip and is stretched as a flat sheet and
- 2) upper plane of the cells, which is not in contact with the coverslip but is still stretched over the nucleus. This however appears as a curved membrane, unlike flat sheet at the lower plane.

These two bleach geometries are quite different and hence we used two different equations to extract D values from the two. The possible differences between these two planes are listed below :

Upper plane	Lower plane
Not in contact with ECM	Is in contact with ECM
No ECM bound integrins	More ECM bound integrins
Integrin mediated signaling : Lower	Integrin mediated signaling : Higher
Tension might be lower	Tension might be higher

**Table 3.2 : Differences between upper plane and lower plane in 2D cells.**

The membrane in 3D cells also appears as a curved sheet, like upper plane in 2D cells. Hence we used same equation for upper plane and 3D, and a different equation for lower plane.

The membrane at **lower plane of cells is perpendicular to the laser beam** which bleaches it however, the membrane of cells embedded in **3D collagen and upper plane in 2D are parallel to the beam**. Confocal laser results in a hourglass kind of bleaching. Bleaching is strongest at the plane of focus in the sample and it decreases as we move away from the focused plane, both, below and above the plane of focus. The lower plane of 2D cells will not be affected by this hourglass effect but 3D membrane will get affected. Hence, we used Ellenberg's equation for analyzing FRAP data from 3D and upper plane, which accounts for this bleaching in the Z direction as it assumes the whole strip of membrane in XZ direction getting bleached. This equation was originally derived and used for ER and nuclear membrane and these bleach geometries are similar to 3D cell membranes (a curved sheet of membrane). The equation assumes diffusion to take place only in one dimension. For lower plane of 2D cells, bleaching will occur in two dimensions and hence for this plane, we chose Ygurabide's equation. This equation assumes diffusion to take place in two dimensions and was originally written and used for a flat sheet of membrane (similar to lower plane of 2D cells).



### **3.3.3 Mobility of K-Ras-CAAX-GFP : 2D v.s. 3D**

Earlier (Chapter 2) we have shown that the recovery of K-Ras-CAAX-GFP during FRAP experiments is majorly via diffusion, as  $T_{\text{half}}$  increased when ROI of bleaching was increased. Thus, looking at mobility of this construct in WT versus Cav1-KO MEFs as well as comparing these two cell types in 2D versus 3D will indirectly comment on the fluidity of the membrane itself.

WT MEFs and Cav1-KO MEFs were transiently transfected with K-Ras-CAAX-GFP and either plated on 2D collagen coated coverslips or embedded in 3D collagen gels (1.5 mg/ml) for 12 hours. A small region of 20X10 pixels was bleached on the plasma membrane and recovery was recorded. Diffusion coefficients (D) were derived from FRAP data and compared across different planes in WT MEFs versus Cav1-KO MEFs.

At lower plane and upper plane in 2D cells, we did not see any difference between diffusion coefficients in WT versus Cav1-KO MEFs (Fig 3.3 a, b). Interestingly, in 3D cells, diffusion coefficient for K-Ras-CAAX-GFP was higher in Cav1-KO MEFs as compared to WT MEFs (Fig 3.3 c).

We further tested whether this difference seen in 3D is dependent on Cav-1 and its phosphorylation. For this, we transiently expressed Cav1-flag or Y14F-Cav1-flag in Cav1-KO MEFs along with K-Ras-CAAX-GFP (expression levels were comparable, Fig 3.3 d). We found that both WT and Y14F-Cav1 flag decreased the mobility of K-Ras-CAAX-GFP to what it is in WT-MEFs (Fig. 3.3 c) suggesting that Cav1 regulates the mobility of K-Ras-CAAX-GFP, however, the phosphorylation of Cav-1 is not needed in regulating mobility of K-Ras-CAAX-GFP. This implies that the altered mobility is only because of presence or absence of caveolae. Since Y14F-Cav1 also makes caveolae, it was able to rescue the phenotype as WT-Cav1 did.

We observed a slight difference (not statistically significant) in how WT versus Y14F-Cav1 regulated diffusion of K-Ras-CAAX-GFP. Y14F-Cav1 had a more pronounced effect on decreasing diffusion of K-Ras-CAAX-GFP as compared to WT-Cav1 (Fig 3.3 c). This could be because of the difference between mobility of WT and Y14F-Cav1 itself. We have earlier shown that Y14F-Cav1 mobile fraction was lesser as compared to WT-Cav1. The mobility of Cav1 constructs was measured earlier by calculating their mobile fractions (Chapter 2).

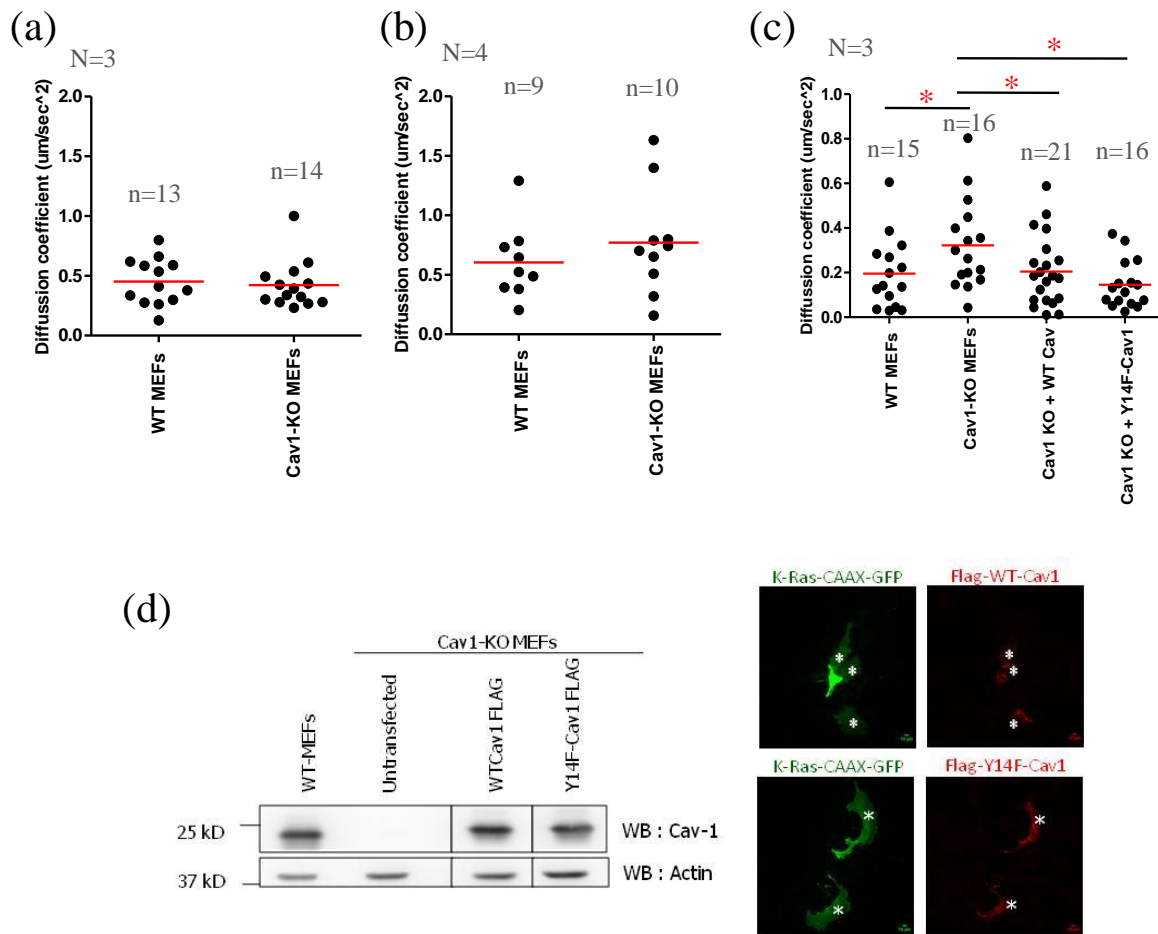


**Fig 3.3 Mobility of K-Ras-CAAX-GFP in WT and Cav1-KO MEFs in 2D v.s. 3D collagen.** Diffusion coefficients calculated from FRAP data for K-Ras-CAAX-GFP at (a) 2D lower plane, (b) 2D upper plane and (c) 3D.  $p < 0.005$ , significance calculated by Mann-Whitney test. (d) shows validation of reconstitution in Cav1-KO MEFs with flag tagged WT-Cav1 and Y14F-Cav1 by Western blot and immunofluorescence (IFA). The levels of over-expressed flag tagged constructs is equivalent to endogenous levels, present in WT MEFs (Cell equivalent loaded, also actin was used as loading control). IFA on the right shows that all the cells got co-transfected with both the constructs. Hence, the cells which were chosen to do FRAP, did also expressed the specified Cav1 construct. For detail statistics refer appendix.

### **3.3.4 Mobility of H-Ras-CAAX-GFP : 2D v.s. 3D**

We next looked at the mobility of another marker which gets localized to the inner leaflet of plasma membrane, H-Ras-CAAX-GFP. WT and Cav1-KO MEFs were transiently transfected with this construct and either plated on 2D collagen coated coverslips or embedded in 3D collagen (1.5 mg/ml) for 12 hours. Diffusion coefficient was derived from FRAP experiments, performed with a bleach box of 20X10 pixels on the plasma membrane.

For H-Ras-CAAX-GFP, there was no difference at upper plane in 2D cells and in 3D cells (Fig. 3.4 b and c). However, at lower plane of 2D cells, diffusion coefficient for H-Ras-CAAX-GFP was significantly higher in Cav1-KO MEFs as compared to WT MEFs (Fig. 3.4 a).

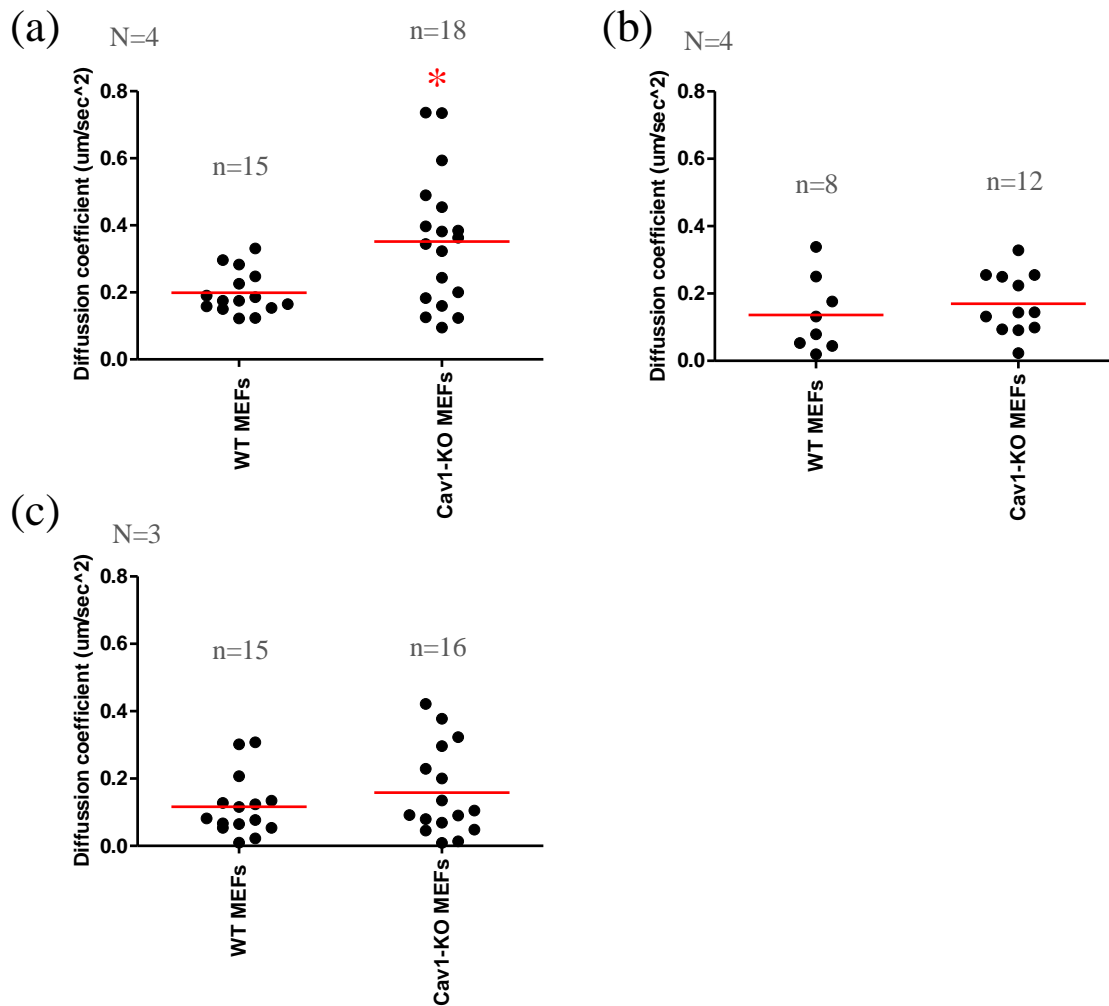


**Fig 3.4 Mobility of H-Ras-CAAX-GFP in WT and Cav1-KO MEFs in 2D v.s. 3D collagen.** Diffusion coefficients calculated from FRAP data for H/-Ras-CAAX-GFP at (a) 2D lower plane, (b) 2D upper plane and (c) 3D. Statistical significance ( $p < 0.005$ ) calculated by Mann-Whitney test. For detail statistics refer appendix.

### **3.3.5 Mobility of GPI-GFP : 2D v.s. 3D**

The third construct we tested was GPI-GFP, which gets anchored to the outer leaflet of the plasma membrane. WT and Cav1-KO MEFs were transfected with GPI-GFP and either plated on 2D collagen coated coverslips or embedded in 3D collagen (1.5 mg/ml) for 12 hours. Diffusion coefficient was derived from FRAP experiments, performed with a bleach box of 20X10 pixels on the plasma membrane.

For GPI-GFP, there was no difference at lower plane in 2D cells and in 3D cells (Fig. 3.5 a). However, at upper plane of 2D cells, diffusion coefficient for GPI-GFP was significantly higher in Cav1-KO MEFs as compared to WT MEFs (Fig. 3.4 b). In 3D, diffusion coefficient for GPI-GFP was slightly higher (not statistically significant) in Cav1-KO MEFs as compared to WT MEFs (Fig. 3.4 c).

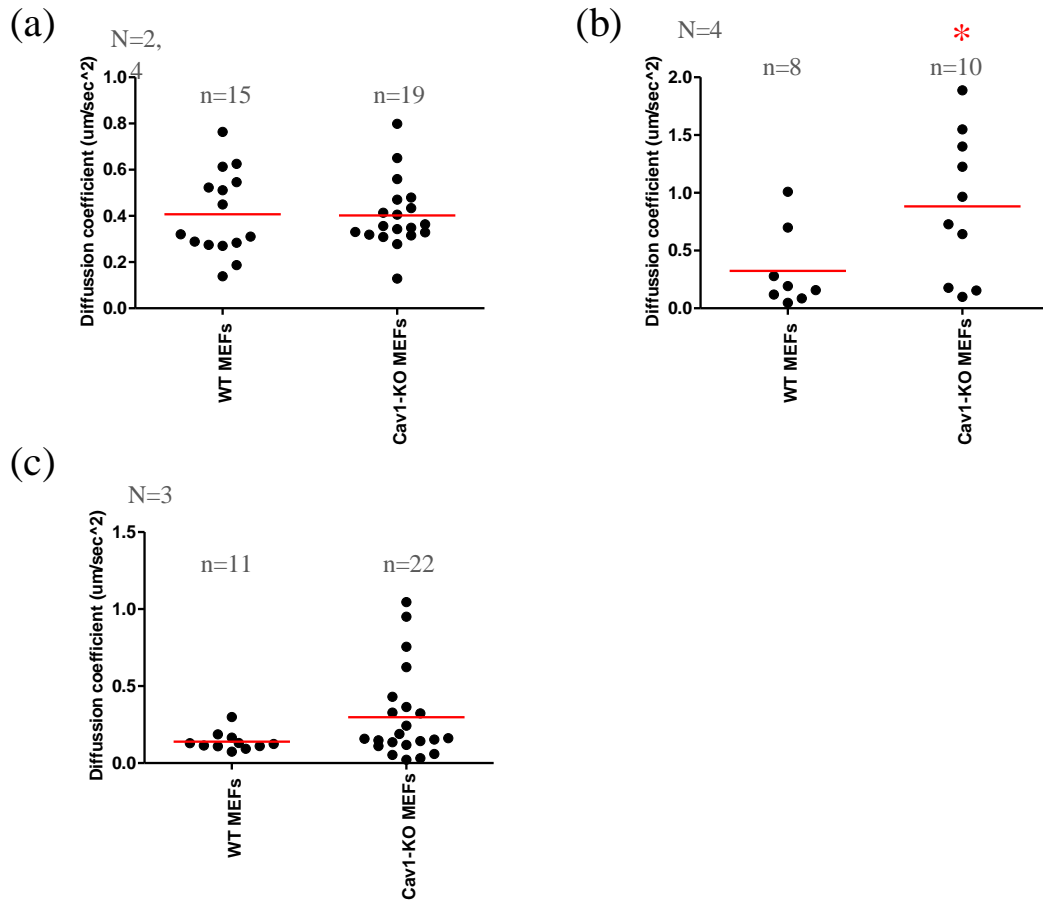


**Fig 3.5 Mobility of GPI-GFP in WT and Cav1-KO MEFs in 2D v.s. 3D collagen.** Diffusion coefficients calculated from FRAP data for GPI-GFP at (a) 2D lower plane, (b) 2D upper plane and (c) 3D. Statistical significance ( $p < 0.005$ ), calculated by Mann-Whitney test. For detail statistics refer appendix.

### **3.3.6 Mobility of EGFR-GFP : 3D**

Since there was difference in 3D for K-Ras-CAAX-GFP (inner leaflet marker) and GPI-GFP (outer leaflet marker), we decided to measure mobility of a transmembrane protein, EGFR-GFP. Cells were transiently transfected with full length EGFP-GFP, embedded in 3D collagen (1.5 mg/ml) and diffusion coefficient was calculated from FRAP experiments. Diffusion coefficient for EGFR-GFP was significantly higher in Cav1-KO MEFs as compared to WT MEFs in 3D.

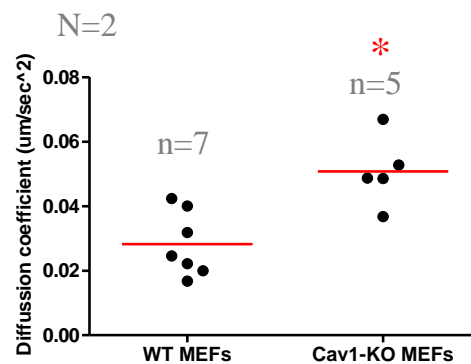


**Fig 3.6 Mobility of EGFR-GFP in WT and Cav1-KO MEFs in 3D collagen.** Diffusion coefficients calculated from FRAP data. Data represented from two independent experiments. Statistical significance ( $p < 0.05$ ) calculated by Mann-Whitney Test. For detail statistics refer appendix.

### **3.4 Discussion**

The classical text book model of plasma membrane is the **fluid-mosaic model** which assumes lipid bilayer as a neutral two-dimensional solvent in which integral membrane proteins are embedded and are free to move (Singer and Nicolson, 1972). In past few decades this model however **has been challenged** by many experimental results and now the accepted view is that the plasma membrane is not a homogenous entity, but **contains many inhomogenities** (Edidin, 1997; Jacobson et al., 1995; Vereb et al., 2003). Proteins and lipids in the plasma membrane hence cannot diffuse freely within the membrane and there are certain barriers known for diffusion. These include membrane associated cytoskeleton, cell-cell junctions, cell-matrix junctions, cilia, nano and microdomains on the plasma membrane like caveolae and CEMMs (cholesterol enriched membrane microdomains), etc (Trimble and Grinstein, 2015).

Membrane associated cytoskeleton or **cortical actin cytoskeleton** acts as a barrier not just for inner leaflet proteins but also of proteins anchored the outer leaflet and even simple lipids (Fujiwara et al., 2002; Suvrajit Saha et al., 2015; Suzuki et al., 2007). **Tight junctions, adherence junctions and as well as focal adhesions** can concentrate and immobilize proteins, hence generating impenetrable barriers (Gulino-Debrac, 2013; Paszek et al., 2014). **Cilia** are projections found in most non-mitotic cells in vertebrates. The membrane which covers cilia is in continuation with rest of the plasma membrane, yet has a unique set of proteins and lipids (Singla and Reiter, 2006). Exclusion of certain membrane proteins (for example, podocyclin) from the cilium is one of the mechanism how cilia act as diffusion barrier (Francis et al., 2011). **Nanodomains and microdomains** on the plasma membrane can be formed by passive association between proteins and/or lipids of compatible structure, hydrophobicity and charge. **Caveolae** are a specialized type of such domain on the plasma membrane which are **different from CEMMs** as they have a definite shape and size because of presence of caveolin proteins.

Caveolae are rich in cholesterol and sphingolipids and hence they harbor certain proteins which have affinity towards these lipids. This causes latching of these proteins (for example H-Ras) inside caveolae and that process limits their diffusion (Prior et al., 2001). Recently, it was shown that **Cav1 alters membrane composition** in fibroblast cells. This affects **membrane organization** and differentially regulates H-Ras and K-Ras clustering and probably signaling too



(Ariotti et al., 2014). However, all these studies have been done in cells plated on 2D coverslips or tissue culture plates, which is an artificial environment for cells. A more physiological system is 3D microenvironment and hence we looked at how caveolae affect diffusion of different membrane associated proteins in a 3D microenvironment. This indirectly gives information about the plasma membrane and its organization in cells in 3D.

For this, we looked at two markers of the inner leaflet of plasma membrane - K-Ras-CAAX-GFP and H-Ras-CAAX-GFP, one marker of outer leaflet - GPI-GFP and one transmembrane protein - EGFR-GFP. **Inner leaflet and outer leaflet of the plasma membrane** are different in their composition as well as organization. CEMMs or so called lipid rafts have been shown to be formed only on the outer leaflet (Bucci, 2013). Not much is known about the organization of the inner leaflet and that is something currently being explored. One more difference between these two leaflets is that the inner leaflet is in close contact with the cortical actin network whereas the outer leaflet is in contact with the extracellular matrix. These different associations can also regulate certain processes like diffusion in these two leaflets differentially.

The constructs we have used in this study are hyper-variable regions and CAAX motifs of K and H Ras respectively, cloned in EGFP-C1 vector. **These two differ in their post-translational modification**, that, the CAAX motif of K-Ras doesn't undergo palmitoylation like H-Ras-CAAX does. K-Ras has a polybasic region just before its CAAX motif and hence there is electrostatic interaction between membrane and polybasic region which is required for its membrane targeting (Prior and Hancock, 2001). K-Ras, irrespective of its activation status, always associates with cholesterol independent nano-domains. And H-Ras is known to shuttle between cholesterol independent (Active H-Ras) and dependent (Inactive H-Ras).

It is shown earlier by FRAP that mobility of H-Ras (but not K-Ras) is sensitive to **cholesterol content** of plasma membrane (Niv et al., 2002). Another membrane lipid, **Phosphatidyl serine (PS)** is shown to be required for K-Ras clustering but not that of H-Ras. Interestingly, inner leaflet PS content is unaltered upon Cav1 knock down however, PS clustering increases upon Cav1 deficiency (Ariotti et al., 2014). Increased PS clustering is shown to increase K-Ras clustering (both whole protein and CAAX motif).

We saw that in 2D (lower plane), mobility of H-Ras-CAAX-GFP was higher in Cav1-KO MEFs than WT MEFs but this difference was not observed in 3D. On the other hand, there was no difference in the mobility of K-Ras-CAAX-GFP in WT versus Cav1-KO MEFs in 2D, but it was higher in Cav1-KO MEFs in 3D collagen. These results indicate to the fact that arrangement of different domains of plasma membrane in cells in 2D versus 3D could be different.

GPI-GFP is localized to the outer leaflet of the plasma membrane, having affinity towards cholesterol rich microdomains. Diffusion of GPI-GFP is mainly governed by cortical actin cytoskeleton, even though it anchors to the outer leaflet of the plasma membrane (Saha et al., 2015). Caveolae have also been shown to limit the mobility of GPI-GFP on the plasma membrane (Hoffmann et al., 2010). EGFR-GFP diffusion is dependent on its activation, clustering and its association with the plasma membrane.

We found that for all three constructs used in this study, their diffusion was differentially regulated at 2D lower plane versus 2D upper plane versus 3D. We further looked at EGFR-GFP mobility and that was found to be higher in Cav1-KO MEFs. We also observed that diffusion coefficients for K-Ras-CAAX-GFP and GPI-GFP were higher in 3D as compared to 2D. This could also mean that the membrane in 3D is more fluid than 2D.

The membrane composition in 3D has already been suggested to be different by others. Particularly, cholesterol and sphingomyelin content in the membrane was more in 3D than 2D. Same study reported that the membrane cholesterol in cells growing in 3D was more susceptible to oxidation and was asymmetrically distributed among the two leaflets of plasma membrane. Because of this asymmetric distribution, differences in the fluidity of the outer and the inner plasma membrane monolayers were less pronounced in 3D than 2D cells (Stefanova et al., 2009). All of this suggests that membrane in 3D could be different in aspects like organization, fluidity, etc than that in 2D. It is also possible that the tension on the membrane will be different in cells in 2D versus 3D and that can regulate certain processes in cells differentially. Caveolae being mechanosensors which buffer the membrane tension, the membrane in WT MEFs when compared to Cav1-KO MEFs could behave differently in 3D matrices.

Our study for the first time has tried to in detail study diffusion of different plasma membrane markers in cells in 3D and have revealed differences between 2D and 3D. Since the diffusion

coefficients of K-Ras-CAAX-GFP are higher in cells embedded in 3D as compared to 2D, there is a possibility that membrane in cells in 3D is more fluid than those in 2D. Increased membrane fluidity affects clustering of receptors on the membrane and hence this could have further effect on downstream signaling. Such altered membrane properties can also regulate other processes in cells like endocytosis, which we have tested in the next chapter.

### **3.5 Summary**

The results for each construct at all three different bleach geometries in WT versus Cav1-KO MEFs are summarized in the following table.

Construct studied	2D : Lower plane	2D : Upper plane	3D
K-Ras-CAAX-GFP	WT MEFs = Cav1-KO MEFs	WT MEFs = Cav1-KO MEFs	WT MEFs < Cav1-KO MEFs
H-Ras-CAAX-GFP	WT MEFs < Cav1-KO MEFs	WT MEFs = Cav1-KO MEFs	WT MEFs = Cav1-KO MEFs
GPI-GFP	WT MEFs = Cav1-KO MEFs	WT MEFs < Cav1-KO MEFs	WT MEFs = Cav1-KO MEFs
EGFR-GFP	Not done	Not done	WT MEFs < Cav1-KO MEFs

**Table 3.3: Summary of FRAP experiments for various membrane associated markers**

## CHAPTER 4

# Regulation of endocytosis in a 3D microenvironment : Role of Cav1 and pTyr14-Cav1

## **4.1 Rationale**

Caveolae were initially thought to be a major endocytic organelles in cells as they resemble clathrin-coated pits. However, unlike clathrin-coated pits, they are very static and stable structures. Caveolae do internalize certain cargos but there are very few which are exclusively taken through caveolae, hence making them redundant. Cargos which are internalized via caveolar route include CTxB (Cholera Toxin B subunit), shiga toxin, GPI linked proteins, BSA, SV40 virus and some bacteria, IL2 receptors, etc (Johannes and Lamaze, 2002; Nichols and Lippincott-Schwartz, 2001; Pelkmans and Helenius, 2002).

Other interesting aspect of regulation of endocytosis by caveolin and cavin is that these proteins regulate the second major endocytic pathway in cells - the clathrin independent pathway. Cav1 and Cavin-1 are shown to negatively regulate the CLIC-GEEC, Cdc42 regulated endocytic pathway (Chaudhary et al., 2014). It was shown that this pathway is up regulated in the absence of Cav1 and Cavin1 and the regulation is independent of caveolae formation. Cav1 reduces the mobility of lipid raft markers on the plasma membrane and Cavin1 influences cholesterol distribution and Cdc42 activity. Both of these eventually resulted in reduced endocytosis of CD-44, a marker specific to CLIC-GEEC pathway.

Altered membrane properties like fluidity or tension can also regulate endocytosis. Increased fluidity and increased membrane tension both trigger the process of endocytosis of certain cargos (Dai et al., 1997; Shi and Baumgart, 2015). It is also shown that membrane tension regulates dynamics of clathrin-coated pits (Tan et al., 2015). All this is however done in cells plated on glass coverslips (2D). Nothing is known how is endocytosis regulated in cells in a 3D microenvironment and how caveolin affects the same. The two key elements, cytoskeleton and plasma membrane, which regulate the process of endocytosis, are either known or speculated to be different in a 3D microenvironment. Hence, it is possible that regulation of endocytosis will be different in 3D and hence we studied that here. We also focused on effect of ECM stiffness on endocytosis by embedding cells in collagen gels with different concentrations.

## **4.2 Materials and methods**

### **4.2.1 Reagents**

Fluorescently conjugated CTxB-488 (Cat. No. C34775), CTxB-594 (Cat. No. C22842), transferrin-texas red conjugate from Human serum (Cat. No. T2875) and DQ-BSA Red (Cat. No. D12051) all were procured from Molecular Probes, Invitrogen. High concentration collagen stock: 10 mg/ml (Cat. No. 354236) was procured from Corning. Actin disrupting drugs, Latrunculin A (Cat. No. L5163) and Cytochalasin D (Cat. No. C8273) were from Sigma.

### **4.2.2 Cell culture**

Mouse embryonic fibroblasts (MEFs) - WT MEFs and Cav1-KO MEFs (from the lab of Dr. Richard Anderson, University of Texas Health Sciences Center, Dallas TX) were cultured in high glucose DMEM medium with 5% fetal bovine serum, penicillin and streptomycin (Invitrogen). For transfections  $1 \times 10^5$  cells were seeded in a 35 mm petri plate. After they had attached and started spreading (after about 2-3 hours), they were transfected with 2  $\mu$ g of DNA. 4  $\mu$ l of Plus reagent and 5  $\mu$ l of Lipofectamine-LTX (Invitrogen Cat. No. 15228100) was added to the transfection mix. Transfection mix was prepared in 500  $\mu$ l OptiMEM (Invitrogen, Cat. No. 5198509) and incubated for 30 minutes before adding to cells. Cells were incubated with 1.5 ml complete DMEM + 0.5 ml transfection mix for 12 hours. Medium was changed after 12 hours and cells were used for further experiment.

### **4.2.3 Labeling cells in 3D collagen**

Cells (WT MEFs or Cav1-KO MEFs) were embedded in specified collagen concentration gel and the gels were allowed to polymerize at 37<sup>0</sup>C. (Detail protocol for embedding - refer to section 2.2.3). After the gels were polymerized properly, labeling with a particular probe was carried out on ice. Medium containing the probe was added and the LabTek chambers were incubated on ice for 20 minutes. Concentrations of the probes used are as follows - CTxB

:1:2000, Transferrin-texas red : 25 µg/ml and DQ-BSA : 30 µl/ml of medium (from 1 mg/ml stock). After 20 minutes, fresh medium was added to the wells and cells were further incubated for 3 hours at 37°C and then imaged .

#### **4.2.4 Cytochalasin D and Latrunculin A treatment**

Drug treatments were performed on WT MEFs after embedding in collagen gels. Cells were first embedded in collagen and drugs were added for 30 minutes before proceeding for labeling. GM1-CTxB labeling was carried out as explained above in a medium which contained drugs. After labeling was done (20 minutes), cells were washed once and again fresh medium containing respective drugs. Latrunculin A was used at a concentration of 0.001 µM and Cytochalasin D was used at a concentration of 1 µM. An equivalent amount of DMSO was added to the control wells as vector controls. Both these drug treatments were for a total duration of 180 min at 37°C.

#### **4.2.5 FRAP**

Cells were transfected 24 hours prior to photobleaching experiment. During FRAP experiments, cells were maintained in CO<sub>2</sub> independent Leibovitz L-15 medium (Invitrogen, 21083-027). Images were acquired using a 63X oil immersion objective on Zeiss LSM 780 confocal microscope, NA 1.4, at 2.2X digital zoom. A region of interest 20X10, 20X20, 20X30 or 20X50 were used for photobleaching on the plasma membrane (1 pixel = 0.12 µM) For photobleaching, we used the 488 nm laser line. 100% laser power was used for photobleaching (200 iterations for bleaching) after 10 scans of pre bleach, and image acquisition was performed every 0.5 sec.

Analysis of FRAP data (done using Ellenberg's equation) - refer to section 3.3.3.

#### **4.2.6 Atomic Force Microscopy (AFM)**

3D gels of rat tail collagen were prepared in a 60 mm petri plate with a glass bottom and probed by atomic force microscopy in DMEM on a Asylum user Bio-AFM. A cantilever (from

Novascan) having spring constant of 0.06 N/m; with a spherical tip (4.5  $\mu\text{m}$  radius) was used to calculate stiffness of collagen. Spring constants calibration was done in PBS on glass by acquiring both deflection sensitivity and thermal noise data subsequently fitted and corrected for a spherical-shaped cantilever. Matrix stiffness was measured at 40 different positions within a particular sample by bringing the cantilever into contact with the surface of the gel (contact force 2-7 nN; approach–retraction distance 26  $\mu\text{m}$ .. Force–distance curves from each measurement were converted into force–indentation (F- $\delta$ )curves and subsequently fitted with the Hertz model to calculate the stiffness:

$$F = \frac{4E(R_c)^{1/2}}{3(1-\gamma^2)} \times \delta^{3/2}$$

with  $F$ , force in Newtons [N];

$R_c$ , bead radius in meters [m];

$E$ , elastic modulus or stiffness in Pascals [Pa];

$\gamma$ , Poisson ratio of 0.5; and

$\delta$ , penetration/ indentation in meters [m].

#### **4.2.7 Second Harmonic Generation (SHG) imaging**

Collagen gels were prepared in a 35mm petri plates with glass bottom. SHG imaging was performed on a upright multiphoton microscope from Leica (TCS SP8). Gel samples were focused and excited with multiphoton laser at 1040 nm. Transmitted light detector was used to collect the signal. To get brighter images, the line averaging of 2 and frame acquisition of 3 was performed. A Z stack of total 10  $\mu\text{m}$  was recorded with a step size of 0.2  $\mu\text{m}$ . The Z stacks were deconvoluted using Huygens software for representative purpose. The images were opened in the deconvolution wizard and automatic background option was selected. Settings used for deconvolution were as follows : number of iterations = 30, signal to noise ratio = 20 and quality threshold = 0.001.



#### **4.2.8 Laser ablations**

WT MEFs were embedded in 1.5 mg/ml or 1 mg/ml collagen as explained earlier. Laser ablation experiments were performed on Zeiss LSM 780 scanning confocal equipped with two-photon laser. Ablation was performed by the MaiTai laser set at 800 nm and around 3000mW power. The actual ablation was done as a line (20 pixels in length, at 2.2 zoom) on the plasma membrane. For fluorescence imaging, the pinhole size was set so as to have Z-sections of about 0.8  $\mu\text{m}$ , thickness. A time lapse movie of 200 images with one image per 0.4 sec was recorded for each cell. After the movie was over, another image of the same cell was acquired after 4 minutes. Analysis was performed using ImageJ software (number of blebs per cell at a particular cross section - calculated manually).

#### **4.2.9 Statistical analysis**

Statistical analysis of data was done using Mann-Whitney test as the data sets had non-normal distribution (confirmed by Shapiro–Wilk test). All analysis was done using Prism Graphpad analysis software. Statistical significance was considered at  $p < 0.05$ .

## 4.3 Results

### 4.3.1 Endocytosis of GM1-CTxB and transferrin upon loss of adhesion

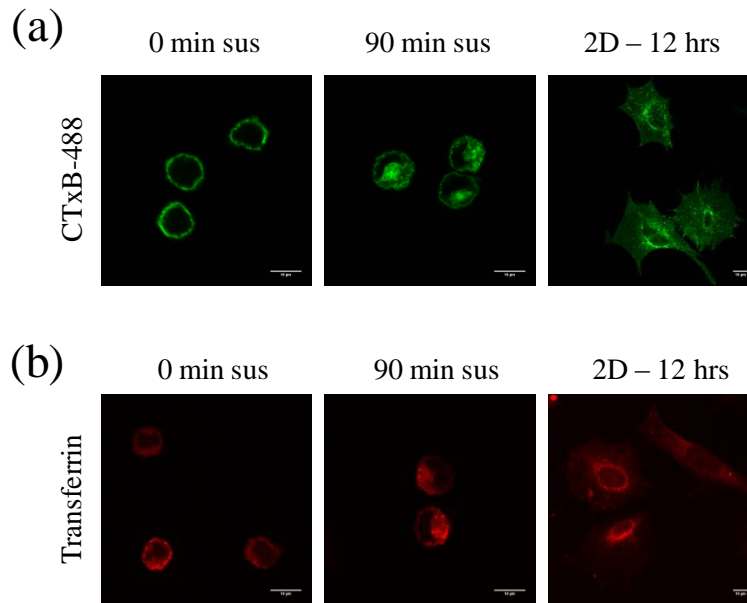


**Fig 4.1 CTxB and transferrin endocytosis in WT MEFs upon loss of adhesion.** Surface labeling of (a) CTxB-488 and (b) transferrin-texas red in WT MEFs. Images taken at 0 min suspension, 90 min suspension and 2D collagen – 12 hours.

Cholera toxin-B subunit (CTxB) binds to the lipid moiety GM1 on the plasma membrane and is endocytosed in cells via various routes. Upon loss of adhesion MEFs internalize CTxB through caveolar route Cav1 (del Pozo et al., 2005) but in 2D adherent cells, even upon Cav1-KD cells were shown to still internalize CTxB through other pathways, which include CLIC/GEEC or Arf6 dependent pathways. On the other hand, transferrin is internalized in cells by clathrin-coated pits. We confirmed that upon loss of adhesion, both these markers are endocytosed as reported earlier. They are also internalized by cells plated on collagen coated coverslips for 12 hours and present in the peri-nuclear region, again as reported earlier . (Fig 4.1).

### 4.3.2 Differential endocytosis of various markers in WT MEFs in 3D collagen

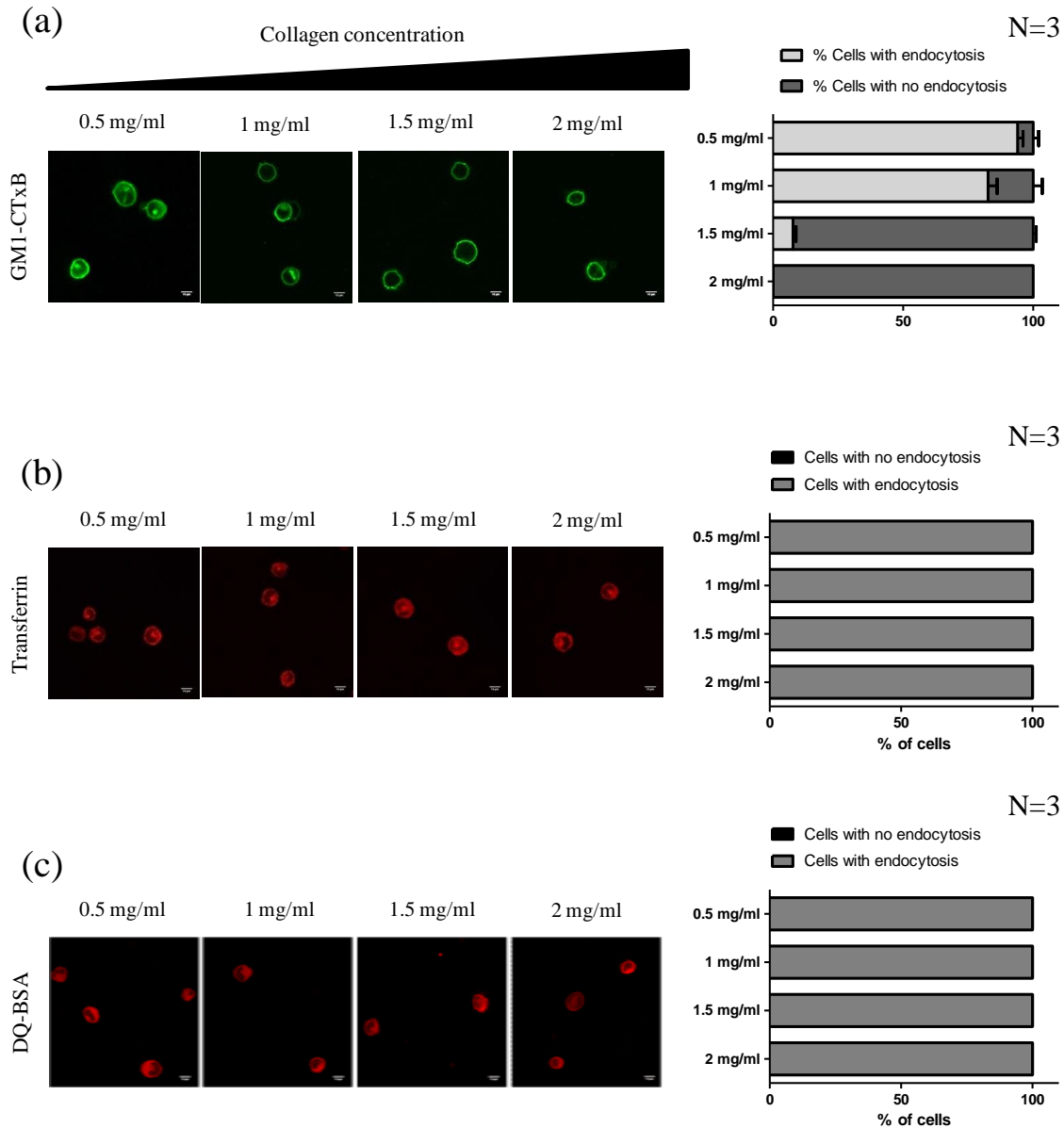


**Fig 4.2 Endocytosis of various markers in WT MEFs embedded in collagen gels of varying concentrations.** Endocytosis of (a) GM1-CTxB (b) Transferrin and (c) DQ-BSA in WT MEFs embedded in a range of concentrations of collagen gel. Quantitation (% of cells with a particular phenotype) is shown on the right. Images are representative from 3 independent experiments for each marker. 100 cells were analyzed in each set.

We next looked at endocytosis of various markers in cells embedded in 3D collagen. Substrate stiffness is shown to regulate endocytosis (Brugnano and Panitch, 2014; Huang et al., 2013). These studies have shown that certain endocytic pathways are responsive to ECM stiffness and generally, at higher substrate stiffness, these pathways are blocked. We looked at three markers : 1. CTxB (internalized majorly by caveolar route upon loss of adhesion and otherwise by other routes like Arf-6 dependent pathway, CLIC-GEEC); 2. Transferrin (internalized by clathrin-coated pits) and 3. DQ-BSA which is a highly self-quenched BODIPY dye conjugated form of BSA that emits a bright fluorescent signal only after proteolytic digestion (Reis et al., 1998). (Fig 4.2).

WT-MEFs were embedded at four different collagen gel concentrations - 0.5 mg/ml, 1 mg/ml, 1.5 mg/ml and 2 mg/ml. Transferrin and DQ-BSA were internalized by all cells (100%) at all 4 concentrations. However, interestingly, CTxB was not internalized by majority of the cells ( $92 \pm 1.2\%$ ) at 1.5 mg/ml collagen and 100% cells at 2 mg/ml collagen. This block at 1.5 mg/ml collagen was further confirmed by various ways, as explained in next two figures).

#### **4.3.3 GM1-CTxB endocytosis is blocked in WT MEFs in 1.5 mg/ml collagen**

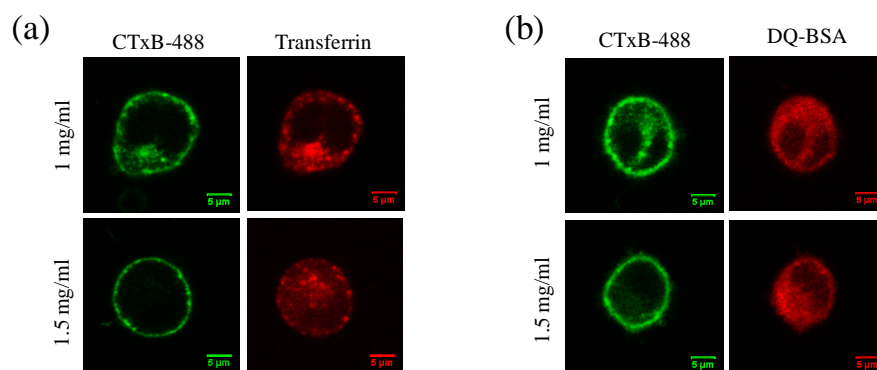


**Fig 4.3 Dual labeling of CTxB and transferrin endocytosis in WT MEFs in 3D collagen.** Co-labeling of (a) CTxB + Transferrin and (b) CTxB + DQ-BSA in WT MEFs at 1 mg/ml and 1.5 mg/ml collagen. Images are representative from 3 independent experiments.

First experiment to confirm that the GM1-CTxB endocytosis is blocked at 1.5 mg/ml but not 1 mg/ml, we looked at the endocytosis of either transferrin + GM1-CTxB (Fig 4.3 a) or DQ-BSA + GM1-CTxB (Fig 4.3 b).

In both the cases, at 1 mg/ml, there was no block of endocytosis for any of the marker. However, at 1.5 mg/ml, GM1-CTxB remained on the plasma membrane completely but transferrin and DQ-BSA both got internalized well. This confirmed that cells are able to use certain endocytic pathways at higher collagen concentrations but some pathways are blocked. Also since DQ-BSA fluorescence was observed in cells at all concentrations, it was confirmed that the lysosomal degradation pathway is working well in these cells in 3D. As, DQ-BSA fluoresces only when degraded (by lysosomes).

We further checked whether the block happens at higher cell density (Fig 4.4 a) as the cells in earlier experiments were very sparsely seeded and that could be one of the reason for blocked endocytosis. We seeded 5 times and 10 times more cells in the same amount of collagen gel and labeled the cells for GM1-CTxB. Even at higher cell densities, the cells did not internalize GM1-CTxB at all. We also checked at longer time points (longer than 4 hours, which was the time point used in earlier experiments) (Fig 4.4 b). There was no internalization of GM1-CTxB even after 12 hours of incubation of cells in 3D collagen at 1.5 mg/ml. Generally, the images are acquired at 2% laser power. We increased it up to 20% and still there was no staining seen inside the cell (Fig 4.4 b - lowermost panel).

All these experiments confirmed that the block in endocytosis for GM1-CTxB seen at 1.5 mg/ml is not an experimental artifact and an interesting observation which was pursued further.

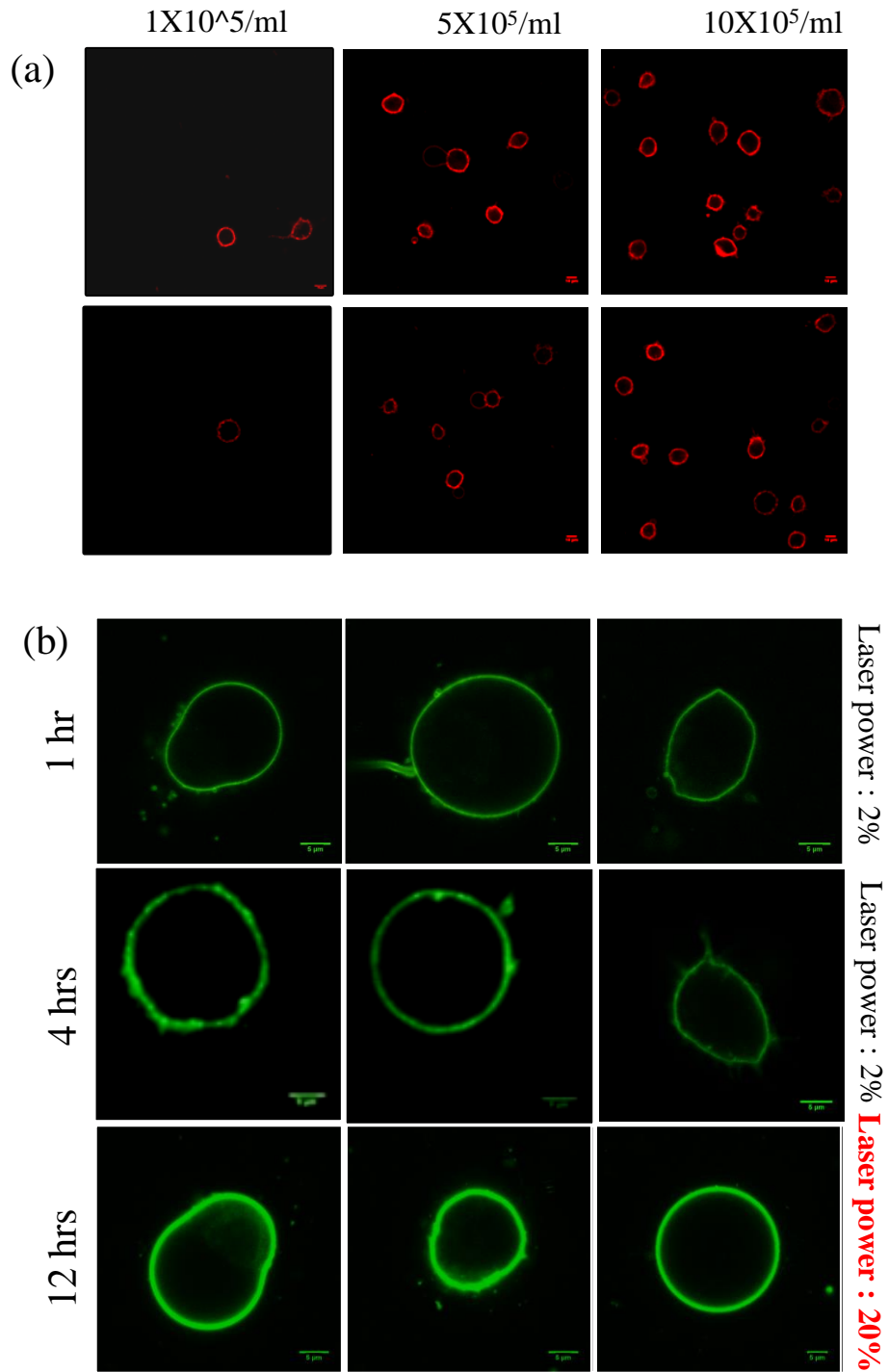


**Fig 4.4 CTxB endocytosis at 1.5 mg/ml is blocked at higher cell density and longer time points.** (a) WT MEFs at indicated cell densities and (b) time course of CTxB internalization.

#### 4.3.4 GM1-CTxB endocytosis in Cav1-KO MEFs

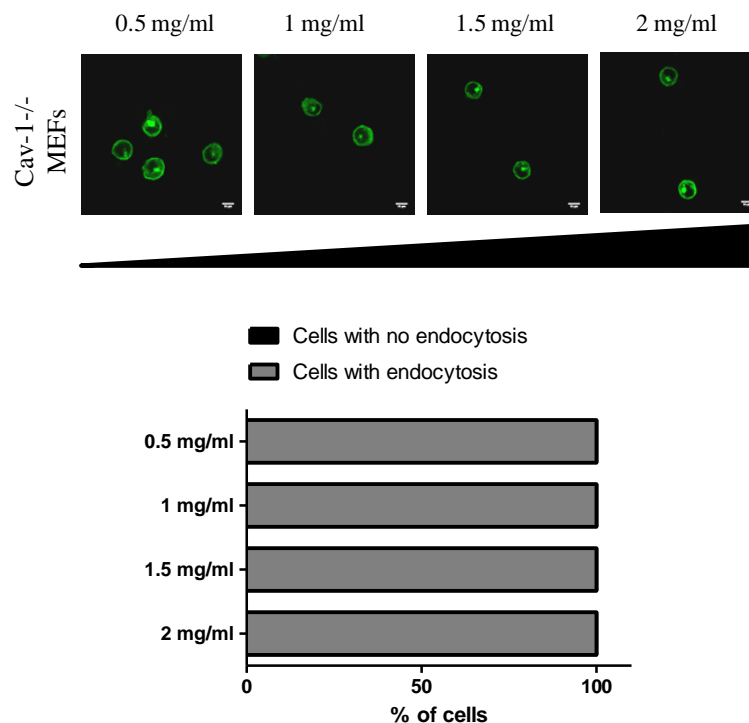


**Fig 4.5 Endocytosis of CTxB in Cav1-KO MEFs at different collagen concentrations.** Cells embedded at increasing collagen concentrations (0.5mg/ml to 2mg/ml) and labeled with CTxB were imaged and representative images shown here from 2 independent experiments. 100 cells were analyzed in each experiment. Graph below shows % distribution of cells with and without endocytosis and represents data from one experiment. Both experiments gave similar results.

As Cav1 has been implicated in CTxB internalization, mainly upon loss of adhesion (del Pozo et al., 2005) we further asked whether it has any role in regulating CTxB endocytosis in 3D collagen. Adhesions made by cells in 3D matrices are quite different than those in 2D (Cukierman et al., 2001a), and hence we can speculate that the processes regulated by adhesion could also be different in 3D than 2D. Surprisingly, in 3D collagen, at all 4 concentrations 100 % of Cav1-KO MEFs internalized CTxB (Fig 4.5).

This suggests that the internalization of GM1-CTxB is taking place through caveolin independent pathways and the block seen in WT MEFs at higher collagen concentrations is dependent on Cav1.

#### **4.3.5 GM1-CTxB endocytosis in WT MEFs and Cav1-KO MEFs at higher collagen concentrations**

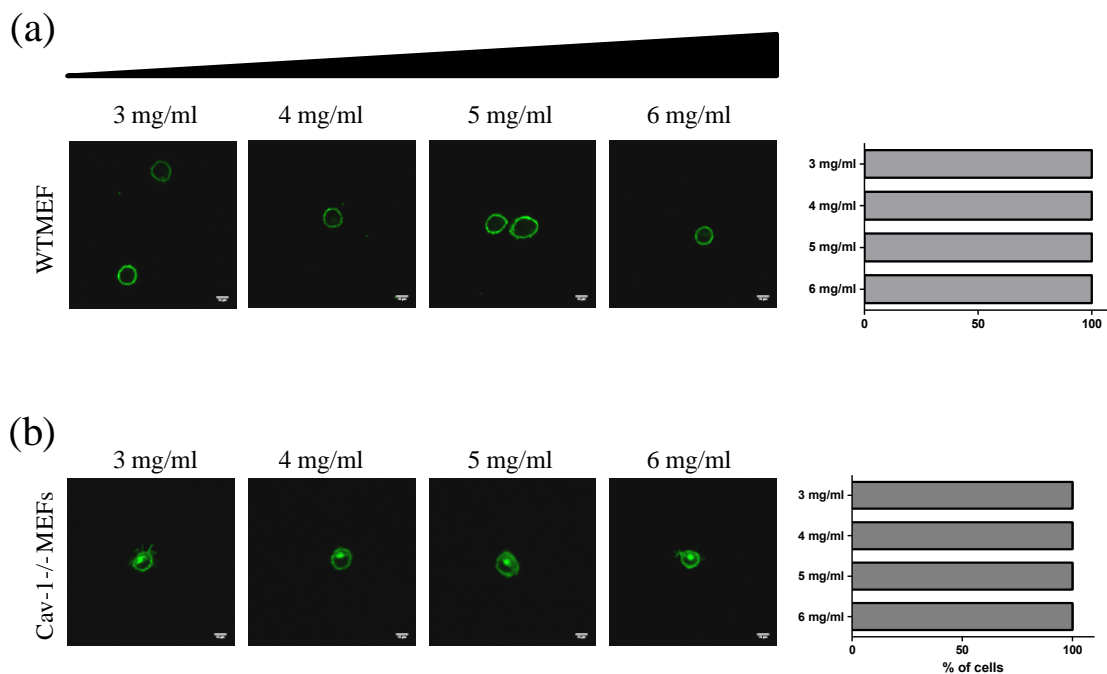


**Fig 4.6 Endocytosis of CTxB in WT MEFs and Cav1-KO MEFs in collagen gels of higher collagen.** Images are representative from 3 independent experiments. 100 cells were analyzed in each experiment. Graphs show % of cells with particular phenotype.

Since the block in endocytosis at higher concentration did not happen in Cav1-KO MEFs (at 1.5 mg/ml and 2 mg/ml), we further increased collagen concentration (up to 6 mg/ml) and checked whether the block happens in any of the further higher concentrations. We also embedded WT



MEFs at these higher concentrations and checked whether GM1-CTxB endocytosis is still blocked. This was to test the possibility whether at higher collagen concentrations Cav1-KO MEFs can sense the ECM stiffness or concentration and block GM1-CtxB endocytosis (like WT MEFs).

Even at these higher concentrations (3 mg/ml, 4 mg/ml, 5 mg/ml and 6 mg/ml), in WT MEFs the endocytosis was blocked. Cav1-KO MEFs continued to internalize GM1-CTxB at all these 4 higher concentrations.

#### **4.3.6 GM1-CTxB endocytosis in WT MEFs surrounded by Cav1-KO MEFs (3D collagen)**

We further elucidated the mechanism for the block of endocytosis in WT MEFs at higher concentrations of collagen. Since Cav1-KO MEFs did not show this block, one of the possible mechanism could be how Cav1-KO MEFs modulate their microenvironment differently than WT MEFs. This modulation could be biochemical (secretion of certain enzymes like MMPs) or biomechanical (differential force generation on the ECM and hence differential arrangement of ECM fibers). All these could alter endocytosis in a particular cell.

To test this, embedded WT MEFs with Cav1-KO MEFs in a 1: 7 ratio (to allow Cav1-KO MEFs to overpopulate WT MEFs in the gel). To distinguish between WT MEFs and Cav1-KO MEFs in a particular frame, we labeled WT MEFs before embedding (with CTxB-488) as well as after embedding (CTxB-594). Hence it was easy to pick up WT MEFs which had both green and red CTxB. We observed that even in a WT MEF cell surrounded by many Cav1-KO MEFs, the endocytosis stayed blocked (Fig 4.7). This indicates that there is a possibility of alternative intracellular mechanism than a neighboring cell affecting endocytosis in other cell.

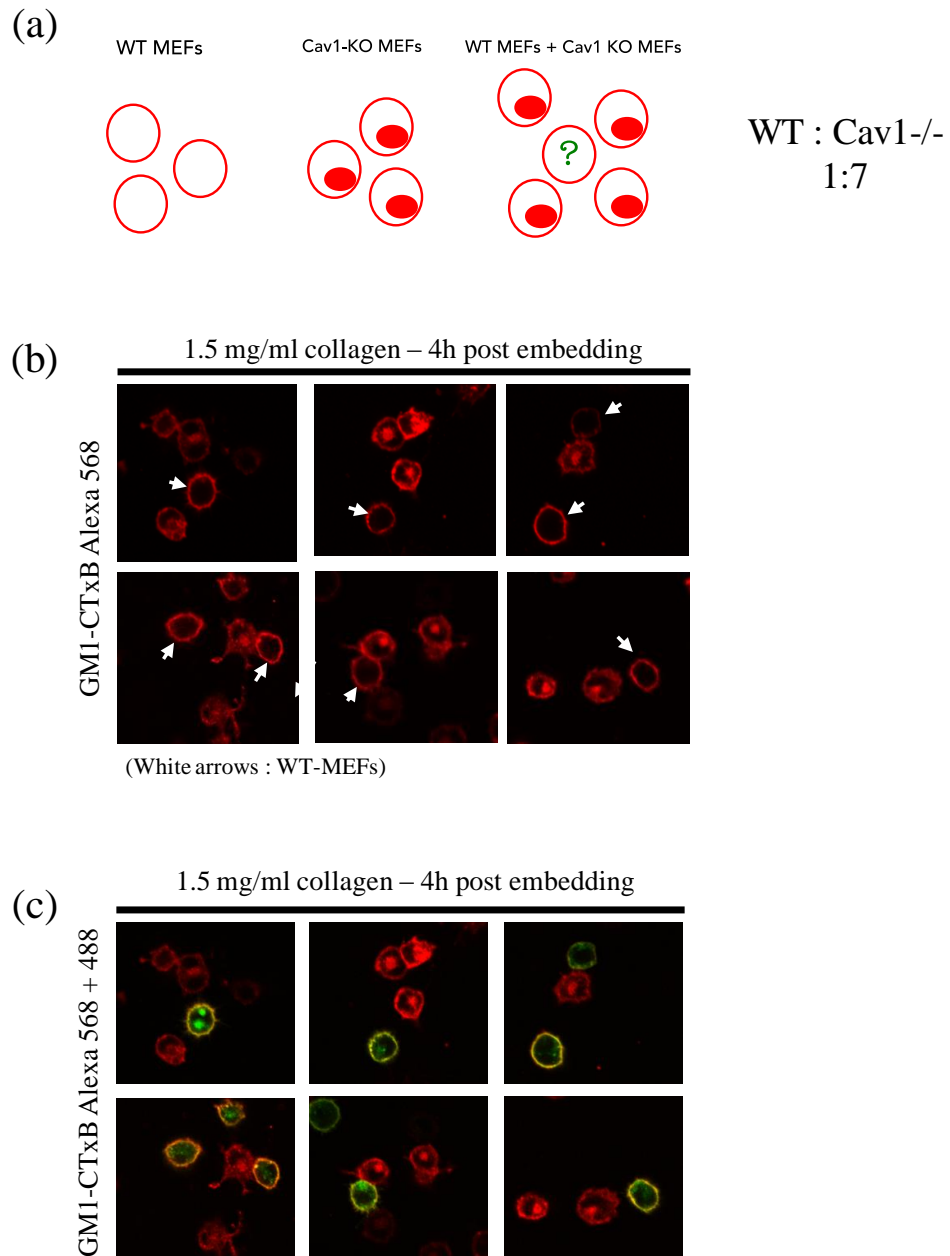


**Fig 4.7 Endocytosis of CTxB in WT MEFs surrounded by Cav1-KO MEFs.**(a) Schematic of the experimental set-up (b) Only CTxB-594 shown which is labeled post embedding and (c) CTxB-594 + CTxB-488 (Read text for details). Images are representative from 2 independent experiments.

### 4.3.7 GM1-CTxB endocytosis in Cav1-KO MEFs expressing WT-Cav1 or Y14F-Cav1

Since Cav1 was negatively regulating GM1-CTxB endocytosis in MEFs at higher concentrations, we reconstituted Cav1-KO MEFs with WT Cav1-GFP and checked whether the phenotype is getting reversed. Checking the effect of pTyr-Cav1 on this was also of interest hence Cav1-KO MEFs were reconstituted with Y14F-Cav1-GFP as well.

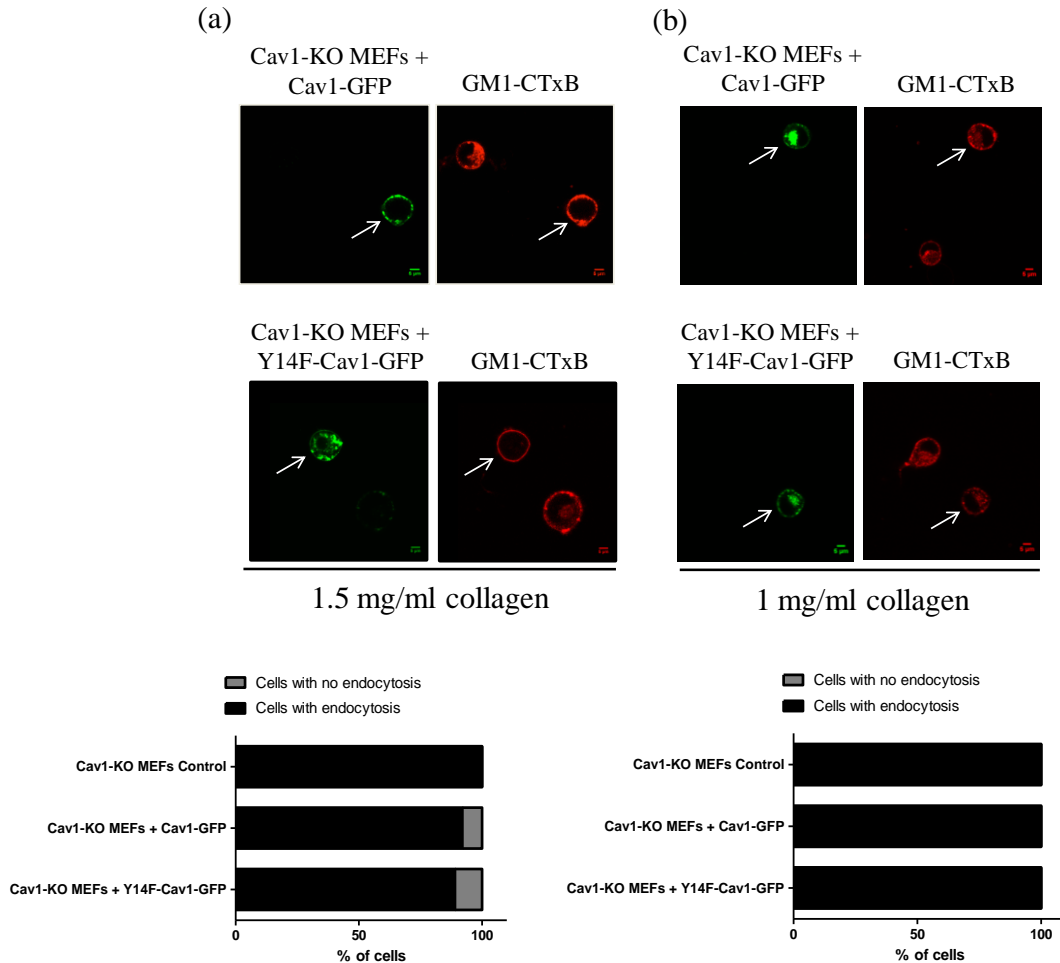


**Fig 4.8 Endocytosis of CTxB in reconstituted Cav1-KO MEFs (WT-Cav1 and Y14F-Cav1-GFP).** (a) Cells embedded at 1.5 mg/ml collagen and (b) Cells embedded at 1 mg/ml collagen. Transfected cells are indicated with white arrows. Images are representative from 3 (for panel a) and 2 (for panel b) independent experiments. 100 cells were analyzed in each experiment. Graphs below show quantitation.

In both cases, WT or Y14F-Cav1, the phenotype was reversed in Cav1-KO MEFs, that the GM1-CTxB endocytosis got blocked at 1.5 mg/ml collagen (like WT MEFs) (Fig 4.8 a). This means that pTyr-Cav1 is not required for this negative regulation of endocytosis. At 1 mg/ml again, re-expression of both WT and Y14F-Cav1 construct did not have any effect on endocytosis, that is Cav1-KO MEFs still continued to internalize GM1-CTxB at 1 mg/ml collagen. This again suggests to the fact that in this case, GM1-CTxB endocytosis is taking place through caveolin independent pathways, most probably clathrin independent pathways.

This result was also interesting if combined with earlier result looking at K-Ras-CAAX-GFP mobility in Cav1-KO MEFs reconstituted with WT or Y14F Cav1 GFP (chapter 3). And there seems to be a correlation between these two phenotypes - mobility of K-Ras-CAAX-GFP and GM1-CTxB endocytosis.

#### **4.3.8 Mobility of K-Ras-CAAX-GFP at different collagen concentrations**

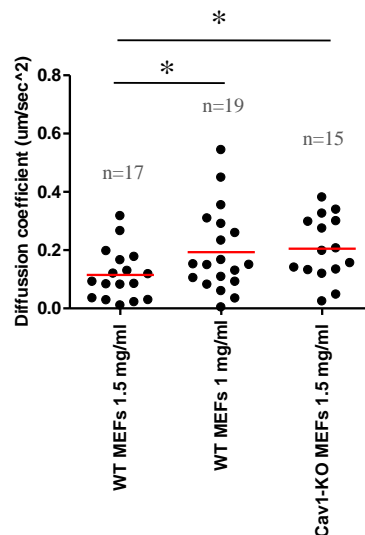


**Fig 4.9 Mobility of K-Ras-CAAX-GFP in WT MEFs embedded at different collagen concentrations.** Diffusion coefficients calculated from FRAP data. Significance calculated by Mann-Whitney Test. Data analyzed from three independent experiments. For detail statistics refer appendix.

Since the only difference in the endocytosis phenotype was observed between 1 and 1.5 mg/ml collagen, we decided to look at the membrane in these two conditions. Endocytosis is highly influenced by properties of the plasma membrane, like fluidity, tension, composition, etc. We had earlier used an assay to comment on how different plasma membrane markers move differentially on the membrane and how that could reflect onto the properties of the membrane (chapter 3). We made use of the same technique, FRAP and looked at mobility of K-Ras-CAAX-GFP construct in WT MEFs at these two different collagen concentrations. This construct was the only one which had showed difference between WT and Cav1-KO MEFs at 1.5 mg/ml. Also, we have checked earlier that the mobility of this construct is majorly diffusion based, hence this was chosen.

We embedded WT MEFs in 1 mg/ml or 1.5 mg/ml collagen and compared this to Cav1-KO MEFs at 1.5 mg/ml collagen. Interestingly, we observed that the diffusion coefficient of K-Ras-CAAX-GFP in WT MEFs embedded in 1 mg/ml collagen ( $0.19 \pm 0.03 \mu\text{m}/\text{sec}^2$ ) was higher as compared to WT MEFs embedded in 1.5 mg/ml gel ( $0.11 \pm 0.02 \mu\text{m}/\text{sec}^2$ ). And it was comparable to that in Cav1-KO MEFs at 1.5 mg/ml ( $0.2 \pm 0.02 \mu\text{m}/\text{sec}^2$ ). This suggests that the membrane of WT MEFs at lower collagen concentration resembles that of Cav1-KO MEFs (with respect to fluidity / composition / order, or all).

#### **4.3.9 Actin disruption triggers GM1-CTxB endocytosis in WT MEFs in 1.5 mg/ml collagen**

We next elucidated the role of a crucial factor required for endocytosis, the actin cytoskeleton. Actin structures are dynamically organized constantly which assists in plasma membrane remodeling and internalization of vesicles. We wanted to check whether GM1-CTxB endocytosis in 3D requires actin cytoskeleton. For this, we used two drugs to disrupt the actin - Cytochalasin D (Cyto D) and Latrunculin A (Lat A). These two act on the actin cytoskeleton differentially, Cyto D disrupts actin microfilaments, whereas Lat A binds to actin monomers and inhibits actin polymerization.

We first embedded the cells in collagen and then pre-incubated the cells for 30 minutes before labeling them with CTxB. After labeling, cells were further incubated with respective drugs for 3 hours and then imaged. Upon treating with both the drugs, the block in WT MEFs at 1.5 mg/ml

was not seen. Both Cyto D and Lat A treatments resulted in internalization of GM1-CTxB at 1.5 mg/ml. At 1 mg/ml, cells still continue to internalize CTxB.

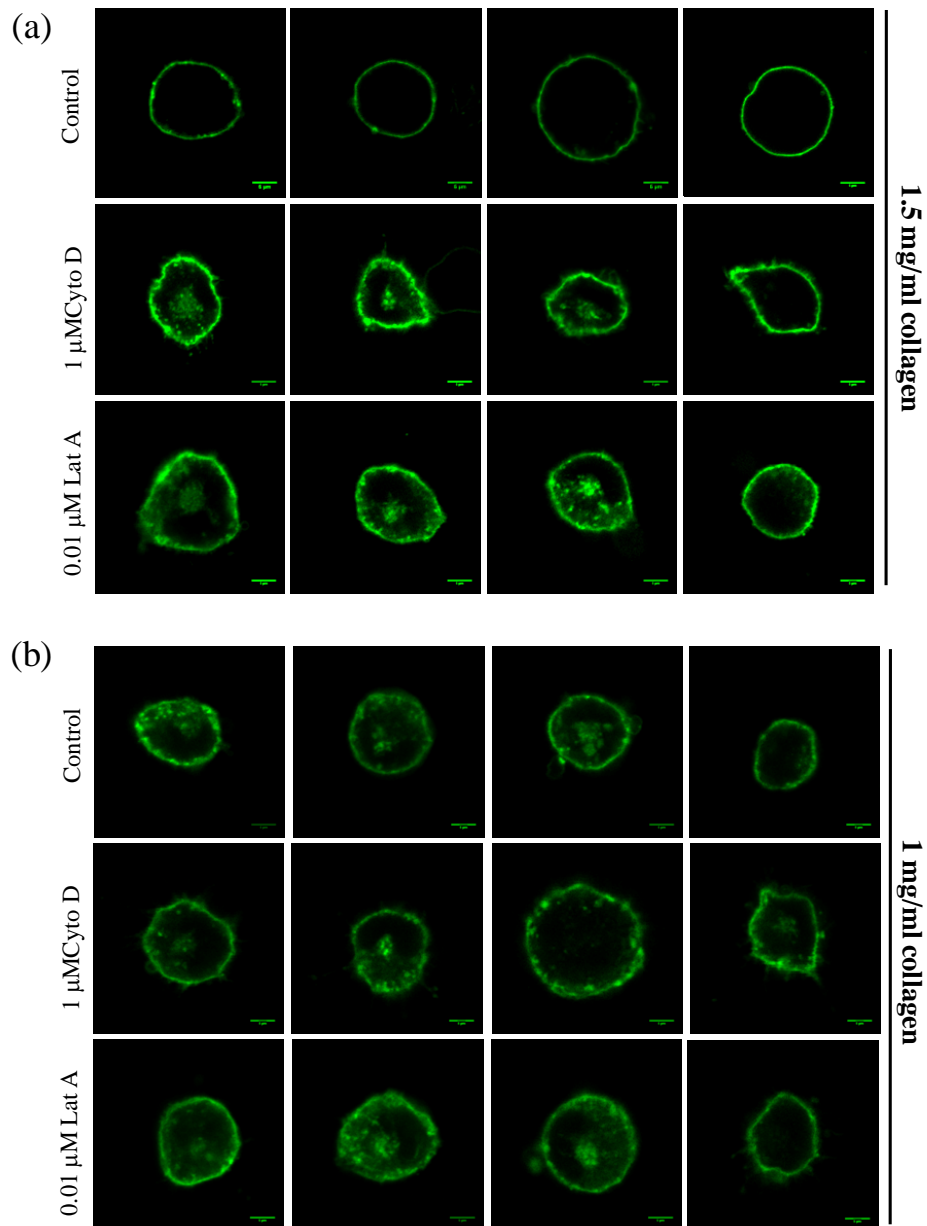


**Fig 4.10 Role of actin in regulating CTxB endocytosis in WT MEFs in 3D collagen.** (a) WT MEFs embedded in 1.5 mg/ml collagen and (b) WT MEFs embedded in 1 mg/ml collagen. Images are representative from 3 independent experiments.

#### **4.3.10 Actin disruption increases K-Ras-CAAX-GFP mobility in WT MEFs in 1.5 mg/ml collagen**

As actin disruption resulted in triggering GM1-CTxB endocytosis, we speculated that one of the possibilities could be because of change in membrane tension. Whether the same affects mobility of K-Ras-CAAX-GFP on the membrane was the next question we asked. Cells were pre-treated with Cyto D 2 hours before performing FRAP. Drug was present in the gel even during the imaging (FRAP) was carried out.

GPI linked proteins get anchored onto the plasma membrane in an actin dependent manner. We used this fact to standardize actin disruption protocol (duration and concentration of the drug). We did find a concentration and time (1  $\mu$ M and 180 minutes) at which upon actin disruption, the mobility of GPI-GFP in WT MEFs increased. 0.5  $\mu$ M did not have any effect (Fig 4.11 a). Also, in Cav1-KO MEFs actin disruption did not affect mobility of GPI-GFP (Fig 4.11 b). This altered mobility of GPI\_GFP could be the result of differential actin organization in WT versus Cav1-KO MEFs. After standardizing this, we further looked at the mobility of K-Ras-CAAX-GFP. Mobility of K-Ras-CAAX-GFP also increased upon actin disruption in WT MEFs (Fig 4.11 c) but not in Cav1-KO MEFs (Fig 4.11 d). All these experiments were carried out in 1.5 mg/ml collagen.

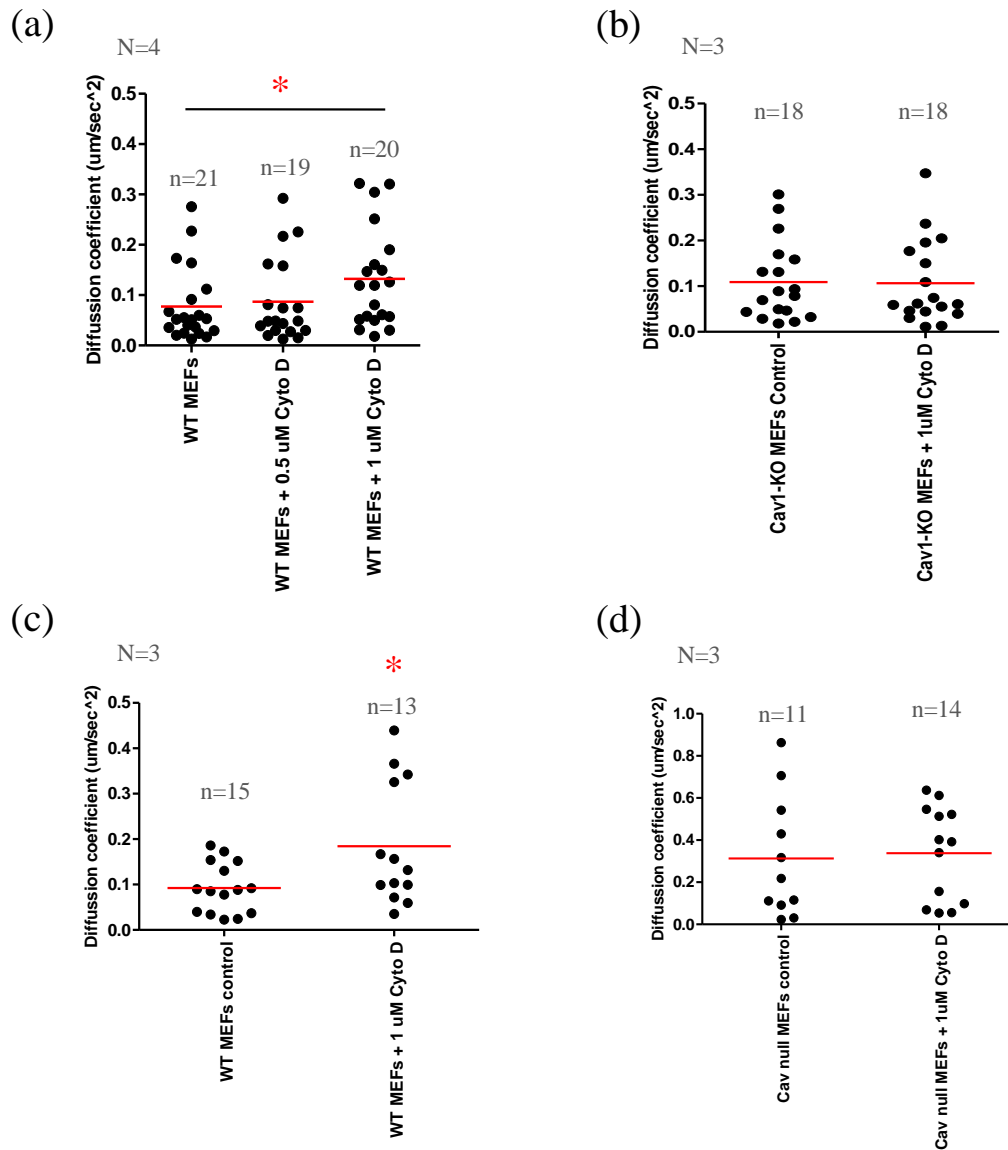


**Fig 4.11 Role of actin in regulating mobility of GPI-GFP and K-Ras-CAAX-GFP in WT MEFs in 3D collagen.** WT MEFs and Cav1-KO MEFs embedded in 1.5 mg/ml collagen expressing GPI-GFP - (a) and (b) or expressing K-Ras-CAAX-GFP - (c) and (d). Diffusion coefficients calculated from FRAP data. Significance calculated by Mann-Whitney Test. For detail statistics refer appendix.



#### **4.4 Discussion**

Endocytosis is a process by which cells internalize various cargo molecules like nutrients, solutes and even pathogens. There are many endocytic pathways present in cells like clathrin-coated pits, caveolar endocytosis, macropinocytosis, phagocytosis and clathrin and caveolin independent pathways. In most of the pathways, a small portion of the plasma membrane invaginates inside and the cargo is taken up. Internalization and transport of the vesicle needs an intact cytoskeleton in most of the cases. Hence, **plasma membrane and cytoskeleton are considered as the key regulators of endocytosis** in cells. During this process, lipid and protein composition of the plasma membrane is also constantly under regulation and this affects how cells interact with their environment.

Both of the regulators - plasma membrane and cytoskeleton - are expected or known to be different in cells present in a 3D microenvironment than a conventional 2D tissue culture plate. As discussed earlier, plasma membrane composition and arrangement of cytoskeleton are shown to be different. Tension on the plasma membrane, order or fluidity, organization of plasma membrane are all speculated to be different in 3D. We hence speculated that the endocytosis in 3D will be differentially regulated too and studied the same in MEFs.

Recently, it is also shown that **endocytosis of certain cargos is regulated by the substrate stiffness** (Brugnano and Panitch, 2014; Huang et al., 2013). Both these studies have shown that when cells were put on a stiff substrates (2D polyacrylamide gels), endocytosis was blocked. 2D PAA (Polyacrylamide) gels provide a very powerful tool to study effect of substrate stiffness on cells. Their stiffness and coating can be easily modulated however, cells still experience a flat two-dimensional environment. One of the above mentioned study has tried to decipher the mechanism for this block and they suggested that membrane tension increases when cells are plated on stiffer substrates and this blocks endocytosis in endothelial cells (in this case, endocytosis of a nanoparticle). We hence looked at endocytosis of various cargos in MEFs embedded at different collagen concentrations. Different concentrations of collagen form gel with different stiffness, with a positive correlation between collagen concentration and stiffness of the gel (Wolf et al., 2013).

We looked at endocytosis of 3 distinct membrane cargos in MEFs - CTxB, transferrin and DQ-BSA across a range of collagen concentrations.

Transferrin (internalized via clathrin-coated pits) and DQ-BSA (internalized majorly via macropinocytosis) both did get internalized in WT MEFs at all four concentrations tested - 0.5 mg/ml, 1 mg/ml, 1.5 mg/ml and 2 mg/ml. However, **CTxB, cholera toxin B subunit** - which binds to a lipid moiety, **GM1** on plasma membrane did not get internalized at 1.5 mg/ml and 2 mg/ml collagen (**Fig 4.2**). Cav1-KO MEFs, interestingly, did not show any dependence on collagen concentration and internalized GM1-CTxB at all four concentrations (**Fig 4.5**).

Since the most striking difference in the endocytosis phenotype was observed between 1 mg/ml and 1.5 mg/ml, we tried to characterize the gels at these two collagen concentrations. We did some preliminary experiments which show differences between the stiffness of these two gels.

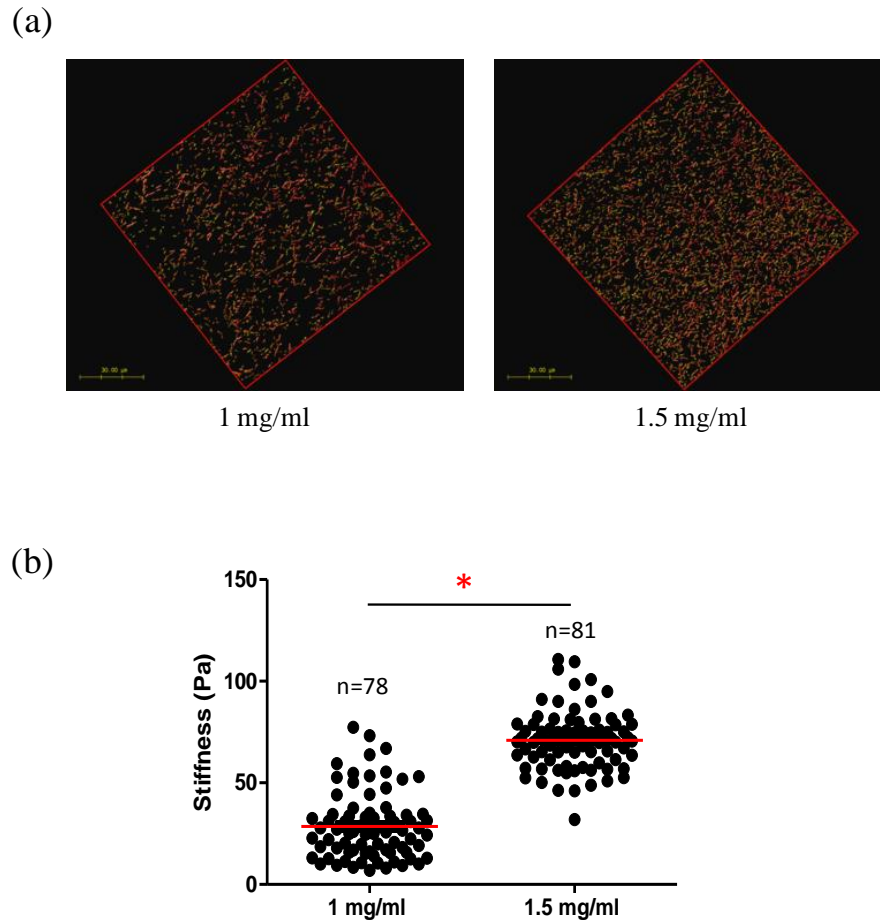


**Fig 4.12. Characterization of collagen gels at 1 mg/ml and 1.5 mg/ml concentrations.** (a) shows representative Z stacks (deconvoluted with Huygens software) of images of gels acquired by second harmonic generation (SHG) imaging. (b) shows stiffness of collagen gels calculated using atomic force microscopy. Significance calculated by Mann-Whitney Test. Data represented from two samples, one experiment. n represents number of readings taken. For detail statistics refer appendix.

SHG, which is a non-destructive and very effective technique to image materials with non-linear symmetry, is useful to image collagen both in vivo and in vitro. This is because collagen fibers exhibit non-linear symmetry. With this technique, we did see differences between the two gels, in their cross-linking and pore area, etc (Fig 4.12 - a). Stiffness of the gels at these two concentrations was calculated by AFM and found to be significantly different (Fig 4.12 - b).

GM1-CTxB is reported to be endocytosed majorly via caveolar route upon loss of integrin mediated adhesion (del Pozo et al., 2005). However, stably adherent cells, internalize it via other pathways. It is not known in literature by what pathways cells internalize GM1-CTxB in 3D collagen. Since Cav1-KO MEFs were able to endocytose GM1-CTxB at all concentrations of collagen, the route of endocytosis is most likely to be one of the **caveolin and clathrin independent pathways**. Interestingly, we found that this pathway is **blocked in WT MEFs at higher collagen concentrations**. Such similar cross-talk between clathrin independent pathways and caveolar proteins, Cav1 and Cavin1 has been shown earlier (Chaudhary et al., 2014). This study however was done in cells in 2D and only at one substrate stiffness.

pTyr14-Cav1 is an important regulator of GM1-CTxB endocytosis (via caveolar route) upon loss of adhesion. We thus tested its role in regulating GM1-CTxB endocytosis in 3D. We reconstituted Cav1-KO MEFs with WT Cav1 or Y14F Cav1 and both these constructs resulted in block of endocytosis at 1.5 mg/ml collagen (**Fig 4.8**). This suggested that the **Cav1 has a role in regulating GM1-CTxB endocytosis in 3D, but pTyr14-Cav1 does not have any role**.

There could be **two possible mechanisms** for regulating this block in endocytosis at higher collagen concentrations, which was seen only in WT MEFs but not in Cav1-KO MEFs. One possibility is as Cav1-KO MEFs remodel the ECM around them differentially as compared to WT MEFs (Goetz et al., 2011) and this alters their behavior. WT MEFs have active Rho which increases the acto-myosin contractility. This was shown to alter arrangement of ECM fibers, making them more parallelly arranged. Cav1-KO MEFs showed a more criss-cross arrangement of ECM fibers. Fibroblast derived matrices (FDMs) derived from WT MEFs were also found to be stiffer as compared to FDMs secreted by Cav1-KO MEFs. Presence of Cav1 in the stromal fibroblasts hence eventually helps cancer cells in migration and metastasis. Cav1 is also considered as essential protein required for formation of normal stroma of different organs like the mammary glands (Thompson et al., 2017).

Another aspect how Cav1 regulates ECM is by regulating MMP secretion. Cells migrate in 3D matrices by two modes - non proteolytic or amoeboid or proteolytic or mesenchymal. In

amoeboid mode of migration, actomyosin contractility and Rho- Rock signaling pathway plays a critical role (Sahai and Marshall, 2003; Sanz-Moreno et al., 2011). Proteolytic mode involves enzymatic degradation of the extracellular matrix which is achieved by various proteases secreted by cells like serine proteases, cysteine proteases and metallo-proteases. **Matrix metalloproteases (MMPs)** are zinc-dependent endopeptidases produced by cells which degrade almost all types of ECM proteins and thus facilitate their migration through surrounding stroma (Visse and Nagase, 2003). There are 25 MMPs known till now and these are classified either as secretory or membrane anchored. MT1-MMP (Membrane type) is considered to be the key regulator of proteolytic cell migration. Interestingly, **caveolae and Cav-1 have been implicated in expression and activation of MT1-MMP (membrane associated) and MMP2, MMP9 (secretory MMPs)** (Chow et al., 2007; Han and Zhu, 2010; Williams et al., 2004). MMP2 and MT1-MMP have also been shown to co-localize with Cav-1 (Puyraimond et al., 2001; Yamaguchi et al., 2009) and MT1-MMP, particularly has been shown to be **trafficked through caveolae** in certain cell types (Galvez et al., 2004; Remacle et al., 2003).

By both these mechanisms, Cav1 can alter how ECM gets remodel and that can eventually affect endocytosis in cells. However, when we mixed WT MEFs with Cav1-KO MEFs (such that one WT MEF was surrounded by at least 4-5 Cav1-KO MEFs), we did not see endocytosis getting triggered in WT MEFs (**Fig 4.7**). There **could be a experimental limitation** as to regulating the number and arrangement of cells uniformly or the distance between the cells might not be enough for one cell to alter neighboring cell's behavior. However, it is also possible that, membrane tension or cortical tension (or both) in WT MEFs could indeed be inherently different from Cav1-KO MEFs when they are embedded in 3D collagen.

Physical properties of the plasma membrane are often considered as significant factors which modulate many intracellular processes and biological functions. This can be mediated by regulation of receptor clustering, opening or closing of stretch induced ion channels, membrane tether formation, etc. Among all such mechanosensory responses, one more process which is directly regulated by membrane tension which is endocytosis. **Rate of endocytosis is low when membrane tension is high and vice versa** (Diz-Muñoz et al., 2013). Increased membrane tension increases both number and size of ordered domains on the membrane making it less fluid. We had earlier seen that mobility of K-Ras-CAAX-GFP was higher in Cav1-KO MEFs

than WT MEFs at 1.5 mg/ml. One of the possible reason for this could be increased fluidity in Cav1-KO MEFs, and hence lesser membrane tension in Cav1-KO MEFs, which further supported endocytosis in these cells. It is shown earlier using Laurdan dye technique it was shown that fibroblast cells which express Cav1 have higher ordered fraction (28.6%) as compared to Cav1 KO MEFs (8.1%) (Gaus et al., 2006).

Cortical actin tension polymerization increases when membrane tension increases (Dai et al., 1999). We **perturbed the cortical actin by laser ablations** in WT MEFs embedded in 1 mg/ml or 1.5 mg/ml collagen. Cells in 1.5 mg/ml showed more blebbing phenotype as compared to those in 1 mg/ml (Fig 4.13 a). Blebs are spherical membrane protrusions driven by the actomyosin cortex which generates hydrostatic pressure in the cytoplasm (Wottawah et al., 2005). The role of cortical tension in bleb growth has been studied earlier and considering cortex as an active elastic material, authors have shown that bleb nucleation and growth strongly depends on cortical tension (Tinevez et al., 2009).

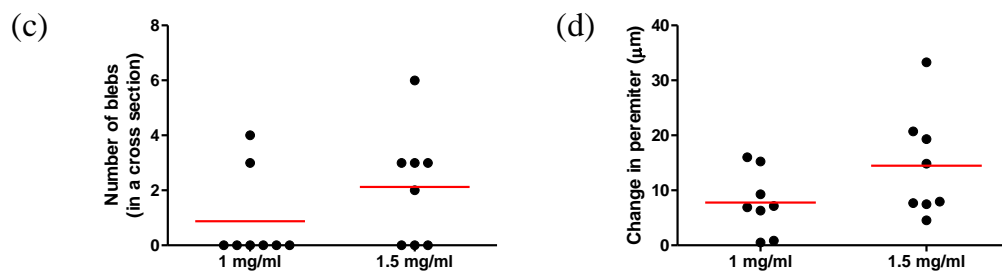
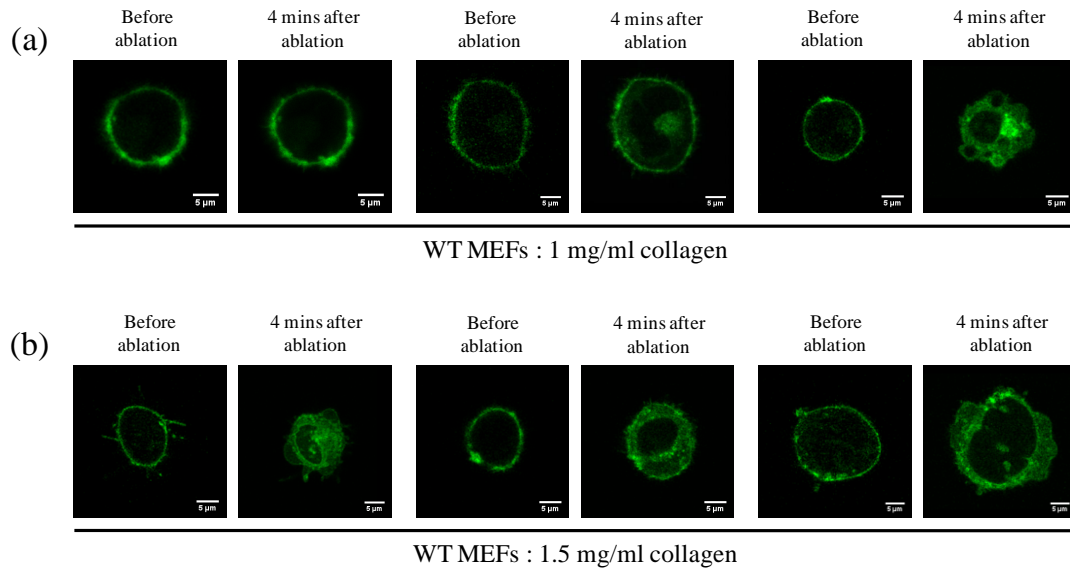


**Fig 4.13 Laser ablations in WT MEFs in 1 mg/ml and 1.5 mg/ml collagen.** (a) shows WT MEFs embedded in 1 mg/ml collagen and (b) shows WT MEFs embedded in 1.5 mg/ml collagen - before ablation and after 4 minutes of ablation. (c) and (d) represent quantitation of number of blebs per cell (in a cross section) and change in perimeter of cells. Data represented from one experiment.

We observed that majority of the cells showed blebbing (75%) in 1.5 mg/ml collagen, whereas only 25% cells showed blebbing in 1 mg/ml collagen. The number of blebs in a particular cells was also high in cells in 1.5 mg/ml (Fig 4.13 c) and so was the change in perimeter of cells (Fig 4.13 d). This could be because of increased cortical tension (and hence probably membrane tension) in cells in 1.5 mg/ml as compared to 1 mg/ml collagen. However, the data is from only one experiment and this needs to be validated further.

We also perturbed the actin by treating cells with actin disruption drugs - Cyto D and Lat A. Treatment with both these drugs triggered GM1-CTxB endocytosis in WT MEFs in 1.5 mg/ml collagen. Cyto D treatment also increased mobility of K-Ras-CAAX-GFP as well in WT MEFs in 1.5 mg/ml collagen. Cyto D treatment is known to decrease cortical actin tension (Pietuch and Janshoff, 2013). Hence, we propose **a possible mechanism** behind this differential regulation of endocytosis that - membrane and / or cortical actin tension is altered in WT MEFs when embedded in collagen gels of different concentrations. Role of membrane tension can also be elucidated in this by performing osmotic shock experiments which modulates membrane tension.

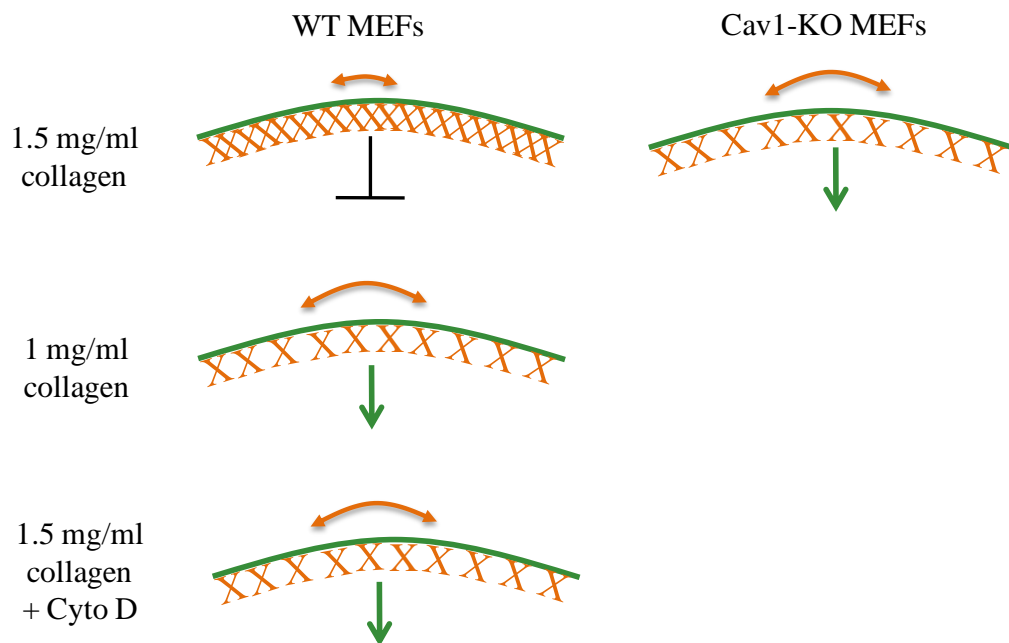


**Fig 4.14 Proposed mechanism for differential regulation of GM1-CTxB endocytosis in MEFs in 3D collagen.**



## 4.5 Summary

In summary, we observed that the two phenotypes - endocytosis and mobility of K-Ras-CAAX-GFP on the plasma membrane have a correlation. The results are summarized in the following schematic.

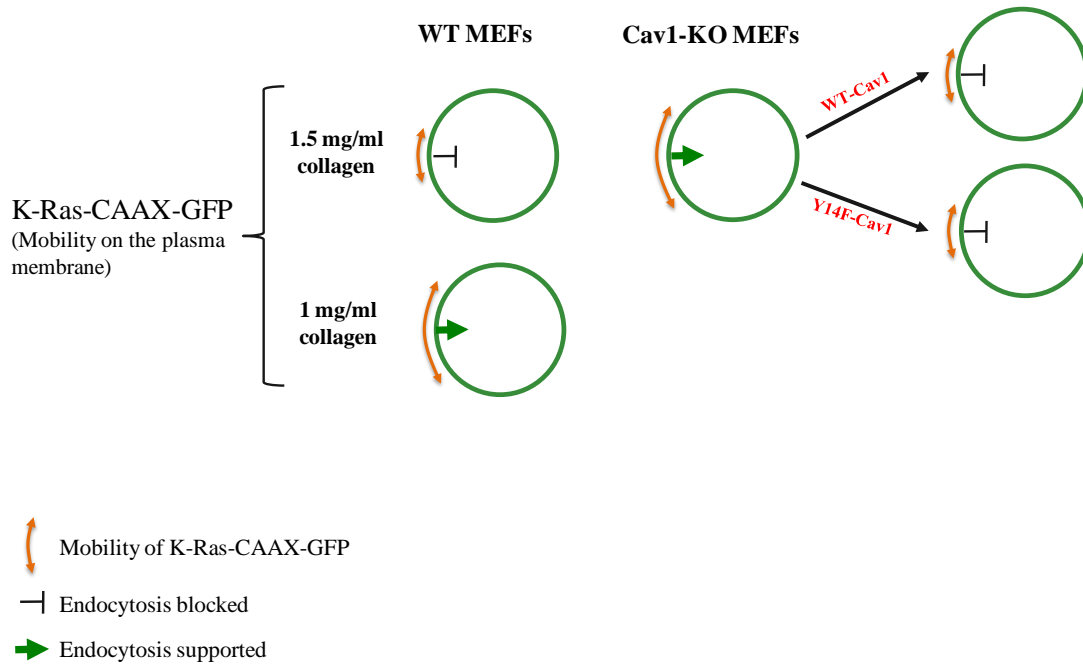


**Fig 4.15 Schematic showing correlation between two phenotypes in WT MEFs v.s. Cav1-KO MEFs in a 3D microenvironment : Mobility of K-Ras CAAX-GFP and GM1-CTxB endocytosis.** Wherever the mobility of K-Ras-CAAX-GFP is higher, GM1-CTxB endocytosis is supported and wherever the mobility is lower, endocytosis is blocked.

Future perspective

The work presented in this thesis looking at caveolar function and trafficking in cells in 3D matrices has opened up quite a few exciting questions to be pursued further. Recently, 3D is being used as a model system increasingly and in this context our study is the first one looking at how caveolae alter the membrane in cells in 3D microenvironment. There are still many more interesting questions which can be pursued further.

### **1. How caveolae alter other membrane properties in cells in 3D?**

Our study indicates to the fact that membrane organization and tension both could be different in WT MEFs versus Cav1-KO MEFs in 3D collagen. Many of the membrane properties are interdependent and hence membrane composition, membrane order or fluidity, membrane potential all these could also be different in presence and absence of caveolae and will be interesting to study in 3D. The most widely used techniques to study these properties are : thin layer chromatography (to study membrane composition), FRAP for membrane dyes or Laurdan dye fluorescence quantitation (to study membrane fluidity or order) and patch clamp (to study membrane potential). Performing experiments with these techniques in cells embedded in 3D gels can be challenging and may need some alterations in the existing techniques or protocols.

Studying membrane potential in 3D will be of great interest as it has been shown to modulate phospholipid dynamics and K-Ras clustering (Zhou et al., 2015). The authors show that plasma membrane depolarization induces phosphatidyl serine (PS) clustering and that increases K-Ras nanoclustering. Presence or absence of caveolae is suggested to modulate membrane polarization as it regulates activity of Na<sup>+</sup>-K<sup>+</sup>-ATPase pump (Liu et al., 2003), and Cav1 deficiency has also been shown to regulate K<sup>+</sup> channel, which leads to depolarization of the membrane (Wang et al., 2015). The membrane potential is closely dependent on membrane tension (Iwasa, 1993; Kakehata and Santos-Sacchi, 1995; Warshaviak et al., 2011) and hence in 3D, whether caveolae regulate membrane potential and hence clustering of membrane proteins is an interesting question.

## **2. Whether and how caveolae regulate signal transduction in 3D?**

Diffusion and clustering of signaling proteins on the plasma membrane influences their downstream signaling to a great extent. Our study looking at diffusion of various membrane associated proteins done in 2D versus 3D indicates to the fact that the diffusion barriers for a particular protein could be different in 2D versus 3D. We also observed that diffusion of EGFR-GFP in Cav1-KO MEFs was higher as compared to that in WT MEFs. It is hence possible that further downstream signaling will be affected by this altered diffusion. It will be worth testing pErk signaling (by Western blotting) or just phosphorylation on Erk (by immunofluorescence) in cells with and without Cav1 in 3D.

## **3. Whether and how ECM remodeling by caveolae dependent stiffness of ECM?**

The concept that interactions of cells with their local microenvironment are important for their function is now well accepted. Both biochemical and biomechanical cues provided by stroma play an important role in regulating many cellular processes in cells. One such biophysical parameter of the microenvironment which is shown to alter cell behavior is the stiffness of the matrix on (or in) which cells are grown (Yeung et al., 2005). Among other cellular processes, matrix stiffness has been shown to regulate expression of various genes (Chiquet et al., 2009; Wang et al., 2007). MMPs are one of the important regulators of microenvironment as they are involved in matrix turnover and cell migration. Hence, knowing whether matrix stiffness directly alters MMP gene expression or their activation or secretion to facilitate cell migration is important to better understand interactions of cells with surrounding stroma.

How substrate stiffness alters MMP expression and function has been studied in various aspects, like during development or morphogenesis and disease progression. Also, majority of the studies are focused on how this phenomenon is regulated in mechanoresponsive cells, for example, Muller cells of the retinal glia (Davis et al., 2012), rat annulus fibrous cells (Zhang et al., 2011), cardiomyocytes (Forte et al., 2012), etc. In fibroblasts, substrate stiffness was shown to regulate MMP1 secretion as well as expression (Petersen et al., 2012). In some cancer cells also matrix rigidity affects MMP expression (Ruppender et al., 2010). However, there are many other

aspects to consider while analyzing data from cancer cell lines as changing substrate stiffness sometimes changes the mode of migration from mesenchymal (MMP dependent) to amoeboid (MMP independent) (Even-Ram and Yamada, 2005; Zaman et al., 2006).

The expression and function of MMPs is altered in many diseases like cardiac myopathies (MMP2 and MMP9) (Cleutjens, 1996), bone abnormalities (MMP13) (Murphy et al., 2002) and cancer (different MMPs are involved depending upon type and stage of cancer) (Jodele et al., 2006; Stetler-Stevenson and Yu, 2001). The common factor in all these diseases is either defect in sensing the stiffness of surrounding microenvironment or responding to the stiffness. However, whether altered MMP expression and function in all these diseases is a cause or a consequence is still unclear in the field. As discussed earlier (section 4.5), Cav1 is involved in MMP activation as well as secretion in many cell types. In 3D collagen gels of varying stiffness, how Cav1 regulates MMP dependent cell migration will be interesting to know.

#### **4. Which other properties of ECM alter endocytosis in cells in 3D?**

In our study, we varied collagen concentrations of gels and observed its effect on endocytosis. Increasing collagen concentration results in increase in stiffness of the gel. There are many other factors than stiffness which can influence cell behavior. For example, fiber thickness, fiber alignment, elasticity of the matrix, composition of the matrix, etc. All these factors could also affect endocytosis in 3D collagen.

#### **5. Whether cells differentially endocytose on 2D substrates with different stiffness as well?**

The GM1-CTxB endocytosis phenotype observed in WT MEFs in 3D collagen is dependent on stiffness of ECM. Whether this is specific to only 3D collagen or also on 2D gels is not known. Inherently, 2D cultures are stiffer than 3D and thus, the response might be visible at a different range in 2D. Whether that happens or not will be interesting to find out.

## **6. Whether and how caveolae regulate endocytosis in 3D in cancer cells?**

Cav-1 has been implicated in many cancers as a known tumor suppressor and is absent in many cancers (Engelman et al., 1998b; Lee et al., 1998). However, there are some reports where Cav1 is known to act as tumor promoter(Williams et al., 2005; Yang et al., 1999). The contribution of Cav1 in cancers is highly stage and tissue type dependent. In the context of cancer cells, how Cav1 regulates endocytosis as a response to substrate stiffness will be exciting to know. Cancer cells experience different range of stiffness from the tumor initiation stage till metastasis. Cav1 is down regulated in many cancers at early stages and reappears in advanced stages. Whether cancer cells use this as a mechanism to regulate endocytosis as well, is not known.

Our understanding of Cav1 in mechanosensitive process of endocytosis has a great potential to be tested in cancer cells and will provide new dimension to drug and nutrient uptake in cancer cells.

# Appendix

**I. Statistics for figure 2.4:**

<b>Cell type</b>	<b>Mean aspect ratio</b>
WT MEFs	$1.798 \pm 0.16$
Cav null MEFs	$1.435 \pm 0.06$
Cav null + WT Cav	$1.963 \pm 0.16$
Cav null + Y14F Cav	$1.579 \pm 0.09$

<b>Comparison (aspect ratio)</b>	<b>p-value</b>
WT vs Cav null MEFs	0.0495
Cav null MEFs vs Cav nulls + WT Cav	0.0055
Cav null MEFs vs Cav nulls + Y14F Cav	0.2042

**II. Statistics for figure 2.6:**

<b>ROI</b>	<b>Mobile fraction (%)</b>	<b>T<sub>half</sub> (min)</b>
20X10	$76.08 \pm 3.25$	$0.09 \pm 0.01$
20X20	$78.71 \pm 3.38$	$0.15 \pm 0.02$
20X30	$79.79 \pm 3.36$	$0.19 \pm 0.01$
20X50	$81.84 \pm 2.85$	$0.25 \pm 0.02$

<b>Comparison (mobile fraction)</b>	<b>p-value</b>
20X10 vs 20X20	0.3443
20X20 vs 20X30	0.8229
20X30 vs 20X50	0.6496

<b>Comparison (T<sub>half</sub>)</b>	<b>p-value</b>
20X10 vs 20X20	0.1627
20X20 vs 20X30	0.2415
20X30 vs 20X50	0.1901



### III. Statistics for figure 2.8:

<b>Construct</b>	<b>Mobile fraction (%)</b>
WT Cav1 GFP	13.57 ± 1.34
Y14F-Cav1 GFP	10.72 ± 1.14

	<b>p-value</b>
WT vs Y14F Cav1 GFP	0.2455

### IV. Statistics for figure 2.9:

<b>Construct (3D)</b>	<b>Mobile fraction (%)</b>
WT Cav1 GFP	10.88 ± 1.18
Y14F-Cav1 GFP	7.20 ± 0.77

<b>Construct (2D edge)</b>	<b>Mobile fraction (%)</b>
WT Cav1 GFP	12.44 ± 1.78
Y14F-Cav1 GFP	7.48 ± 1.56

<b>Comparison</b>	<b>p-value</b>
WT vs Y14F Cav1 GFP (3D)	0.0374
WT vs Y14F Cav1 GFP (2D edge)	0.0428

**V. Statistics for figure 3.3:**

	<b>D (<math>\mu\text{m}/\text{sec}^2</math>)</b>	
	<b>WT MEFs</b>	<b>Cav1-KO MEFs</b>
2D Lower plane	0.45 $\pm$ 0.05	0.42 $\pm$ 0.05
2D upper plane	0.60 $\pm$ 0.10	0.77 $\pm$ 0.14

<b>Bleach geometry</b>	<b>WT vs Cav1-KO MEFs (p-value)</b>
2D Lower plane	0.6104
2D upper plane	0.3154

<b>3D collagen</b>	<b>D (<math>\mu\text{m}/\text{sec}^2</math>)</b>
WT MEFs	0.19 $\pm$ 0.04
Cav1-KO MEFs	0.32 $\pm$ 0.05
Cav1-KO MEFs + WT Cav1	0.20 $\pm$ 0.03
Cav1-KO MEFs + Y14F Cav1	0.14 $\pm$ 0.02

<b>Comparison (3D)</b>	<b>p-value</b>
WT vs Cav1-KO MEFs	0.0418
Cav1-KO MEFs vs Cav1-KO MEFs + WT Cav1	0.0436
Cav1-KO MEFs vs Cav1-KO MEFs + Y14F Cav1	0.0037

**VI. Statistics for figure 3.4:**

	<b>D (<math>\mu\text{m}/\text{sec}^2</math>)</b>	
	<b>WT MEFs</b>	<b>Cav1-KO MEFs</b>
2D Lower plane	0.19 $\pm$ 0.01	0.35 $\pm$ 0.04
2D upper plane	0.13 $\pm$ 0.03	0.16 $\pm$ 0.02
3D	0.11 $\pm$ 0.02	0.15 $\pm$ 0.03

<b>Bleach geometry</b>	<b>WT vs Cav1-KO MEFs (p-value)</b>
2D Lower plane	0.0179
2D upper plane	0.375
3D	0.5143

**VII. Statistics for figure 3.5:**

	<b>D (<math>\mu\text{m}/\text{sec}^2</math>)</b>	
	<b>WT MEFs</b>	<b>Cav1-KO MEFs</b>
2D Lower plane	0.40 $\pm$ 0.04	0.40 $\pm$ 0.03
2D upper plane	0.32 $\pm$ 0.12	0.88 $\pm$ 0.19
3D	0.13 $\pm$ 0.01	0.29 $\pm$ 0.06

<b>Bleach geometry</b>	<b>WT vs Cav1-KO MEFs (p-value)</b>
2D Lower plane	0.6773
2D upper plane	0.0312
3D	0.0967

**VIII. Statistics for figure 3.6:**

	<b>D (<math>\mu\text{m}/\text{sec}^2</math>)</b>	
	<b>WT MEFs</b>	<b>Cav1-KO MEFs</b>
3D	0.02 $\pm$ 0.003	0.05 $\pm$ 0.004

<b>Bleach geometry</b>	<b>WT vs Cav1-KO MEFs (p-value)</b>
3D	0.0101

**IX. Statistics for figure 4.9:**

	<b>D (<math>\mu\text{m}/\text{sec}^2</math>)</b>
WT MEFs 1.5 mg/ml collagen	0.11 $\pm$ 0.02
WT MEFs 1 mg/ml collagen	0.19 $\pm$ 0.03
Cav1-KO MEFs 1.5 mg/ml collagen	0.20 $\pm$ 0.02

<b>Comparison</b>	<b>p-value</b>
WT MEFs 1.5 mg/ml collagen vs WT MEFs 1 mg/ml collagen	0.0431
WT MEFs 1.5 mg/ml collagen vs Cav1-KO MEFs 1.5 mg/ml collagen	0.0127

**X. Statistics for figure 4.11:**

<b>GPI-GFP</b>		<b>D (<math>\mu\text{m}/\text{sec}^2</math>)</b>	<b>Comparison</b>	<b>p-value</b>
WT MEFs		$0.07 \pm 0.01$	WT MEFs vs WT MEFs + 0.5 $\mu\text{M}$ Cyto D	0.9352
WT MEFs + 0.5 $\mu\text{M}$ Cyto D		$0.08 \pm 0.01$		
WT MEFs + 1 $\mu\text{M}$ Cyto D		$0.13 \pm 0.02$	WT MEFs vs WT MEFs + 1 $\mu\text{M}$ Cyto D	0.0335

<b>GPI-GFP</b>		<b>D (<math>\mu\text{m}/\text{sec}^2</math>)</b>	<b>Comparison</b>	<b>p-value</b>
Cav1-KO MEFs control		$0.10 \pm 0.02$	Cav1-KO MEFs control vs Cav1-KO MEFs + 1 $\mu\text{M}$ Cyto D	0.9388
Cav1-KO MEFs + 1 $\mu\text{M}$ Cyto D		$0.10 \pm 0.02$		

<b>K-Ras-CAAX-GFP</b>		<b>D (<math>\mu\text{m}/\text{sec}^2</math>)</b>	<b>Comparison</b>	<b>p-value</b>
WT MEFs		$0.09 \pm 0.01$	WT MEFs vs WT MEFs + 1 $\mu\text{M}$ Cyto D	0.0228
WT MEFs + 1 $\mu\text{M}$ Cyto D		$0.18 \pm 0.03$		

<b>K-Ras-CAAX-GFP</b>		<b>D (<math>\mu\text{m}/\text{sec}^2</math>)</b>	<b>Comparison</b>	<b>p-value</b>
Cav1-KO MEFs control		$0.31 \pm 0.08$	Cav1-KO MEFs control vs Cav1-KO MEFs + 1 $\mu\text{M}$ Cyto D	0.8122
Cav1-KO MEFs + 1 $\mu\text{M}$ Cyto D		$0.33 \pm 0.06$		

**XI. Statistics for figure 4.12:**

<b>Collagen concentration</b>	<b>Stiffness (Pa)</b>
1 mg/ml	$28.60 \pm 1.85$
1.5 mg/ml	$70.90 \pm 1.60$

<b>Comparison</b>	<b>p-value</b>
1 mg/ml vs 1.5 mg/ml	<0.0001

## Bibliography

Achilli, M., and Mantovani, D. (2010). Tailoring Mechanical Properties of Collagen-Based Scaffolds for Vascular Tissue Engineering: The Effects of pH, Temperature and Ionic Strength on Gelation. *Polymers* 2, 665-680.

Agelaki, S., Spiliotaki, M., Markomanolaki, H., Kallergi, G., Mavroudis, D., Georgoulas, V., and Stournaras, C. (2009). Caveolin-1 regulates EGFR signaling in MCF-7 breast cancer cells and enhances gefitinib-induced tumor cell inhibition. *Cancer Biol Ther* 8, 1470-1477.

Alavi, A., and Stupack, D.G. (2007). Cell survival in a three-dimensional matrix. *Methods Enzymol* 426, 85-101.

Albinsson, S., Nordstrom, I., Sward, K., and Hellstrand, P. (2008). Differential dependence of stretch and shear stress signaling on caveolin-1 in the vascular wall. *Am J Physiol Cell Physiol* 294, C271-279.

An, K.N., Sun, Y.L., and Luo, Z.P. (2004). Flexibility of type I collagen and mechanical property of connective tissue. *Biorheology* 41, 239-246.

Ariotti, N., Fernandez-Rojo, M.A., Zhou, Y., Hill, M.M., Rodkey, T.L., Inder, K.L., Tanner, L.B., Wenk, M.R., Hancock, J.F., and Parton, R.G. (2014). Caveolae regulate the nanoscale organization of the plasma membrane to remotely control Ras signaling. *J Cell Biol* 204, 777-792.

Arjonen, A., Alanko, J., Veltel, S., and Ivaska, J. (2012). Distinct recycling of active and inactive beta1 integrins. *Traffic* 13, 610-625.

Asterholm, I.W., Mundy, D.I., Weng, J., Anderson, R.G., and Scherer, P.E. (2012). Altered mitochondrial function and metabolic inflexibility associated with loss of caveolin-1. *Cell Metab* 15, 171-185.

Aung, C.S., Hill, M.M., Bastiani, M., Parton, R.G., and Parat, M.O. (2011). PTRF-cavin-1 expression decreases the migration of PC3 prostate cancer cells: role of matrix metalloprotease 9. *Eur J Cell Biol* 90, 136-142.

Baker, B.M., and Chen, C.S. (2012). Deconstructing the third dimension: how 3D culture microenvironments alter cellular cues. *J Cell Sci* 125, 3015-3024.

Beacham, D.A., Amatangelo, M.D., and Cukierman, E. (2002). Preparation of extracellular matrices produced by cultured and primary fibroblasts. *Curr Protoc Cell Biol Chapter 10*, Unit 10 19.

Beningo, K.A., Dembo, M., and Wang, Y.L. (2004). Responses of fibroblasts to anchorage of dorsal extracellular matrix receptors. *Proc Natl Acad Sci USA* 101, 18024-18029.

- Biedi, C., Panetta, D., Segat, D., Cordera, R., and Maggi, D. (2003). Specificity of insulin-like growth factor I and insulin on Shc phosphorylation and Grb2 recruitment in caveolae. *Endocrinology* *144*, 5497-5503.
- Bilderback, T.R., Gazula, V.R., Lisanti, M.P., and Dobrowsky, R.T. (1999). Caveolin interacts with Trk A and p75(NTR) and regulates neurotrophin signaling pathways. *J Biol Chem* *274*, 257-263.
- Bilderback, T.R., Grigsby, R.J., and Dobrowsky, R.T. (1997). Association of p75(NTR) with caveolin and localization of neurotrophin-induced sphingomyelin hydrolysis to caveolae. *J Biol Chem* *272*, 10922-10927.
- Bode, J., Goetze, S., Heng, H., Krawetz, S.A., and Benham, C. (2003). From DNA structure to gene expression: mediators of nuclear compartmentalization and dynamics. *Chromosome Res* *11*, 435-445.
- Bosch, M., Mari, M., Herms, A., Fernandez, A., Fajardo, A., Kassan, A., Giralt, A., Colell, A., Balgoma, D., Barbero, E., *et al.* (2011). Caveolin-1 deficiency causes cholesterol-dependent mitochondrial dysfunction and apoptotic susceptibility. *Curr Biol* *21*, 681-686.
- Boucrot, E., Howes, M.T., Kirchhausen, T., and Parton, R.G. (2011). Redistribution of caveolae during mitosis. *J Cell Sci* *124*, 1965-1972.
- Brasaemle, D.L., Dolios, G., Shapiro, L., and Wang, R. (2004). Proteomic analysis of proteins associated with lipid droplets of basal and lipolytically stimulated 3T3-L1 adipocytes. *J Biol Chem* *279*, 46835-46842.
- Briand, N., Dugail, I., and Le Lay, S. (2011). Cavin proteins: New players in the caveolae field. *Biochimie* *93*, 71-77.
- Brugnano, J.L., and Panitch, A. (2014). Matrix stiffness affects endocytic uptake of MK2-inhibitor peptides. *PLoS One* *9*, e84821.
- Bucci, M. (2013). Leaflets out of order. *Nature Chemical Biology* *9*, 2011-2019.
- Cai, C., Weisleder, N., Ko, J.K., Komazaki, S., Sunada, Y., Nishi, M., Takeshima, H., and Ma, J. (2009). Membrane repair defects in muscular dystrophy are linked to altered interaction between MG53, caveolin-3, and dysferlin. *J Biol Chem* *284*, 15894-15902.
- Cao, S., Yao, J., McCabe, T.J., Yao, Q., Katusic, Z.S., Sessa, W.C., and Shah, V. (2001). Direct interaction between endothelial nitric-oxide synthase and dynamin-2. Implications for nitric-oxide synthase function. *J Biol Chem* *276*, 14249-14256.
- Cerezo, A., Guadamillas, M.C., Goetz, J.G., Sanchez-Perales, S., Klein, E., Assoian, R.K., and del Pozo, M.A. (2009). The absence of caveolin-1 increases proliferation and anchorage-

independent growth by a Rac-dependent, Erk-independent mechanism. *Mol Cell Biol* 29, 5046-5059.

Chaudhary, N., Gomez, G.A., Howes, M.T., Lo, H.P., McMahon, K.A., Rae, J.A., Schieber, N.L., Hill, M.M., Gaus, K., Yap, A.S., *et al.* (2014). Endocytic crosstalk: caveolins, caveolins, and caveolae regulate clathrin-independent endocytosis. *PLoS Biol* 12, e1001832.

Chiquet, M., Gelman, L., Lutz, R., and Maier, S. (2009). From mechanotransduction to extracellular matrix gene expression in fibroblasts. *Biochim Biophys Acta* 1793, 911-920.

Choquet, D., Felsenfeld, D.P., and Sheetz, M.P. (1997). Extracellular matrix rigidity causes strengthening of integrin-cytoskeleton linkages. *Cell* 88, 39-48.

Chow, A.K., Cena, J., El-Yazbi, A.F., Crawford, B.D., Holt, A., Cho, W.J., Daniel, E.E., and Schulz, R. (2007). Caveolin-1 inhibits matrix metalloproteinase-2 activity in the heart. *Journal of Molecular and Cellular Cardiology* 42, 896-901.

Clark, R.A.F., Lin, F., Greiling, D., an, J., and Couchman, J.R. (2004). Fibroblast invasive migration into fibronectin/fibrin gels requires a previously uncharacterized dermatan sulfate-CD44 proteoglycan. *J Invest Dermatol* 122, 266-277.

Cleutjens, J.P. (1996). The role of matrix metalloproteinases in heart disease. *Cardiovasc Res* 32, 816-821.

Collins, B.M., Davis, M.J., Hancock, J.F., and Parton, R.G. (2012). Structure-based reassessment of the caveolin signaling model: do caveolae regulate signaling through caveolin-protein interactions? *Dev Cell* 23, 11-20.

Couet, J., Li, S., Okamoto, T., Ikezu, T., and Lisanti, M.P. (1997a). Identification of peptide and protein ligands for the caveolin-scaffolding domain. Implications for the interaction of caveolin with caveolae-associated proteins. *J Biol Chem* 272, 6525-6533.

Couet, J., Sargiacomo, M., and Lisanti, M.P. (1997b). Interaction of a receptor tyrosine kinase, EGF-R, with caveolins. Caveolin binding negatively regulates tyrosine and serine/threonine kinase activities. *J Biol Chem* 272, 30429-30438.

Crisp, M., Liu, Q., Roux, K., Rattner, J.B., Shanahan, C., Burke, B., Stahl, P.D., and Hodzic, D. (2006). Coupling of the nucleus and cytoplasm: role of the LINC complex. *J Cell Biol* 172, 41-53.

Cukierman, E., Pankov, R., Stevens, D.R., and Yamada, K.M. (2001a). Taking cell-matrix adhesions to the third dimension. *Science* 294, 1708-1712.

Cukierman, E., Pankov, R., Stevens, D.R., and Yamada, K.M. (2001b). Taking Cell-Matrix Adhesions to the Third Dimension. *Science* 294, 1708-1712.



- Czarny, M., Fiucci, G., Lavie, Y., Banno, Y., Nozawa, Y., and Liscovitch, M. (2000). Phospholipase D2: functional interaction with caveolin in low-density membrane microdomains. *FEBS Lett* 467, 326-332.
- Dai, J., Ting-Beall, H.P., Hochmuth, R.M., Sheetz, M.P., and Titus, M.A. (1999). Myosin I contributes to the generation of resting cortical tension. *Biophys J* 77, 1168-1176.
- Dai, J., Ting-Beall, H.P., and Sheetz, M.P. (1997). The secretion-coupled endocytosis correlates with membrane tension changes in RBL 2H3 cells. *J Gen Physiol* 110, 1-10.
- Damm, E.M., Pelkmans, L., Kartenbeck, J., Mezzacasa, A., Kurzchalia, T., and Helenius, A. (2005). Clathrin- and caveolin-1-independent endocytosis: entry of simian virus 40 into cells devoid of caveolae. *J Cell Biol* 168, 477-488.
- Davis, J.T., Wen, Q., Janmey, P.A., Otteson, D.C., and Foster, W.J. (2012). Muller cell expression of genes implicated in proliferative vitreoretinopathy is influenced by substrate elastic modulus. *Invest Ophthalmol Vis Sci* 53, 3014-3019.
- del Pozo, M.A., Alderson, N.B., Kiosses, W.B., Chiang, H.H., Anderson, R.G., and Schwartz, M.A. (2004). Integrins regulate Rac targeting by internalization of membrane domains. *Science* 303, 839-842.
- del Pozo, M.A., Balasubramanian, N., Alderson, N.B., Kiosses, W.B., Grande-Garcia, A., Anderson, R.G., and Schwartz, M.A. (2005). Phospho-caveolin-1 mediates integrin-regulated membrane domain internalization. *Nat Cell Biol* 7, 901-908.
- Dietzen, D.J., W.R. Hastings, and Lublin, D.M. (1995). Caveolin is palmitoylated on multiple cysteine residues. Palmitoylation is not necessary for localization of caveolin to caveolae. *J Biol Chem* 270, 6838-6842.
- Diz-Muñoz, A., Fletcher, D.A., and Weiner, O.D. (2013). Use the force: membrane tension as an organizer of cell shape and motility. *Trends in Cell Biology* 23, 47-53.
- Doyle, A.D., Carvajal, N., Jin, A., Matsumoto, K., and Yamada, K.M. (2015). Local 3D matrix microenvironment regulates cell migration through spatiotemporal dynamics of contractility-dependent adhesions. *Nat Commun* 6, 8720.
- Doyle, A.D., Wang, F.W., Matsumoto, K., and Yamada, K.M. (2009). One dimensional topography underlies three-dimensional fibrillar cell migration. *Journal of Cell Biology* 184, 481-490.
- Doyle, A.D., and Yamada, K.M. (2016). Mechanosensing via cell-matrix adhesions in 3D microenvironments. *Exp Cell Res* 343, 60-66.

Du, J., Chen, X., Liang, X., Zhang, G., Xu, J., He, L., Zhan, Q., Feng, X.Q., Chien, S., and Yang, C. (2011). Integrin activation and internalization on soft ECM as a mechanism of induction of stem cell differentiation by ECM elasticity. *Proc Natl Acad Sci U S A* *108*, 9466-9471.

Dulhunty, A.F., and Franzini-Armstrong, C. (1975). The relative contributions of the folds and caveolae to the surface membrane of frog skeletal muscle fibres at different sarcomere lengths. *J Physiol* *250*, 513-539.

Echarri, A., Muriel, O., Pavon, D.M., Azegrouz, H., Escolar, F., Terron, M.C., Sanchez-Cabo, F., Martinez, F., Montoya, M.C., Llorca, O., *et al.* (2012). Caveolar domain organization and trafficking is regulated by Abl kinases and mDia1. *J Cell Sci* *125*, 3097-3113.

Eddidin, M. (1997). Lipid microdomains in cell surface membranes. *Curr Opin Struct Biol* *7*, 528-532.

Ellenberg, J., Siggia, E.D., Moreira, J.E., Smith, C.L., Presley, J.F., Worman, H.J., and Lippincott-Schwartz, J. (1997). Nuclear membrane dynamics and reassembly in living cells: targeting of an inner nuclear membrane protein in interphase and mitosis. *J Cell Biol* *138*, 1193-1206.

Elsdale, T., and Bard, J. (1972). Collagen substrata for studies on cell behavior. *Journal of Cell Biology* *54*, 626-637.

Engelman, J.A., Chu, C., Lin, A., Jo, H., Ikezu, T., Okamoto, T., Kohtz, D.S., and Lisanti, M.P. (1998a). Caveolin-mediated regulation of signaling along the p42/44 MAP kinase cascade in vivo. A role for the caveolin-scaffolding domain. *FEBS Lett* *428*, 205-211.

Engelman, J.A., Zhang, X.L., Galbiati, F., and Lisanti, M.P. (1998b). Chromosomal localization, genomic organization, and developmental expression of the murine caveolin gene family (Cav-1, -2, and -3). Cav-1 and Cav-2 genes map to a known tumor suppressor locus (6-A2/7q31). *FEBS Lett* *429*, 330-336.

Even-Ram, S., and Yamada, K.M. (2005). Cell migration in 3D matrix. *Curr Opin Cell Biol* *17*, 524-532.

Fairn, G.D., Schieber, N.L., Ariotti, N., Murphy, S., Kuerschner, L., Webb, R.I., Grinstein, S., and Parton, R.G. (2011). High-resolution mapping reveals topologically distinct cellular pools of phosphatidylserine. *J Cell Biol* *194*, 257-275.

Fang, P.K., Solomon, K.R., Zhuang, L., Qi, M., McKee, M., Freeman, M.R., and Yelick, P.C. (2006). Caveolin-1 $\alpha$  and -1 $\beta$  perform nonredundant roles in early vertebrate development. *Am J Pathol* *169*, 2209-2222.

Fielding, C.J., and Fielding, P.E. (2000). Cholesterol and caveolae: structural and functional relationships. *Biochim Biophys Acta* *1529*, 210-222.

- Fielding, P.E., Chau, P., Liu, D., Spencer, T.A., and Fielding, C.J. (2004). Mechanism of platelet-derived growth factor-dependent caveolin-1 phosphorylation: relationship to sterol binding and the role of serine-80. *Biochemistry* *43*, 2578-2586.
- Forte, G., Pagliari, S., Ebara, M., Uto, K., Tam, J.K., Romanazzo, S., Escobedo-Lucea, C., Romano, E., Di Nardo, P., Traversa, E., *et al.* (2012). Substrate stiffness modulates gene expression and phenotype in neonatal cardiomyocytes in vitro. *Tissue Eng Part A* *18*, 1837-1848.
- Fra, A.M., Williamson, E., Simons, K., and Parton, R.G. (1995). De novo formation of caveolae in lymphocytes by expression of VIP21-caveolin. *Proc Natl Acad Sci U S A* *92*, 8655-8659.
- Fraley, S.I., Feng, Y., Krishnamurthy, R., Kim, D.H., Celedon, A., Longmore, G.D., and Wirtz, D. (2010). A distinctive role for focal adhesion proteins in three-dimensional cell motility. *Nat Cell Biol* *12*, 598-604.
- Francis, S.S., Sfakianos, J., Lo, B., and Mellman, I. (2011). A hierarchy of signals regulates entry of membrane proteins into the ciliary membrane domain in epithelial cells. *J Cell Biol* *193*, 219-233.
- Fujiwara, T., Ritchie, K., Murakoshi, H., Jacobson, K., and Kusumi, A. (2002). Phospholipids undergo hop diffusion in compartmentalized cell membrane. *J Cell Biol* *157*, 1071-1081.
- Galbiati, F., Volonte, D., Engelman, J.A., Watanabe, G., Burk, R., Pestell, R.G., and Lisanti, M.P. (1998). Targeted downregulation of caveolin-1 is sufficient to drive cell transformation and hyperactivate the p42/44 MAP kinase cascade. *EMBO J* *17*, 6633-6648.
- Galvez, B.G., Matias-Roman, S., Yanez-Mo, M., Vicente-Manzanares, M., Sanchez-Madrid, F., and Arroyo, A.G. (2004). Caveolae are a novel pathway for membrane-type 1 matrix metalloproteinase traffic in human endothelial cells. *Mol Biol Cell* *15*, 678-687.
- Garcia-Cardena, G., Martasek, P., Masters, B.S., Skidd, P.M., Couet, J., Li, S., Lisanti, M.P., and Sessa, W.C. (1997). Dissecting the interaction between nitric oxide synthase (NOS) and caveolin. Functional significance of the nos caveolin binding domain in vivo. *J Biol Chem* *272*, 25437-25440.
- Gaus, K., Le Lay, S., Balasubramanian, N., and Schwartz, M.A. (2006). Integrin-mediated adhesion regulates membrane order. *J Cell Biol* *174*, 725-734.
- Glenney, J.R. (1989). Tyrosine phosphorylation of a 22k-Da protein is correlated with transformation by rous sarcoma virus. *Journal of Biological Chemistry* *264*, 20163-20166.
- Glenney, J.R., Jr., and Soppet, D. (1992). Sequence and expression of caveolin, a protein component of caveolae plasma membrane domains phosphorylated on tyrosine in Rous sarcoma virus-transformed fibroblasts. *Proc Natl Acad Sci U S A* *89*, 10517-10521.

Goetz, J.G., Lajoie, P., Wiseman, S.M., and Nabi, I.R. (2008). Caveolin-1 in tumor progression: the good, the bad and the ugly. *Cancer Metastasis Rev* 27, 715-735.

Goetz, J.G., Minguet, S., Navarro-Lerida, I., Lazcano, J.J., Samaniego, R., Calvo, E., Tello, M., Osteso-Ibanez, T., Pellinen, T., Echarri, A., *et al.* (2011). Biomechanical remodeling of the microenvironment by stromal caveolin-1 favors tumor invasion and metastasis. *Cell* 146, 148-163.

Gould, M.L., Williams, G., and Nicholson, H.D. (2010). Changes in caveolae, caveolin, and polymerase 1 and transcript release factor (PTRF) expression in prostate cancer progression. *Prostate* 70, 1609-1621.

Grande-Garcia, A., Echarri, A., de Rooij, J., Alderson, N.B., Waterman-Storer, C.M., Valdivielso, J.M., and del Pozo, M.A. (2007). Caveolin-1 regulates cell polarization and directional migration through Src kinase and Rho GTPases. *J Cell Biol* 177, 683-694.

Grinnell, F. (2003). Fibroblast biology in three-dimensional collagen matrices. *Trends Cell Biol* 13, 264-269.

Gulino-Debrac (2013). Mechanotransduction at the basis of endothelial barrier function. *Tissue Barriers* 1, e24180-24181-e241807.

Guthold, M., Liu, W., Sparks, E.A., Jawerth, L.M., Peng, L., Falvo, M., Superfine, R., Hantgan, R.R., and Lord, S.T. (2007). A comparison of the mechanical and structural properties of fibrin fibers with other protein fibers. *Cell Biochem Biophys* 49, 165-181.

Han, B., Tiwari, A., and Kenworthy, A.K. (2015). Tagging strategies strongly affect the fate of overexpressed caveolin-1. *Traffic* 16, 417-438.

Han, F., and Zhu, H.G. (2010). Caveolin-1 regulating the invasion and expression of matrix metalloproteinase (MMPs) in pancreatic carcinoma cells. *J Surg Res* 159, 443-450.

Hansen, C.G., Bright, N.A., Howard, G., and Nichols, B.J. (2009). SDPR induces membrane curvature and functions in the formation of caveolae. *Nat Cell Biol* 11, 807-814.

Hansen, C.G., Howard, G., and Nichols, B.J. (2011). Pacsin 2 is recruited to caveolae and functions in caveolar biogenesis. *J Cell Sci* 124, 2777-2785.

Hanson, C.A., Drake, K.R., Baird, M.A., Han, B., Kraft, L.J., Davidson, M.W., and Kenworthy, A.K. (2013). Overexpression of caveolin-1 is sufficient to phenocopy the behavior of a disease-associated mutant. *Traffic* 14, 663-677.

Hayer, A., Stoeber, M., Bissig, C., and Helenius, A. (2010a). Biogenesis of caveolae: stepwise assembly of large caveolin and cavin complexes. *Traffic* 11, 361-382.

- Hayer, A., Stoeber, M., Ritz, D., Engel, S., Meyer, H.H., and Helenius, A. (2010b). Caveolin-1 is ubiquitinated and targeted to intraluminal vesicles in endolysosomes for degradation. *J Cell Biol* *191*, 615-629.
- Henley, J.R., Krueger, E.W., Oswald, B.J., and McNiven, M.A. (1998). Dynamin-mediated internalization of caveolae. *J Cell Biol* *141*, 85-99.
- Hill, M.M., Bastiani, M., Luetterforst, R., Kirkham, M., Kirkham, A., Nixon, S.J., Walser, P., Abankwa, D., Oorschot, V.M., Martin, S., *et al.* (2008). PTRF-Cavin, a conserved cytoplasmic protein required for caveola formation and function. *Cell* *132*, 113-124.
- Hill, M.M., Daud, N.H., Aung, C.S., Loo, D., Martin, S., Murphy, S., Black, D.M., Barry, R., Simpson, F., Liu, L., *et al.* (2012). Co-regulation of cell polarization and migration by caveolar proteins PTRF/Cavin-1 and caveolin-1. *PLoS One* *7*, e43041.
- Hill, M.M., Scherbakov, N., Schiefermeier, N., Baran, J., Hancock, J.F., Huber, L.A., Parton, R.G., and Parat, M.O. (2007). Reassessing the role of phosphocaveolin-1 in cell adhesion and migration. *Traffic* *8*, 1695-1705.
- Hoffmann, C., Berking, A., Agerer, F., Buntru, A., Neske, F., Chhatwal, G.S., Ohlsen, K., and Hauck, C.R. (2010). Caveolin limits membrane microdomain mobility and integrin-mediated uptake of fibronectin-binding pathogens. *J Cell Sci* *123*, 4280-4291.
- Howes, M.T., Kirkham, M., Riches, J., Cortese, K., Walser, P.J., Simpson, F., Hill, M.M., Jones, A., Lundmark, R., Lindsay, M.R., *et al.* (2010). Clathrin-independent carriers form a high capacity endocytic sorting system at the leading edge of migrating cells. *J Cell Biol* *190*, 675-691.
- Huang, C., Butler, P.J., Tong, S., Muddana, H.S., Bao, G., and Zhang, S. (2013). Substrate stiffness regulates cellular uptake of nanoparticles. *Nano Lett* *13*, 1611-1615.
- Hughes, C.S., Postovit, L.M., and Lajoie, G.A. (2010). Matrigel: a complex protein mixture required for optimal growth of cell culture. *Proteomics* *10*, 1886-1890.
- Ingber, D.E. (2006). Cellular mechanotransduction: putting all the pieces together again. *FASEB J* *20*, 811-827.
- Isshiki, M., Ando, J., Yamamoto, K., Fujita, T., Ying, Y., and Anderson, R.G. (2002). Sites of Ca(2+) wave initiation move with caveolae to the trailing edge of migrating cells. *J Cell Sci* *115*, 475-484.
- Iwasa, K.H. (1993). Effect of stress on the membrane capacitance of the auditory outer hair cell. *Biophys J* *65*, 492-498.
- Jacobson, K., Sheets, E.D., and Simson, R. (1995). Revisiting the fluid mosaic model of membranes. *Science* *268*, 1441-1442.

- Jang, I.H., Kim, J.H., Lee, B.D., Bae, S.S., Park, M.H., Suh, P.G., and Ryu, S.H. (2001). Localization of phospholipase C-gamma1 signaling in caveolae: importance in EGF-induced phosphoinositide hydrolysis but not in tyrosine phosphorylation. *FEBS Lett* 491, 4-8.
- Jayo, A., and Parsons, M. (2012). Imaging of cell adhesion events in 3D matrix environments. *European Journal of Cell Biology* 50686, 1-10.
- Jodele, S., Blavier, L., Yoon, J.M., and DeClerck, Y.A. (2006). Modifying the soil to affect the seed: role of stromal-derived matrix metalloproteinases in cancer progression. *Cancer Metastasis Rev* 25, 35-43.
- Johannes, L., and Lamaze, C. (2002). Clathrin-dependent or not: is it still the question? *Traffic* 3, 443-451.
- Joshi, B., Bastiani, M., Strugnelli, S.S., Boscher, C., Parton, R.G., and Nabi, I.R. (2012). Phosphocaveolin-1 is a mechanotransducer that induces caveola biogenesis via Egr1 transcriptional regulation. *J Cell Biol* 199, 425-435.
- Joshi, B., Strugnelli, S.S., Goetz, J.G., Kojic, L.D., Cox, M.E., Griffith, O.L., Chan, S.K., Jones, S.J., Leung, S.P., Masoudi, H., *et al.* (2008). Phosphorylated caveolin-1 regulates Rho/ROCK-dependent focal adhesion dynamics and tumor cell migration and invasion. *Cancer Res* 68, 8210-8220.
- Ju, H., Zou, R., Venema, V.J., and Venema, R.C. (1997). Direct interaction of endothelial nitric-oxide synthase and caveolin-1 inhibits synthase activity. *J Biol Chem* 272, 18522-18525.
- K. Bloch (1991). Cholesterol: evolution of structure and function. *Biochemistry of Lipids, Lipoprotein and Membranes*, 363-381.
- Kakehata, S., and Santos-Sacchi, J. (1995). Membrane tension directly shifts voltage dependence of outer hair cell motility and associated gating charge. *Biophys J* 68, 2190-2197.
- Kalluri, R. (2003). Basement membranes: structure, assembly and role in tumour angiogenesis. *Nat Rev Cancer* 3, 422-433.
- Kanzaki, M., and Pessin, J.E. (2002). Caveolin-associated filamentous actin (Cav-actin) defines a novel F-actin structure in adipocytes. *J Biol Chem* 277, 25867-25869.
- Kim, J.H., Han, J.M., Lee, S., Kim, Y., Lee, T.G., Park, J.B., Lee, S.D., Suh, P.G., and Ryu, S.H. (1999). Phospholipase D1 in caveolae: regulation by protein kinase Calpha and caveolin-1. *Biochemistry* 38, 3763-3769.
- Kim, Y.N., Wiepz, G.J., Guadarrama, A.G., and Bertics, P.J. (2000). Epidermal growth factor-stimulated tyrosine phosphorylation of caveolin-1. Enhanced caveolin-1 tyrosine phosphorylation following aberrant epidermal growth factor receptor status. *J Biol Chem* 275, 7481-7491.

- Kirkham, M., Nixon, S.J., Howes, M.T., Abi-Rached, L., Wakeham, D.E., Hanzal-Bayer, M., Ferguson, C., Hill, M.M., Fernandez-Rojo, M., Brown, D.A., *et al.* (2008). Evolutionary analysis and molecular dissection of caveola biogenesis. *J Cell Sci* *121*, 2075-2086.
- Kisiday, J., Jin, M., Kurz, B., Hung, H., Semino, C., Zhang, S., and Grodzinsky, A.J. (2002). Self-assembling peptide hydrogel fosters chondrocyte extracellular matrix production and cell division: implications for cartilage tissue repair. *Proc Natl Acad Sci U S A* *99*, 9996-10001.
- Kovtun, O., Tillu, V.A., Ariotti, N., Parton, R.G., and Collins, B.M. (2015). Cavin family proteins and the assembly of caveolae. *J Cell Sci* *128*, 1269-1278.
- Kozera, L., White, E., and Calaghan, S. (2009). Caveolae act as membrane reserves which limit mechanosensitive I(Cl,swell) channel activation during swelling in the rat ventricular myocyte. *PLoS One* *4*, e8312.
- Kubow, K.E., Conrad, S.K., and Horwitz, A.R. (2013). Matrix microarchitecture and myosin II determine adhesion in 3D matrices. *Curr Biol* *23*, 1607-1619.
- Kubow, K.E., and Horwitz, A.R. (2011). Reducing background fluorescence reveals adhesions in 3D matrices. *Nat Cell Biol* *13*, 3-5; author reply 5-7.
- Lajoie, P., Partridge, E.A., Guay, G., Goetz, J.G., Pawling, J., Lagana, A., Joshi, B., Dennis, J.W., and Nabi, I.R. (2007). Plasma membrane domain organization regulates EGFR signaling in tumor cells. *J Cell Biol* *179*, 341-356.
- Lauffenburger, D.A., and Horwitz, A.F. (1996). Cell migration: a physically integrated molecular process. *Cell* *84*, 359-369.
- Lee, B., Zhou, X., Riching, K., Eliceiri, K.W., Keely, P.J., Guelcher, S.A., Weaver, A.M., and Jiang, Y. (2014). A three-dimensional computational model of collagen network mechanics. *PLoS One* *9*, e111896.
- Lee, H., Park, D.S., Wang, X.B., Scherer, P.E., Schwartz, P.E., and Lisanti, M.P. (2002). Src-induced phosphorylation of caveolin-2 on tyrosine 19. Phospho-caveolin-2 (Tyr(P)19) is localized near focal adhesions, remains associated with lipid rafts/caveolae, but no longer forms a high molecular mass hetero-oligomer with caveolin-1. *J Biol Chem* *277*, 34556-34567.
- Lee, J., and Glover, K.J. (2012). The transmembrane domain of caveolin-1 exhibits a helix-break-helix structure. *Biochim Biophys Acta* *1818*, 1158-1164.
- Lee, J., and Schmid-Schonbein, G.W. (1995). Biomechanics of skeletal muscle capillaries: hemodynamic resistance, endothelial distensibility, and pseudopod formation. *Ann Biomed Eng* *23*, 226-246.
- Lee, S.W., Reimer, C.L., Oh, P., Campbell, D.B., and Schnitzer, J.E. (1998). Tumor cell growth inhibition by caveolin re-expression in human breast cancer cells. *Oncogene* *16*, 1391-1397.

- Lepzelter, D., Bates, O., and Zaman, M. (2012). Integrin clustering in two and three dimensions. *Langmuir* 28, 5379-5386.
- Liu, A.P., Chaudhuri, O., and Parekh, S.H. (2017). New advances in probing cell-extracellular matrix interactions. *Integr Biol (Camb)* 9, 383-405.
- Liu, L., Brown, D., McKee, M., Lebrasseur, N.K., Yang, D., Albrecht, K.H., Ravid, K., and Pilch, P.F. (2008). Deletion of Cavin/PTRF causes global loss of caveolae, dyslipidemia, and glucose intolerance. *Cell Metab* 8, 310-317.
- Liu, L., Mohammadi, K., Aynafshar, B., Wang, H., Li, D., Liu, J., Ivanov, A.V., Xie, Z., and Askari, A. (2003). Role of caveolae in signal-transducing function of cardiac Na<sup>+</sup>/K<sup>+</sup>-ATPase. *Am J Physiol Cell Physiol* 284, C1550-1560.
- Liu, P., Li, W.P., Machleidt, T., and Anderson, R.G. (1999). Identification of caveolin-1 in lipoprotein particles secreted by exocrine cells. *Nat Cell Biol* 1, 369-375.
- Liu, Y.J., Le Berre, M., Lautenschlaeger, F., Maiuri, P., Callan-Jones, A., Heuze, M., Takaki, T., Voituriez, R., and Piel, M. (2015). Confinement and low adhesion induce fast amoeboid migration of slow mesenchymal cells. *Cell* 160, 659-672.
- Lo, C.M., Wang, H.B., Dembo, M., and Wang, Y.L. (2000). Cell movement is guided by the rigidity of the substrate. *Biophys J* 79, 144-152.
- Lord, S.T. (2007). Fibrinogen and fibrin: scaffold proteins in hemostasis. *Curr Opin Hematol* 14, 236-241.
- Lutolf, M.P., and Hubbell, J.A. (2005). Synthetic biomaterials as instructive extracellular microenvironments for morphogenesis in tissue engineering. *Nat Biotechnol* 23, 47-55.
- Mann, B.K., Gobin, A.S., Tsai, A.T., Schmedlen, R.H., and West, J.L. (2001). Smooth muscle cell growth in photopolymerized hydrogels with cell adhesive and proteolytically degradable domains: synthetic ECM analogs for tissue engineering. *Biomaterials* 22, 3045-3051.
- Mata, A., Hsu, L., Capito, R., Aparicio, C., Henrikson, K., and Stupp, S.I. (2009). Micropatterning of bioactive self-assembling gels. *Soft Matter* 5, 1228-1236.
- Meshulam, T., Simard, J.R., Wharton, J., Hamilton, J.A., and Pilch, P.F. (2006). Role of caveolin-1 and cholesterol in transmembrane fatty acid movement. *Biochemistry* 45, 2882-2893.
- Miller, J.S., Shen, C.J., Legant, W.R., Baranski, J.D., Blakely, B.L., and Chen, C.S. (2010). Bioactive hydrogels made from step-growth derived PEG-peptide macromers. *Biomaterials* 31, 3736-3743.



- Monier, S., Parton, R.G., Vogel, F., Behlke, J., Henske, A., and Kurzchalia, T.V. (1995). VIP21-caveolin, a membrane protein constituent of the caveolar coat, oligomerizes in vivo and in vitro. *Mol Biol Cell* 6, 911-927.
- Mundy, D.I., Machleidt, T., Ying, Y.S., Anderson, R.G., and Bloom, G.S. (2002). Dual control of caveolar membrane traffic by microtubules and the actin cytoskeleton. *J Cell Sci* 115, 4327-4339.
- Murata M, Peranen J, Schreiner R, Wieland F, Kurzchalia TV, and K., S. (1995). VIP21/caveolin is a cholesterol-binding protein. *Proc Natl Acad Sci* 22, 10339-10343.
- Muriel, O., Echarri, A., Hellriegel, C., Pavon, D.M., Beccari, L., and Del Pozo, M.A. (2011). Phosphorylated filamin A regulates actin-linked caveolae dynamics. *J Cell Sci* 124, 2763-2776.
- Murphy, G., Knauper, V., Atkinson, S., Butler, G., English, W., Hutton, M., Stracke, J., and Clark, I. (2002). Matrix metalloproteinases in arthritic disease. *Arthritis Res* 4 Suppl 3, S39-49.
- Murshid, S.A., Kamioka, H., Ishihara, Y., Ando, R., Sugawara, Y., and Takano-Yamamoto, T. (2007). Actin and microtubule cytoskeletons of the processes of 3D-cultured MC3T3-E1 cells and osteocytes. *J Bone Miner Metab* 25, 151-158.
- Nichols, B. (2003). Caveosomes and endocytosis of lipid rafts. *J Cell Sci* 116, 4707-4714.
- Nichols, B.J., and Lippincott-Schwartz, J. (2001). Endocytosis without clathrin coats. *Trends Cell Biol* 11, 406-412.
- Niv, H., Gutman, O., Kloog, Y., and Henis, Y.I. (2002). Activated K-Ras and H-Ras display different interactions with saturable nonraft sites at the surface of live cells. *J Cell Biol* 157, 865-872.
- Nixon, S.J., Carter, A., Wegner, J., Ferguson, C., Floetenmeyer, M., Riches, J., Key, B., Westerfield, M., and Parton, R.G. (2007). Caveolin-1 is required for lateral line neuromast and notochord development. *J Cell Sci* 120, 2151-2161.
- Norica Branza-Nichita, Macovei, A., and Lazar, C. (2012). Caveolae-Dependent Endocytosis in Viral Infection. *Molecular Regulation of Endocytosis*.
- Oh, P., Borgstrom, P., Witkiewicz, H., Li, Y., Borgstrom, B.J., Chrastina, A., Iwata, K., Zinn, K.R., Baldwin, R., Testa, J.E., *et al.* (2007). Live dynamic imaging of caveolae pumping targeted antibody rapidly and specifically across endothelium in the lung. *Nat Biotechnol* 25, 327-337.
- Okamoto, T., Schlegel, A., Scherer, P.E., and Lisanti, M.P. (1998). Caveolins, a family of scaffolding proteins for organizing "preassembled signaling complexes" at the plasma membrane. *J Biol Chem* 273, 5419-5422.

Onoprishvili, I., Andria, M.L., Kramer, H.K., Ancevska-Taneva, N., Hiller, J.M., and Simon, E.J. (2003). Interaction between the mu opioid receptor and filamin A is involved in receptor regulation and trafficking. *Mol Pharmacol* *64*, 1092-1100.

Palade, G.E. (1953). Fine structure of blood capillaries. *J Appl Phys* *24*, 1424-1436.

Pani, B., Ong, H.L., Brazer, S.C., Liu, X., Rauser, K., Singh, B.B., and Ambudkar, I.S. (2009). Activation of TRPC1 by STIM1 in ER-PM microdomains involves release of the channel from its scaffold caveolin-1. *Proc Natl Acad Sci U S A* *106*, 20087-20092.

Parat, M.O., Anand-Apte, B., and Fox, P.L. (2003). Differential caveolin-1 polarization in endothelial cells during migration in two and three dimensions. *Mol Biol Cell* *14*, 3156-3168.

Parton, R.G. (1994). Ultrastructural localization of gangliosides; GM1 is concentrated in caveolae. *J Histochem Cytochem* *42*, 155-166.

Parton, R.G., and del Pozo, M.A. (2013). Caveolae as plasma membrane sensors, protectors and organizers. *Nat Rev Mol Cell Biol* *14*, 98-112.

Paszek, M.J., DuFort, C.C., Rossier, O., Bainer, R., Mouw, J.K., Godula, K., Hudak, J.E., Lakins, J.N., Wijekoon, A.C., Cassereau, L., *et al.* (2014). The cancer glycocalyx mechanically primes integrin-mediated growth and survival. *Nature* *511*, 319-325.

Pedersen, J.A., and Swartz, M.A. (2005). Mechanobiology in the third dimension. *Ann Biomed Eng* *33*, 1469-1490.

Pelkmans, L., and Helenius, A. (2002). Endocytosis via caveolae *Traffic* *3*, 311-320.

Petersen, A., Joly, P., Bergmann, C., Korus, G., and Duda, G.N. (2012). The impact of substrate stiffness and mechanical loading on fibroblast-induced scaffold remodeling. *Tissue Eng Part A* *18*, 1804-1817.

Pietuch, A., and Janshoff, A. (2013). Mechanics of spreading cells probed by atomic force microscopy. *Open Biol* *3*, 130084.

Pol, A., Martin, S., Fernandez, M.A., Ferguson, C., Carozzi, A., Luetterforst, R., Enrich, C., and Parton, R.G. (2004). Dynamic and regulated association of caveolin with lipid bodies: modulation of lipid body motility and function by a dominant negative mutant. *Mol Biol Cell* *15*, 99-110.

Prevostel, C., Alice, V., Joubert, D., and Parker, P.J. (2000). Protein kinase C(alpha) actively downregulates through caveolae-dependent traffic to an endosomal compartment. *J Cell Sci* *113* ( Pt 14), 2575-2584.

Prior, I.A., and Hancock, J.F. (2001). Compartmentalization of Ras proteins. *J Cell Sci* *114*, 1603-1608.

- Prior, I.A., Harding, A., Yan, J., Sluimer, J., Parton, R.G., and Hancock, J.F. (2001). GTP-dependent segregation of H-ras from lipid rafts is required for biological activity. *Nat Cell Biol* 3, 368-375.
- Puyraimond, A., Fridman, R., Lemesle, M., Arbeille, B., and Menashi, S. (2001). MMP-2 colocalizes with caveolae on the surface of endothelial cells. *Exp Cell Res* 262, 28-36.
- Ravid, D., Chuderland, D., Landsman, L., Lavie, Y., Reich, R., and Liscovitch, M. (2008). Filamin A is a novel caveolin-1-dependent target in IGF-I-stimulated cancer cell migration. *Exp Cell Res* 314, 2762-2773.
- Razani, B., Combs, T.P., Wang, X.B., Frank, P.G., Park, D.S., Russell, R.G., Li, M., Tang, B., Jelicks, L.A., Scherer, P.E., *et al.* (2002). Caveolin-1-deficient mice are lean, resistant to diet-induced obesity, and show hypertriglyceridemia with adipocyte abnormalities. *J Biol Chem* 277, 8635-8647.
- Razani, B., and Lisanti, M.P. (2001). Two distinct caveolin-1 domains mediate the functional interaction of caveolin-1 with protein kinase A. *Am J Physiol Cell Physiol* 281, C1241-1250.
- Razani, B., Zhang, X.L., Bitzer, M., von Gersdorff, G., Bottinger, E.P., and Lisanti, M.P. (2001). Caveolin-1 regulates transforming growth factor (TGF)-beta/SMAD signaling through an interaction with the TGF-beta type I receptor. *J Biol Chem* 276, 6727-6738.
- Reis, R.C., Sorgine, M.H., and Coelho-Sampaio, T. (1998). A novel methodology for the investigation of intracellular proteolytic processing in intact cells. *Eur J Cell Biol* 75, 192-197.
- Remacle, A., Murphy, G., and Roghi, C. (2003). Membrane type I-matrix metalloproteinase (MT1-MMP) is internalised by two different pathways and is recycled to the cell surface. *J Cell Sci* 116, 3905-3916.
- Rhee, S., and Grinnell, F. (2007). Fibroblast mechanics in 3D collagen matrices. *Adv Drug Deliv Rev* 59, 1299-1305.
- Ridley, A.J., Schwartz, M.A., Burridge, K., Firtel, R.A., Ginsberg, M.H., Borisy, G., Parsons, J.T., and Horwitz, A.R. (2003). Cell migration: integrating signals from front to back. *Science* 302, 1704-1709.
- Rothberg, K.G., Heuser, J.E., Donzell, W.C., Ying, Y.S., Glenney, J.R., and Anderson, R.G. (1992). Caveolin, a protein component of caveolae membrane coats. *Cell* 68, 673-682.
- Ruppender, N.S., Merkel, A.R., Martin, T.J., Mundy, G.R., Sterling, J.A., and Guelcher, S.A. (2010). Matrix rigidity induces osteolytic gene expression of metastatic breast cancer cells. *PLoS One* 5, e15451.

- Ruprecht, V., Wieser, S., Callan-Jones, A., Smutny, M., Morita, H., Sako, K., Barone, V., Ritsch-Marte, M., Sixt, M., Voituriez, R., *et al.* (2015). Cortical contractility triggers a stochastic switch to fast amoeboid cell motility. *Cell* *160*, 673-685.
- Saha, S., Lee, H., Polley, A., Groves, J.T., Rao, M., and Mayor, S. (2015). Diffusion of GPI-anchored proteins is influenced by the activity of dynamic cortical actin. *Molecular Biology of The Cell* *26*, 4033-4045.
- Sahai, E., and Marshall, C.J. (2003). Differing modes of tumour cell invasion have distinct requirements for Rho/ROCK signalling and extracellular proteolysis. *Nat Cell Biol* *5*, 711-719.
- Sanguinetti, A.R., Cao, H., and Corley Mastick, C. (2003). Fyn is required for oxidative- and hyperosmotic-stress-induced tyrosine phosphorylation of caveolin-1. *Biochem J* *376*, 159-168.
- Sanguinetti, A.R., and Mastick, C.C. (2003). c-Abl is required for oxidative stress-induced phosphorylation of caveolin-1 on tyrosine 14. *Cell Signal* *15*, 289-298.
- Sanz-Moreno, V., Gaggioli, C., Yeo, M., Albregues, J., Wallberg, F., Viros, A., Hooper, S., Mitter, R., Feral, C.C., Cook, M., *et al.* (2011). ROCK and JAK1 signaling cooperate to control actomyosin contractility in tumor cells and stroma. *Cancer Cell* *20*, 229-245.
- Scheiffele, P., Verkade, P., Fra, A.M., Virta, H., Simons, K., and Ikonen, E. (1998). Caveolin-1 and -2 in the exocytic pathway of MDCK cells. *J Cell Biol* *140*, 795-806.
- Scherer, P.E., Lewis, R.Y., Volonte, D., Engelman, J.A., Galbiati, F., Couet, J., Kohtz, D.S., van Donselaar, E., Peters, P., and Lisanti, M.P. (1997). Cell-type and tissue-specific expression of caveolin-2. Caveolins 1 and 2 co-localize and form a stable hetero-oligomeric complex in vivo. *J Biol Chem* *272*, 29337-29346.
- Scherer, P.E., Tang, Z., Chun, M., Sargiacomo, M., Lodish, H.F., and Lisanti, M.P. (1995). Caveolin isoforms differ in their N-terminal protein sequence and subcellular distribution. Identification and epitope mapping of an isoform-specific monoclonal antibody probe. *J Biol Chem* *270*, 16395-16401.
- Schlegel, A., Arvan, P., and Lisanti, M.P. (2001). Caveolin-1 binding to endoplasmic reticulum membranes and entry into the regulated secretory pathway are regulated by serine phosphorylation. Protein sorting at the level of the endoplasmic reticulum. *J Biol Chem* *276*, 4398-4408.
- Seck, T., Baron, R., and Horne, W.C. (2003). Binding of filamin to the C-terminal tail of the calcitonin receptor controls recycling. *J Biol Chem* *278*, 10408-10416.
- Shi, F., and Sottile, J. (2008). Caveolin-1-dependent beta1 integrin endocytosis is a critical regulator of fibronectin turnover. *J Cell Sci* *121*, 2360-2371.

- Shi, Z., and Baumgart, T. (2015). Membrane tension and peripheral protein density mediate membrane shape transitions. *Nat Commun* 6, 5974.
- Simone, L.C., Caplan, S., and Naslavsky, N. (2013). Role of phosphatidylinositol 4,5-bisphosphate in regulating EHD2 plasma membrane localization. *PLoS One* 8, e74519.
- Simons, K., and Sampaio, J.L. (2011). Membrane organization and lipid rafts. *Cold Spring Harb Perspect Biol* 3, a004697.
- Singer, S.J., and Nicolson, G.L. (1972). The fluid mosaic model of the structure of cell membranes. *Science* 175, 720-731.
- Singh, R.D., Marks, D.L., Holicky, E.L., Wheatley, C.L., Kaptzan, T., Sato, S.B., Kobayashi, T., Ling, K., and Pagano, R.E. (2010). Gangliosides and beta1-integrin are required for caveolae and membrane domains. *Traffic* 11, 348-360.
- Singla, V., and Reiter, J.F. (2006). The primary cilium as cell's antenna : signaling at a sensory organelle. *Science* 313, 629-633.
- Sinha, B., Koster, D., Ruez, R., Gonnord, P., Bastiani, M., Abankwa, D., Stan, R.V., Butler-Browne, G., Védie, B., Johannes, L., *et al.* (2011). Cells respond to mechanical stress by rapid disassembly of caveolae. *Cell* 144, 402-413.
- Stahlhut, M., and van Deurs, B. (2000). Identification of filamin as a novel ligand for caveolin-1: evidence for the organization of caveolin-1-associated membrane domains by the actin cytoskeleton. *Mol Biol Cell* 11, 325-337.
- Stefanova, N., Staneva, G., Petkova, D., Lupanova, T., Pankov, R., and Momchilova, A. (2009). Cell culturing in a three-dimensional matrix affects the localization and properties of plasma membrane cholesterol. *Cell Biol Int* 33, 1079-1086.
- Stetler-Stevenson, W.G., and Yu, A.E. (2001). Proteases in invasion: matrix metalloproteinases. *Semin Cancer Biol* 11, 143-152.
- Stroka, K.M., Jiang, H., Chen, S.H., Tong, Z., Wirtz, D., Sun, S.X., and Konstantopoulos, K. (2014). Water permeation drives tumor cell migration in confined microenvironments. *Cell* 157, 611-623.
- Suvrajit Saha, Il-Hyung Lee, Anirban Polley, Jay T. Groves, Madan Rao, and Mayor, S. (2015). Diffusion of GPI-anchored proteins is influenced by the activity of dynamic cortical actin. *Molecular Biology of The Cell* 26, 4033-4045.
- Suzuki, K.G., Fujiwara, T.K., Sanematsu, F., Ino, R., Edidin, M., and Kusumi, A. (2007). GPI-anchored receptor clusters transiently recruit Lyn and G alpha for temporary cluster immobilization and Lyn activation: single-molecule tracking study 1. *J Cell Biol* 177, 717-730.

- Sverdlov, M., Shinin, V., Place, A.T., Castellon, M., and Minshall, R.D. (2009). Filamin A regulates caveolae internalization and trafficking in endothelial cells. *Mol Biol Cell* *20*, 4531-4540.
- Tagawa, A., Mezzacasa, A., Hayer, A., Longatti, A., Pelkmans, L., and Helenius, A. (2005). Assembly and trafficking of caveolar domains in the cell: caveolae as stable, cargo-triggered, vesicular transporters. *J Cell Biol* *170*, 769-779.
- Tan, X., Heureaux, J., and Liu, A.P. (2015). Cell spreading area regulates clathrin-coated pit dynamics on micropatterned substrate. *Integr Biol (Camb)* *7*, 1033-1043.
- Thompson, C., Rahim, S., Arnold, J., and Hielscher, A. (2017). Loss of caveolin-1 alters extracellular matrix protein expression and ductal architecture in murine mammary glands. *PLoS One* *12*, e0172067.
- Thomsen, P., Roepstorff, K., Stahlhut, M., and Deurs, B.v. (2002). Caveolae Are Highly Immobile Plasma Membrane Microdomains, Which Are not Involved in Constitutive Endocytic Trafficking. *Mol Biol Cell* *13*, 238-250.
- Tinevez, J.Y., Schulze, U., Salbreux, G., Roensch, J., Joanny, J.F., and Paluch, E. (2009). Role of cortical tension in bleb growth. *Proc Natl Acad Sci U S A* *106*, 18581-18586.
- Trimble, W.S., and Grinstein, S. (2015). Barriers to the free diffusion of proteins and lipids in the plasma membrane. *J Cell Biol* *208*, 259-271.
- Upla, P., Marjomaki, V., Kankaanpaa, P., Ivaska, J., Hyypia, T., Van Der Goot, F.G., and Heino, J. (2004). Clustering induces a lateral redistribution of alpha 2 beta 1 integrin from membrane rafts to caveolae and subsequent protein kinase C-dependent internalization. *Mol Biol Cell* *15*, 625-636.
- Venema, V.J., Zou, R., Ju, H., Marrero, M.B., and Venema, R.C. (1997). Caveolin-1 detergent solubility and association with endothelial nitric oxide synthase is modulated by tyrosine phosphorylation. *Biochem Biophys Res Commun* *236*, 155-161.
- Vereb, G., Szollosi, J., Matko, J., Nagy, P., Farkas, T., Vigh, L., Matyus, L., Waldmann, T.A., and Damjanovich, S. (2003). Dynamic, yet structured: The cell membrane three decades after the Singer-Nicolson model. *Proc Natl Acad Sci U S A* *100*, 8053-8058.
- Visse, R., and Nagase, H. (2003). Matrix metalloproteinases and tissue inhibitors of metalloproteinases: structure, function, and biochemistry. *Circ Res* *92*, 827-839.
- Volonte, D., Galbiati, F., Pestell, R.G., and Lisanti, M.P. (2001). Cellular stress induces the tyrosine phosphorylation of caveolin-1 (Tyr(14)) via activation of p38 mitogen-activated protein kinase and c-Src kinase. Evidence for caveolae, the actin cytoskeleton, and focal adhesions as mechanical sensors of osmotic stress. *J Biol Chem* *276*, 8094-8103.

- Walser, P.J., Ariotti, N., Howes, M., Ferguson, C., Webb, R., Schwudke, D., Leneva, N., Cho, K.J., Cooper, L., Rae, J., *et al.* (2012). Constitutive formation of caveolae in a bacterium. *Cell* *150*, 752-763.
- Wang, J.H., Thampatty, B.P., Lin, J.S., and Im, H.J. (2007). Mechanoregulation of gene expression in fibroblasts. *Gene* *391*, 1-15.
- Wang, L., Zhang, C., Su, X., Lin, D.H., and Wang, W. (2015). Caveolin-1 Deficiency Inhibits the Basolateral K<sup>+</sup> Channels in the Distal Convolute Tubule and Impairs Renal K<sup>+</sup> and Mg<sup>2+</sup> Transport. *J Am Soc Nephrol* *26*, 2678-2690.
- Warshaviak, D.T., Muellner, M.J., and Chachisvilis, M. (2011). Effect of membrane tension on the electric field and dipole potential of lipid bilayer membrane. *Biochim Biophys Acta* *1808*, 2608-2617.
- Wary, K.K., Mariotti, A., Zurzolo, C., and Giancotti, F.G. (1998). A requirement for caveolin-1 and associated kinase Fyn in integrin signaling and anchorage-dependent cell growth. *Cell* *94*, 625-634.
- Waschke, J., Golenhofen, N., Kurzchalia, T.V., and Drenckhahn, D. (2006). Protein kinase C-mediated endothelial barrier regulation is caveolin-1-dependent. *Histochem Cell Biol* *126*, 17-26.
- Weaver, V.M., Petersen, O.W., Wang, F., Larabell, C.A., Briand, P., Damsky, C., and Bissell, M.J. (1997). Reversion of the malignant phenotype of human breast cells in three-dimensional culture and in vivo by integrin blocking antibodies. *J Cell Biol* *137*, 231-245.
- Weiss, P., and Garber, B. (1952). Shape and Movement of Mesenchyme Cells as Functions of the Physical Structure of the Medium: Contributions to a Quantitative Morphology. *Proc Natl Acad Sci U S A* *38*, 264-280.
- Wickstrom, S.A., Lange, A., Hess, M.W., Polleux, J., Spatz, J.P., Kruger, M., Pfaller, K., Lambacher, A., Bloch, W., Mann, M., *et al.* (2010). Integrin-linked kinase controls microtubule dynamics required for plasma membrane targeting of caveolae. *Dev Cell* *19*, 574-588.
- Williams, T.M., Hassan, G.S., Li, J., Cohen, A.W., Medina, F., Frank, P.G., Pestell, R.G., Di Vizio, D., Loda, M., and Lisanti, M.P. (2005). Caveolin-1 promotes tumor progression in an autochthonous mouse model of prostate cancer: genetic ablation of Cav-1 delays advanced prostate tumor development in tramp mice. *J Biol Chem* *280*, 25134-25145.
- Williams, T.M., Medina, F., Badano, I., Hazan, R.B., Hutchinson, J., Muller, W.J., Chopra, N.G., Scherer, P.E., Pestell, R.G., and Lisanti, M.P. (2004). Caveolin-1 Gene Disruption Promotes Mammary Tumorigenesis and Dramatically Enhances Lung Metastasis in Vivo. *Journal of Biological Chemistry* *279*, 51630-51645.
- Wolf, K., Mazo, I., Leung, H., Engelke, K., von Andrian, U.H., Deryugina, E.I., Strongin, A.Y., Brocker, E.B., and Friedl, P. (2003). Compensation mechanism in tumor cell migration:

mesenchymal-amoeboid transition after blocking of pericellular proteolysis. *J Cell Biol* 160, 267-277.

Wolf, K., Te Lindert, M., Krause, M., Alexander, S., Te Riet, J., Willis, A.L., Hoffman, R.M., Figdor, C.G., Weiss, S.J., and Friedl, P. (2013). Physical limits of cell migration: control by ECM space and nuclear deformation and tuning by proteolysis and traction force. *J Cell Biol* 201, 1069-1084.

Wottawah, F., Schinkinger, S., Lincoln, B., Ananthakrishnan, R., Romeyke, M., Guck, J., and Kas, J. (2005). Optical rheology of biological cells. *Phys Rev Lett* 94, 098103.

Wozniak, M.A., Desai, R., Solski, P.A., Der, C.J., and Keely, P.J. (2003). ROCK-generated contractility regulates breast epithelial cell differentiation in response to the physical properties of a three-dimensional collagen matrix. *J Cell Biol* 163, 583-595.

Yamada, E. (1955). The fine structures of the gall bladder epithelium of the mouse. *J Biophys Biochem Cytol* 1, 445-458.

Yamaguchi, H., Takeo, Y., Yoshida, S., Kouchi, Z., Nakamura, Y., and Fukami, K. (2009). Lipid rafts and caveolin-1 are required for invadopodia formation and extracellular matrix degradation by human breast cancer cells. *Cancer Res* 69, 8594-8602.

Yamamoto, M., Toya, Y., Schwencke, C., Lisanti, M.P., Myers, M.G., Jr., and Ishikawa, Y. (1998). Caveolin is an activator of insulin receptor signaling. *J Biol Chem* 273, 26962-26968.

Yang, G., Truong, L.D., Wheeler, T.M., and Thompson, T.C. (1999). Caveolin-1 expression in clinically confined human prostate cancer: a novel prognostic marker. *Cancer Res* 59, 5719-5723.

Yeung, T., Georges, P.C., Flanagan, L.A., Marg, B., Ortiz, M., Funaki, M., Zahir, N., Ming, W., Weaver, V., and Janmey, P.A. (2005). Effects of substrate stiffness on cell morphology, cytoskeletal structure, and adhesion. *Cell Motil Cytoskeleton* 60, 24-34.

Yguerabide, J., Schmidt, J.A., and Yguerabide, E.E. (1982). Lateral mobility in membranes as detected by fluorescence recovery after photobleaching. *Biophys J* 40, 69-75.

Zaman, M.H., Trapani, L.M., Sieminski, A.L., Mackellar, D., Gong, H., Kamm, R.D., Wells, A., Lauffenburger, D.A., and Matsudaira, P. (2006). Migration of tumor cells in 3D matrices is governed by matrix stiffness along with cell-matrix adhesion and proteolysis. *Proc Natl Acad Sci U S A* 103, 10889-10894.

Zamir, E., and Geiger, B. (2001). Molecular complexity and dynamics of cell-matrix adhesions. *J Cell Sci* 114, 3583-3590.



- Zhang, B., Peng, F., Wu, D., Ingram, A.J., Gao, B., and Krepinsky, J.C. (2007). Caveolin-1 phosphorylation is required for stretch-induced EGFR and Akt activation in mesangial cells. *Cell Signal* 19, 1690-1700.
- Zhang, Y.H., Zhao, C.Q., Jiang, L.S., and Dai, L.Y. (2011). Substrate stiffness regulates apoptosis and the mRNA expression of extracellular matrix regulatory genes in the rat annular cells. *Matrix Biol* 30, 135-144.
- Zhong, J., Baquiran, J.B., Bonakdar, N., Lees, J., Ching, Y.W., Pugacheva, E., Fabry, B., and O'Neill, G.M. (2012). NEDD9 stabilizes focal adhesions, increases binding to the extra-cellular matrix and differentially effects 2D versus 3D cell migration. *PLoS One* 7, e35058.
- Zhou, X., Rowe, R.G., Hiraoka, N., George, J.P., Wirtz, D., Mosher, D.F., Virtanen, I., Chernousov, M.A., and Weiss, S.J. (2008). Fibronectin fibrillogenesis regulates three-dimensional neovessel formation. *Genes Dev* 22, 1231-1243.
- Zhou, Y., Wong, C.O., Cho, K.J., van der Hoeven, D., Liang, H., Thakur, D.P., Luo, J., Babic, M., Zinsmaier, K.E., Zhu, M.X., *et al.* (2015). SIGNAL TRANSDUCTION. Membrane potential modulates plasma membrane phospholipid dynamics and K-Ras signaling. *Science* 349, 873-876.
- Zhu, H., Lin, P., De, G., Choi, K.H., Takeshima, H., Weisleder, N., and Ma, J. (2011). Polymerase transcriptase release factor (PTRF) anchors MG53 protein to cell injury site for initiation of membrane repair. *J Biol Chem* 286, 12820-12824.
- Zhuang, L., Lin, J., Lu, M.L., Solomon, K.R., and Freeman, M.R. (2002). Cholesterol-rich lipid rafts mediate akt-regulated survival in prostate cancer cells. *Cancer Res* 62, 2227-2231.
- Zimnicka, A.M., Husain, Y.S., Shajahan, A.N., Sverdlov, M., Chaga, O., Chen, Z., Toth, P.T., Klomp, J., Karginov, A.V., Tirupathi, C., *et al.* (2016). Src-dependent phosphorylation of caveolin-1 Tyr-14 promotes swelling and release of caveolae. *Mol Biol Cell* 27, 2090-2106.